Bridge River Power Development Water Use Plan

Seton River Sockeye Smolt Monitoring

Implementation Year 3

Reference: BRGMON-13

2014 Data Report

Study Period: April 1, 2014 - March 31, 2015

Jessica Hopkins, Bonnie Adolph and Dave Levy
St'at'imc Eco-Resources
Box 1420
Lillooet, B.C.
V0K 1V0

Prepared for:

BC Hydro
6911 Southpoint Drive
Burnaby, BC V3N 4X8

October 2, 2014

Executive Summary

Since 2006, St'át'imc and BC Hydro have collaborated to monitor sockeye smolt mortality associated with entrainment into the Seton powercanal. Turbine mortality is mitigated by shutting down the generator for 6-h duration outages that overlap peak nighttime smolt migrations. In those years when there is a maintenance outage that overlaps the smolt migration, impacts can be fully avoided for the period of overlap. As part of the St'át'imc - BC Hydro Settlement Agreement, monitoring is conducted annually to evaluate compliance with a 5% smolt mortality target.

Sampling was conducted in 2014 to monitor the seasonal timing, magnitude, and diel migrations of sockeye smolts out of Seton Lake, along with physical conditions in the Seton River. Sampling included:

- operating an inclined plane trap (IPT) in the Seton River below Seton Dam for 6 weeks during the sockeye smolt migration period;
- sampling during day- and nighttime hours to monitor diel migration patterns;
- conducting mark-recapture trials, including the release of marks below the dam;
- collecting biological data (i.e., forklengths) from a subset of sampled smolts to enable analysis of trends in smolt size between years;
- monitoring water temperature at the sampling site.

During 2014, a 24h/day maintenance outage overlapped the entire smolt migration period rendering a zero entrainment mortality. Scheduling of future maintenance outages within the April 20 - May 20 smolt migration window will provide optimal survival benefits, including protection of daytime migrators.

Results from 2014 indicated a moderate-sized smolt run totaling an estimated 2.3 million smolts . Sockeye smolts in 2014 were close to average in body size, consistent with density dependence in growth patterns in Seton Lake.

To describe and explore current velocity dynamics at the forebay and approach channel of Seton Dam, a Computational Fluid Dynamics model was constructed to predict water current velocities. The model successfully predicted flow dynamics at the face of the dam under different generator shutdown scenarios. A brief survey of the literature provided insight into sockeye smolt swimming capacity in relation to entrainment. A remote sensing/tagging project is recommended to directly measure entrainment.

Table of Contents

1.0 Introduction

The St'at'imc and BC Hydro have worked together since 2006 to devise practical methods for mitigating sockeye salmon smolt mortality of at the Seton Powerhouse (Figure 1). This mortality is a consequence of entrainment into the Power Canal and subsequent smolt passage through the turbine. Smolt mortality rates have been monitored since 2006.

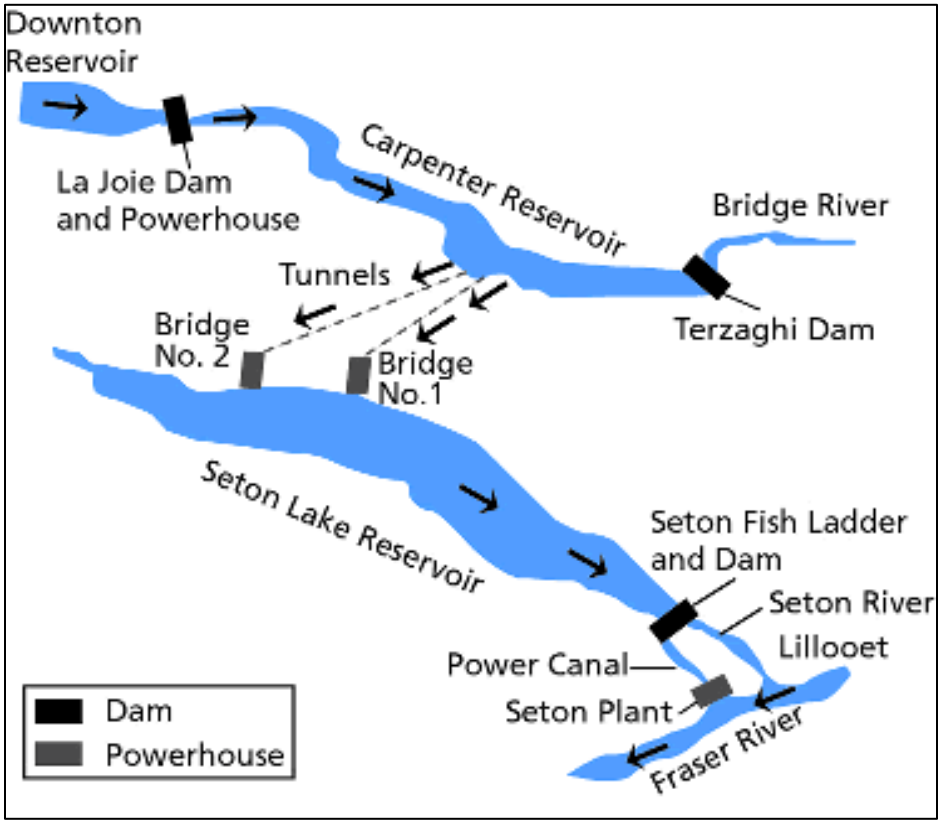

Figure 1. Location of BC Hydro facilities in the Bridge/Seton watersheds.

This data report presents the 2014 data set and compares results with previous findings. In view of budgetary considerations, a decision was taken in 2013 to streamline the annual reporting procedure to include full presentation of the data together with a focused and succinct report write-up. This approach has been carried over to 2014. Further descriptive information including methods are contained in the previous reports that cover the 9-year monitoring period, as listed in the Table below. These reports are available from BC Hydro via the authors upon request. The 2012 and previous reports contain a complete description of methods that have been consistently followed since 2006.

Date	Authors	Title
2014	J. Hopkins, B. Adolph and D.A. Levy	Seton River sockeye smolt monitoring: implementation year 9 (present report)
2013	B.Adolph and D.A. Levy	Seton River sockeye smolt monitoring: implementation year 8.
2012	J. Sneep, B. Adolph and D.A. Levy	Seton sockeye smolt monitoring in 2012 with a summary of historical data.
2011	J. Sneep,S. Hall and Lillooet Tribal Council	Seton River sockeye smolt monitoring program: 2011 sampling results.
2010	J. Sneep	Seton River sockeye smolt monitoring program: 2010 sampling results.
2009	D.A. Levy and J. Sneep	Effectiveness of Seton Powerhouse shutdowns for reducing entrainment mortality of sockeye salmon smolts during 2009.
2008	D.A. Levy, J. Sneep and S. Hall	Effectiveness of Seton Powerhouse shutdowns for reducing entrainment mortality of sockeye salmon smolts during 2008.
2007	D.A. Levy and J. Sneep	Effectiveness of Seton Powerhouse shutdowns for reducing entrainment mortality of sockeye salmon smolts during 2007.
2006	D.A. Levy and J. Sneep	Effectiveness of Seton Powerhouse shutdowns for reducing entrainment mortality of sockeye salmon smolts during 2006.

In an effort to better understand flow management alternatives for minimizing smolt entrainment, a proposal was developed in 2013 to measure the current flow field at the face of Seton Dam under different flow routing scenarios. However, safety concerns precluded the use of a boat-mounted Acoustic Doppler Current Profiler (ADCP) in the forebay of Seton Dam to obtain this information. In 2014, an alternate approach was followed using Computational Fluid Dynamics Modeling conducted by the University of Alberta (Appendix 1). Results were compared with published literature information to assess sockeye smolt swimming behavior in relation to entrainment (Appendix 2). The latter 2 approaches are novel ones for BRGMON13 that are evaluated in the Discussion Section.

2.0 Results

2.1 Physical Characteristics

2.1.1 Discharge

Discharge records into the Seton River and powercanal are maintained by BC Hydro. Discharge through the mid-April to late May smolt migration was relatively stable until May 22 when the river was ramped from 38 cms to 62 cms. (Figure 2). The increase in flow during the latter part of sampling required that the smolt trap be brought close to shore for safe operation.

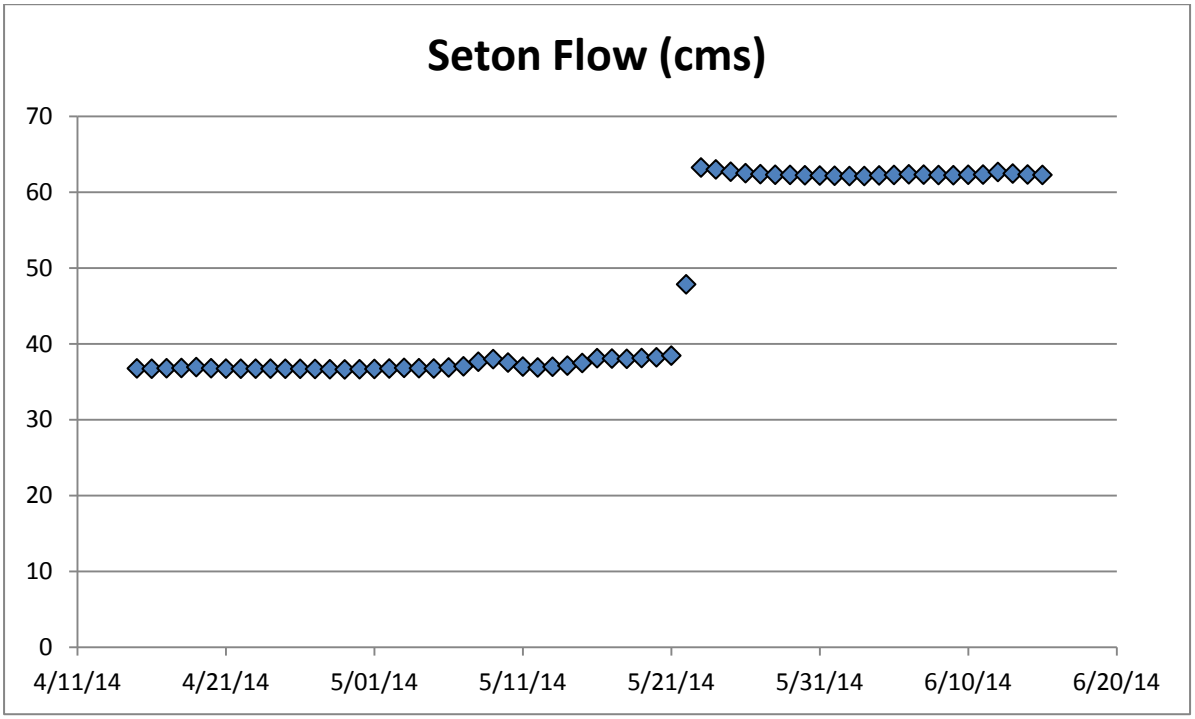

Figure 2. Seton River discharges during the 2014 smolt migration period.

Discharges into the Seton River were relatively low (38 cms) during the first part of the smolt migration period between April 20 - May 21 (Figure 3). Thereafter flows increased to around 61-62 cms until June 20. The generator and powercanal were shut off for maintenance (prior to the start-up of smolt sampling on April 14) until June 11, well after the end of the smolt migration. Due to the extended outage, there was no associated turbine mortality in 2014.

During 2013, hourly discharges were documented to reflect shutdown hours in relation to diel smolt migrations. The analysis for 2014 (Table 1) documents the total closure of the plant in relation to the normal operating practice of a 6-hr nightly shutdown period between 20:00 - 02:00.

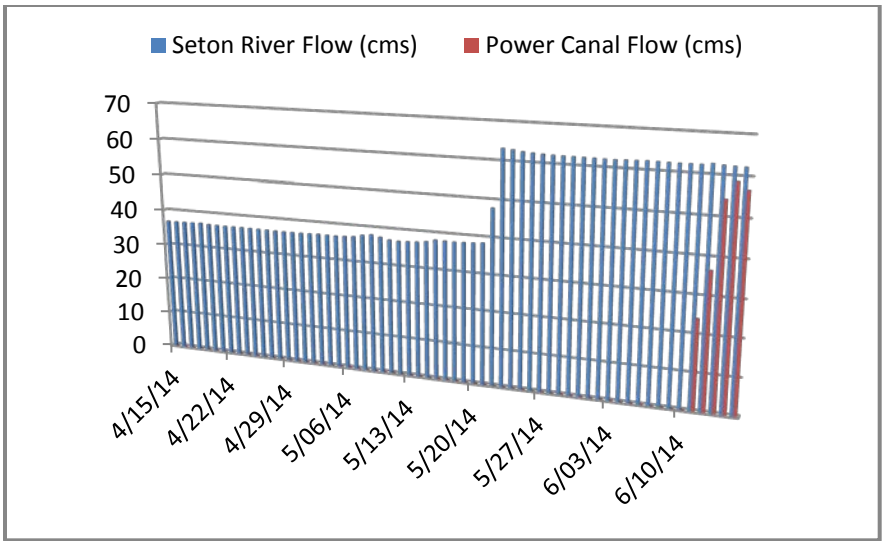

Figure 3. Daily averaged water flows into the Seton River and the Seton Powercanal during the smolt migration period in 2014.

Table 1. Hourly shutdowns in 2014 (black dots) and recommended shutdown schedule (20:00 - 02:00 hours) designed for optimal smolt protection (red-shaded cells). Numbers in the top row indicate time of day. During 2014 a maintenance outage extended over the entire smolt migration period.

	1	2	3	4	5	6	7	8	9	10	11	12	13	14	15	16	17	18	19	20	21	22	23	24
Apr. 20	•	•	•	•	•	•	•	•	•	•	•	•	•	•	•	•	•	•	•	•	•	•	•	•
Apr. 21	•	•	•	•	•	•	•	•	•	•	•	•	•	•	•	•	•	•	•	•	•	•	•	•
Apr. 22	•	•	•	•	•	•	•	•	•	•	•	•	•	•	•	•	•	•	•	•	•	•	•	•
Apr. 23	•	•	•	•	•	•	•	•	•	•	•	•	•	•	•	•	•	•	•	•	•	•	•	•
Apr. 24	•	•	•	•	•	•	•	•	•	•	•	•	•	•	•	•	•	•	•	•	•	•	•	•
Apr. 25	•	•	•	•	•	•	•	•	•	•	•	•	•	•	•	•	•	•	•	•	•	•	•	•
Apr. 26	•	•	•	•	•	•	•	•	•	•	•	•	•	•	•	•	•	•	•	•	•	•	•	•
Apr. 27	•	•	•	•	•	•	•	•	•	•	•	•	•	•	•	•	•	•	•	•	•	•	•	•
Apr. 28	•	•	•	•	•	•	•	•	•	•	•	•	•	•	•	•	•	•	•	•	•	•	•	•
Apr. 29	•	•	•	•	•	•	•	•	•	•	•	•	•	•	•	•	•	•	•	•	•	•	•	•
Apr. 30	•	•	•	•	•	•	•	•	•	•	•	•	•	•	•	•	•	•	•	•	•	•	•	•
May 1	•	•	•	•	•	•	•	•	•	•	•	•	•	•	•	•	•	•	•	•	•	•	•	•
May 2	•	•	•	•	•	•	•	•	•	•	•	•	•	•	•	•	•	•	•	•	•	•	•	•
May 3	•	•	•	•	•	•	•	•	•	•	•	•	•	•	•	•	•	•	•	•	•	•	•	•
May 4	•	•	•	•	•	•	•	•	•	•	•	•	•	•	•	•	•	•	•	•	•	•	•	•
May 5	•	•	•	•	•	•	•	•	•	•	•	•	•	•	•	•	•	•	•	•	•	•	•	•
May 6	•	•	•	•	•	•	•	•	•	•	•	•	•	•	•	•	•	•	•	•	•	•	•	•
May 7	•	•	•	•	•	•	•	•	•	•	•	•	•	•	•	•	•	•	•	•	•	•	•	•
May 8	•	•	•	•	•	•	•	•	•	•	•	•	•	•	•	•	•	•	•	•	•	•	•	•
May 9	•	•	•	•	•	•	•	•	•	•	•	•	•	•	•	•	•	•	•	•	•	•	•	•
May 10	•	•	•	•	•	•	•	•	•	•	•	•	•	•	•	•	•	•	•	•	•	•	•	•
May 11	•	•	•	•	•	•	•	•	•	•	•	•	•	•	•	•	•	•	•	•	•	•	•	•
May 12	•	•	•	•	•	•	•	•	•	•	•	•	•	•	•	•	•	•	•	•	•	•	•	•
May 13	•	•	•	•	•	•	•	•	•	•	•	•	•	•	•	•	•	•	•	•	•	•	•	•
May 14	•	•	•	•	•	•	•	•	•	•	•	•	•	•	•	•	•	•	•	•	•	•	•	•
May 15	•	•	•	•	•	•	•	•	•	•	•	•	•	•	•	•	•	•	•	•	•	•	•	•
May 16	•	•	•	•	•	•	•	•	•	•	•	•	•	•	•	•	•	•	•	•	•	•	•	•
May 17	•	•	•	•	•	•	•	•	•	•	•	•	•	•	•	•	•	•	•	•	•	•	•	•
May 18	•	•	•	•	•	•	•	•	•	•	•	•	•	•	•	•	•	•	•	•	•	•	•	•
May 19	•	•	•	•	•	•	•	•	•	•	•	•	•	•	•	•	•	•	•	•	•	•	•	•
May 20	•	•	•	•	•	•	•	•	•	•	•	•	•	•	•	•	•	•	•	•	•	•	•	•

2.1.2 Temperature

River and air temperatures throughout the smolt migration are shown in Figure 4. 2014 was a relatively cool year at the beginning of the migration period compared to previous years. It is likely that a river temperature of 5^0C serves as a migration cue for sockeye smolts (Sneep et al. 2012) and this temperature was surpassed in late April. There was a spike in temperature at the beginning of May followed by a week-long cooling period. Following steady heating in early May air temperatures decreased through mid-May. Water temperatures stabilized for around 10 days, also in mid-May, and then increased, albeit erratically, over the rest of the monitoring period. It was evident (Figure 4 - bottom panel) that changes in air temperature were driving the water temperature fluctuations and co-varied with a time lag of several days, a pattern that has been observed in previous years.

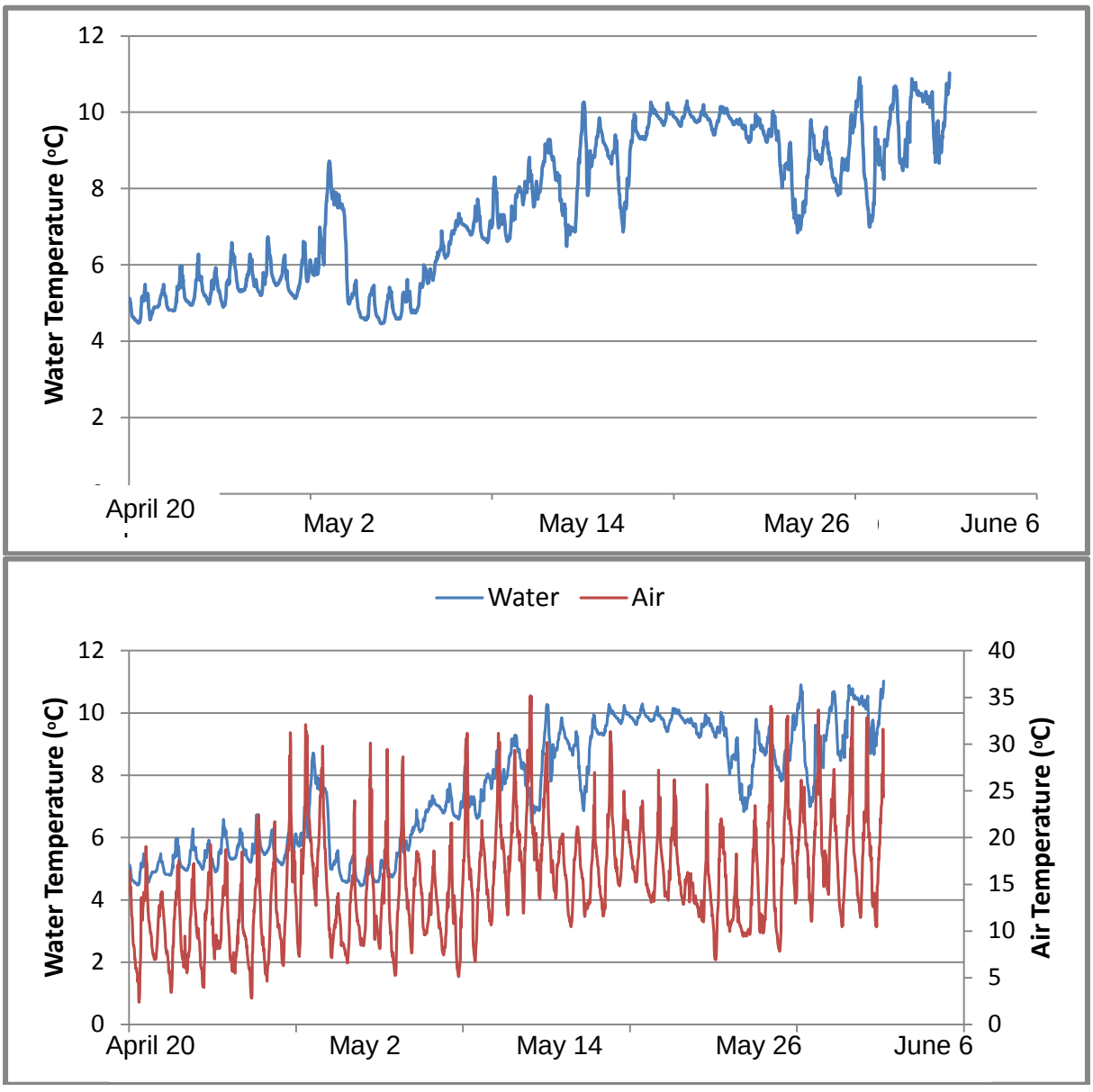

Figure 4. Top: Seton River temperatures; Bottom: Seton River air and water temperatures.

2.2 Sockeye Smolt Monitoring Data

2.2.1 Inclined Plane Trap Catches

There were intermediate smolt catches in 2014 compared with 2006-2013 IPT results. Table 2 provides the total annual catches, broken out by daytime and nighttime sampling periods, as well as the maximum daily or nightly catch results. Nighttime and daytime periods yielded catches of 34,447 and 5,706 smolts, respectively, during 45 days of trapping. In contrast, during 2012 a single daytime catch yielded 45,817 smolts, greater than the total seasonal smolt catch of 40,153 in 2014. The numbers captured in 2014 were similar to those in 2010 which was the same cycle year (Seton sockeye are 4-yr old fish), a reflection of cyclic dominance in Gates and Portage sockeye (Levy and Wood 1992). The total catch numbers are shown graphically in Figure 5.

Table 2. Total and maximum daily catches of sockeye smolts between 2006-2014.

	Total Catch	Total nighttime Catch	Total daytime Catch	Daytime - Nighttime ratio	Maximum 1-day catch (nighttime)	Maximum 1-day catch (daytime)
2006	34,143	34,143	---------	---------	6,705	---------
2007	43,450	43,450	---------	---------	7,059	---------
2008	8,694	7,026	1,668	0.19	632	731
2009	18,048	13,486	4,562	0.25	1,641	717
2010	27,335	20,532	6,803	0.25	3,096	2,167
2011	144,128	136,388	7,740	0.05	12,177	1,561
2012	249,979	129,153	120,826	0.48	40,574	45,817
2013	16,330	15,534	796	0.05	1,540	141
2014	39,492	34,447	5,045	0.15	5,706	592

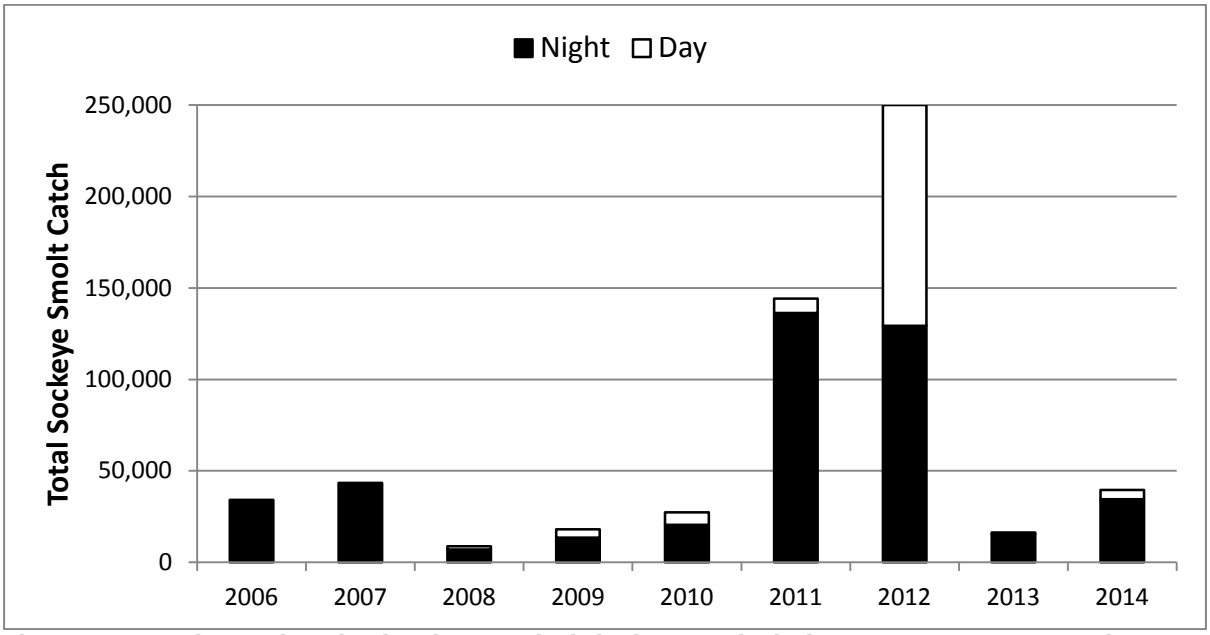

Figure 5. Smolt catches in daytime and nighttime periods between 2006-2014. There was no daytime sampling undertaken in 2006 and 2007.

2.2.2 Seasonal Migration Timing

As in previous years, the smolt outmigration spanned the period between mid-April through the termination of sampling at the end of May. Figure 6 shows the nighttime and daytime smolt catch results plotted on a logarithmic axis to effectively display the data which cover 4 orders of magnitude. Seasonal catches in 2013 were distributed over time in a similar fashion as in previous years and showed an intermediate level of abundance, consistent with the total catch and maximum 1-day catch data (Table 2).

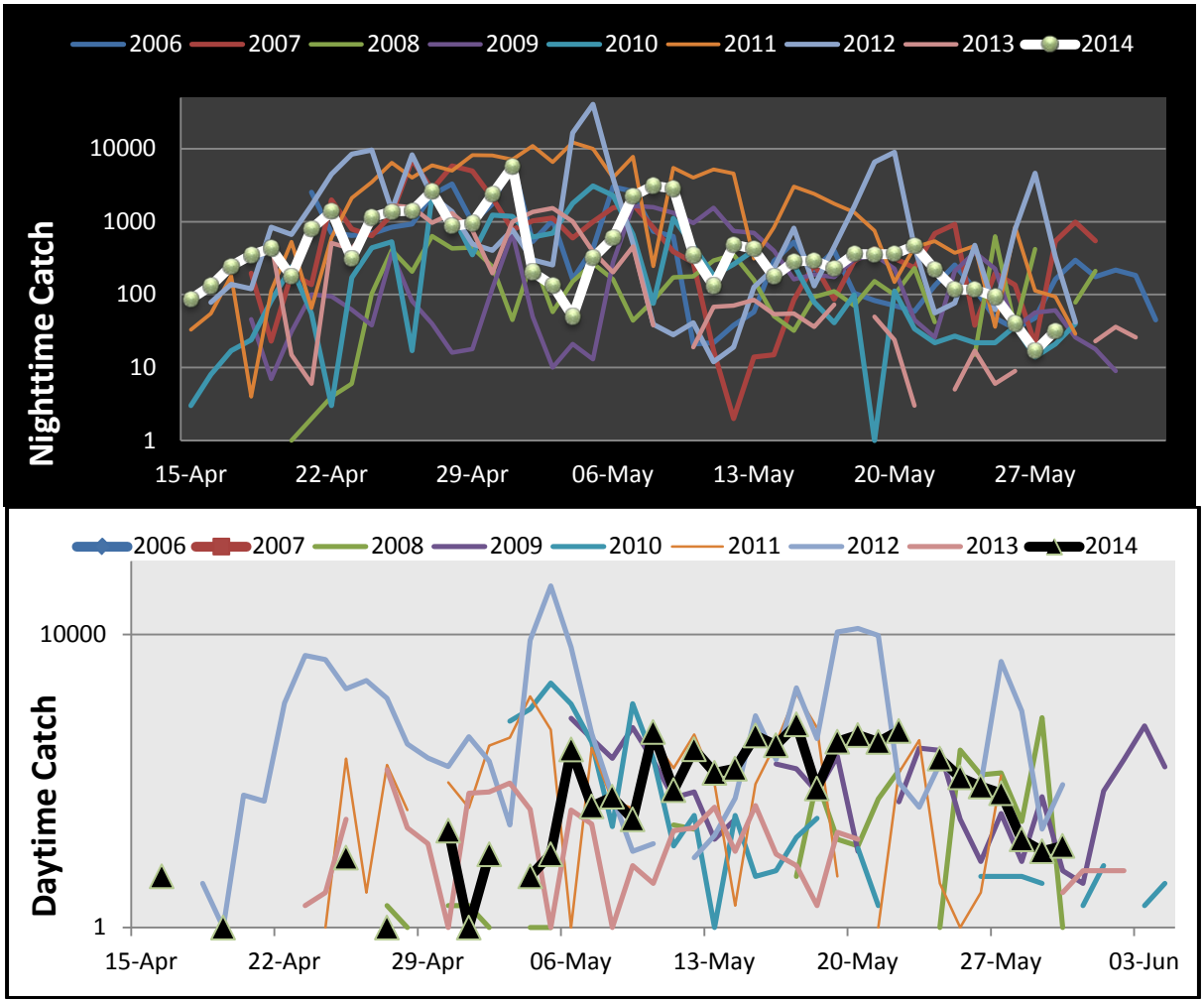

Figure 6. Night vs. daytime smolt catches plotted with a logarithmic axis.

Comparison of the mean proportion of smolt catches over the migration period (Figure 7) indicated different patterns between nighttime and daytime. Whereas the nighttime proportions were uniformly distributed (seasonally), there was a higher proportion of daytime migrators from May onwards at the tail end of the migration with only low proportions

occurring during April[1]. The data have been plotted on a log scale due to the large variation (5 orders of magnitude) in the catch records when plotted as a proportion of the annual smolt run.

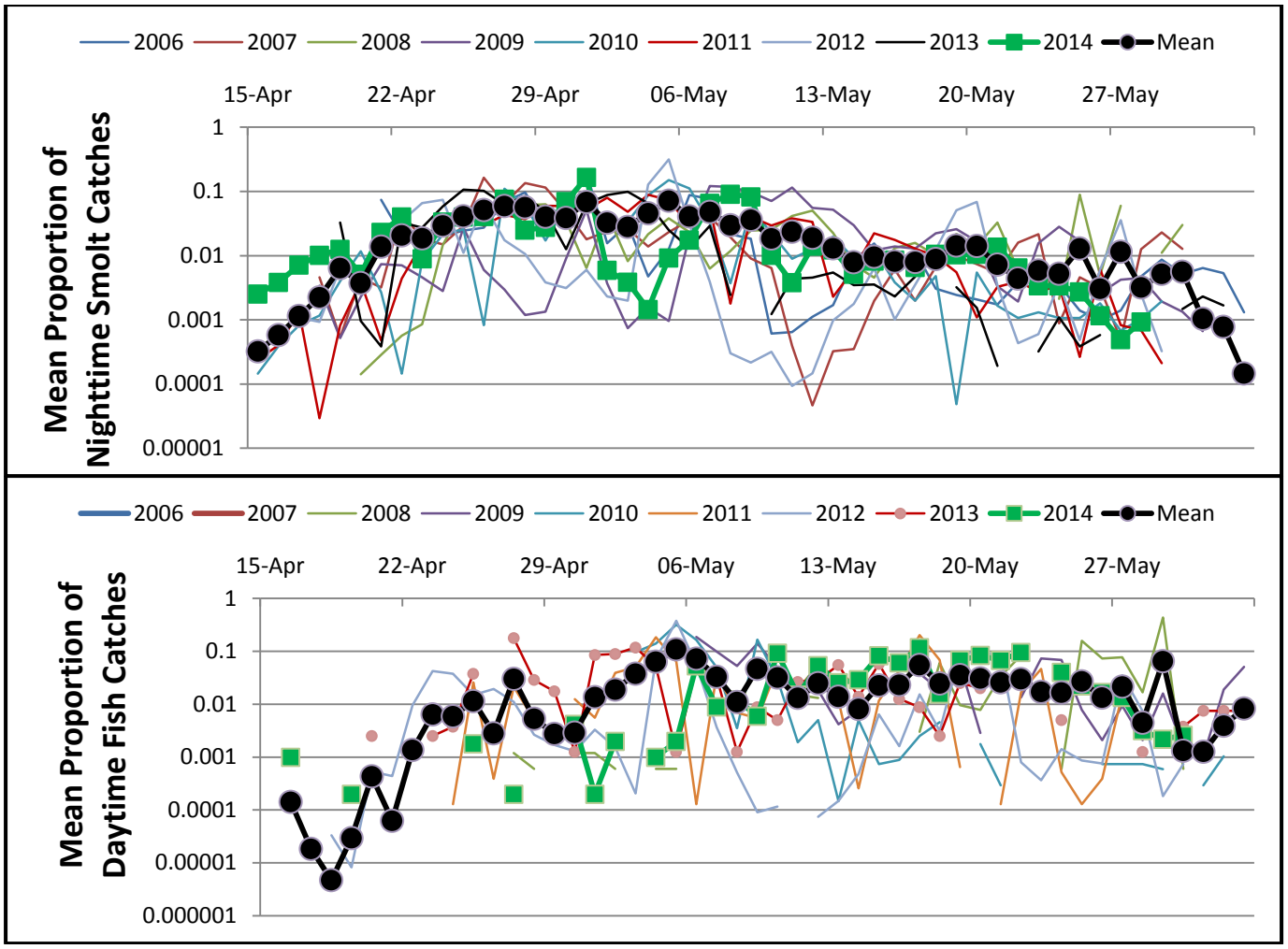

Figure 7. Seasonal proportions of daytime and nighttime smolt catches plotted with a logarithmic axis.

As in previous years, the catch data were transformed into time-density plots to measure the median migration dates and to compare migration patterns between years (Figure 8). The median migration dates in 2014 were May 1 and May 17 for nighttime and daytime migrations respectively. Median migration dates are May 3 and May 11 for the consolidated data set (Figure 8; lower panel) indicating that the 2014 nighttime smolt migration was similar to previous years while the daytime migration was about 1 week later than average. Median outmigration timing across all of the 9 years shows that daytime migrations on average occur later in the outmigration period, by about 1 week.

[1] There was no daytime sampling during the month of April in 2009 and 2010.

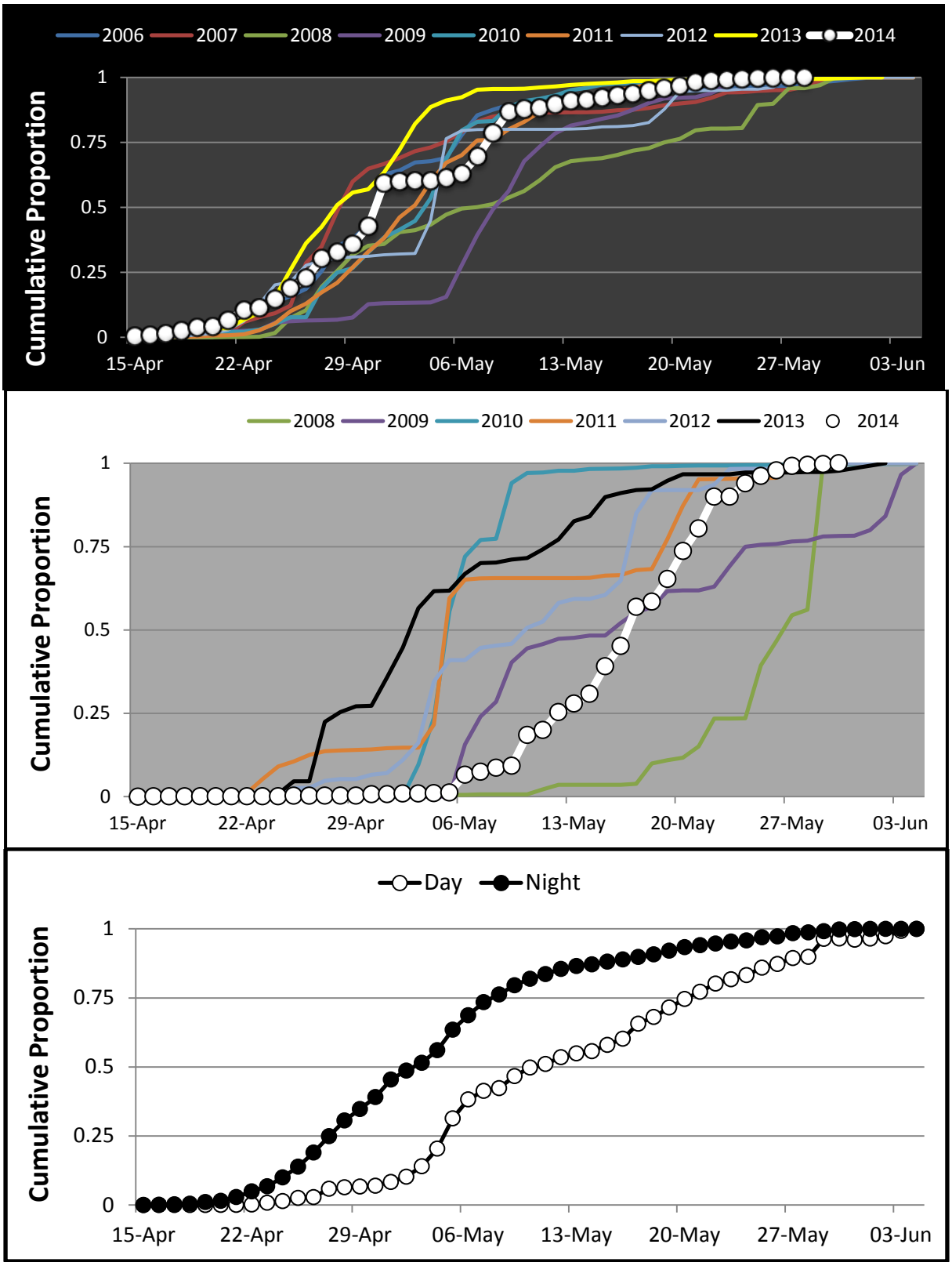

Figure 8. Time-density plots for (top to bottom) nighttime, daytime and average proportional catches for the 9 years of observations.

Seasonal timing together with day-night catch comparisons were also evaluated by plotting day and night catch histograms (Figure 9). Patterns varied between years with some years (nightime - 2011) being unimodal, others being skewed (nighttime - 2008 and 2010) and others being multimodal (2012 both daytime and nighttime). The differences between night and day catches were most strongly reflected in the 2011, 2013 and 2014 data sets.

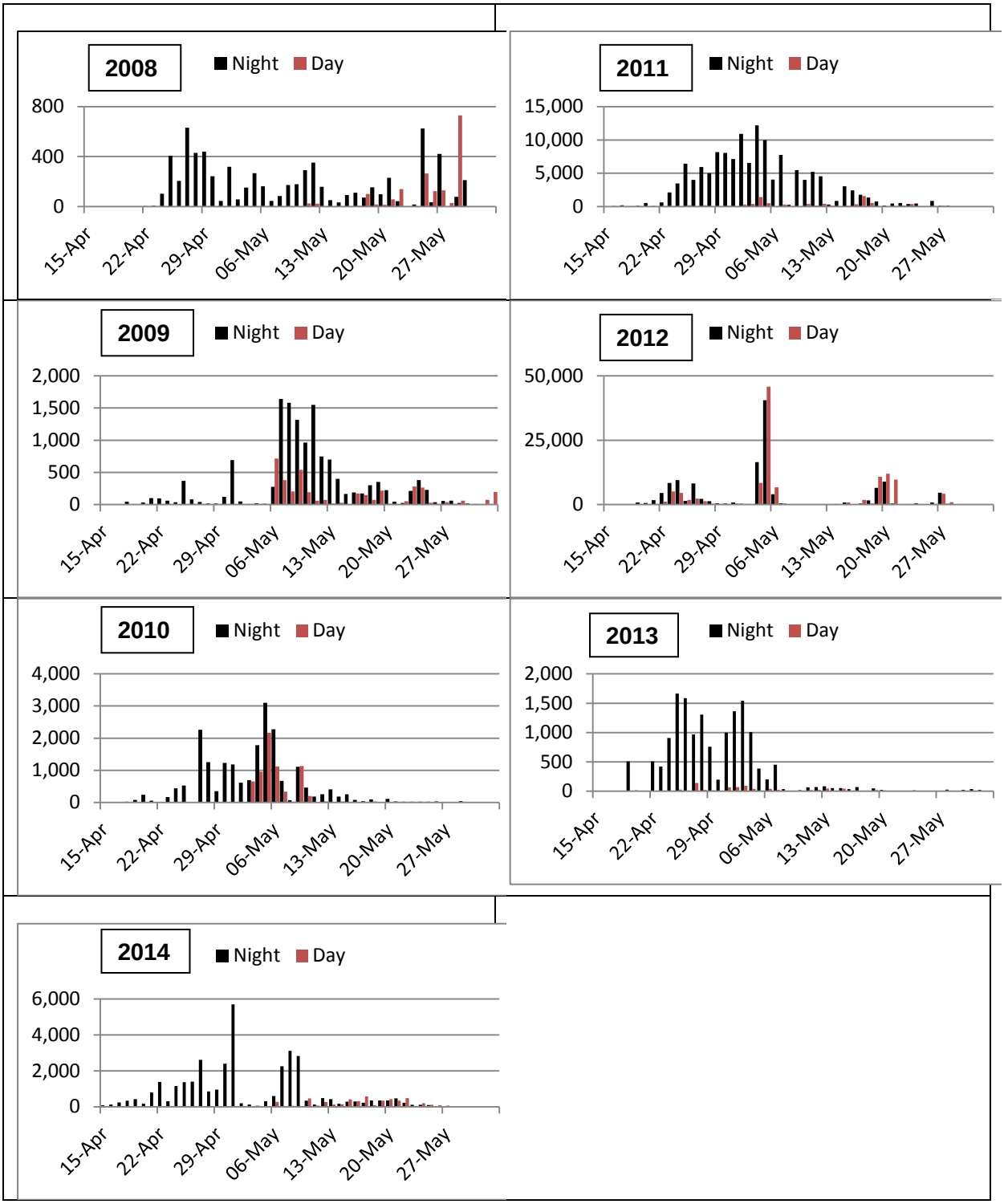

Figure 9. Day and night catch histograms for 2008 - 2014 when daytime and nighttime periods were consistently sampled.

2.2.3 Diel Timing

Understanding of smolt diel timing patterns is essential for scheduling 6-h shutdowns so as to maximize the mortality mitigation benefits. In 2006 it was determined that a 6-h period between 20:00 and 02:00 would be optimal for 6-hr duration shutdowns and that has been followed annually. In every year, including 2014 this was the optimal protection window (Figure 10). During 2014, 83% of the nightly migration occurred between 20:00 - 02:00 justifying this diel shutdown scheduling to optimize the protective benefits of the 6-hr shutdowns. As in previous years, daytime catches generally increased from early morning through to early evening[2] (Figure 10 - lower panel).

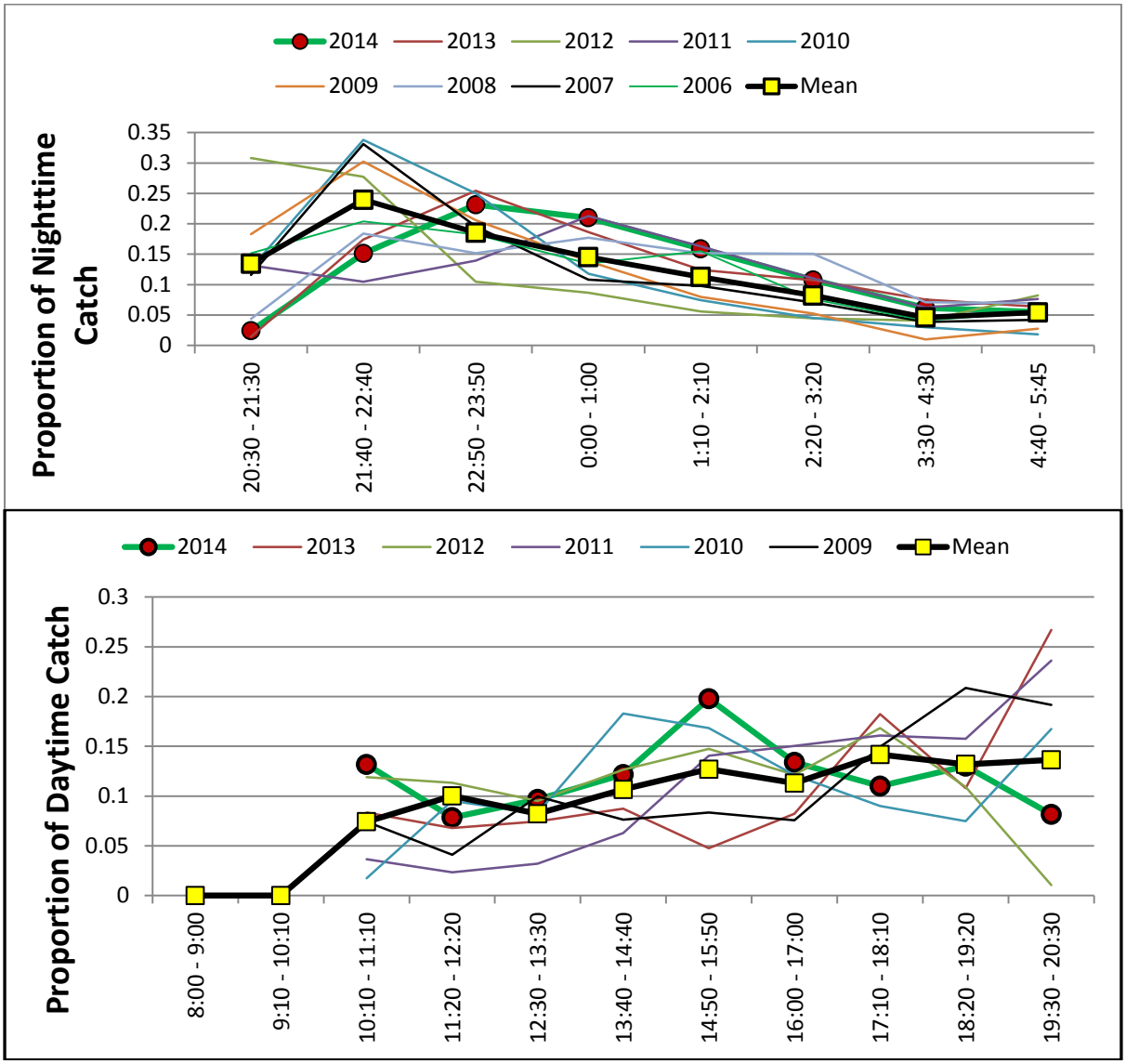

Figure 10. Hourly variation in the proportion of nighttime and daytime catches.

[2] Sampling did not occur between 06:00 - 10:00 in order to optimize the available personpower within the available budget envelope.

2.2.4 Smolt Size Characteristics

Sockeye smolts in the Seton River showed large interannual differences in fork length distribution (Table 3, Figure 11). Largest smolts were captured in 2009 (mean = 109 mm) and smallest smolts occurred in 2012 (mean = 77 mm). During 2013, smolts were relatively large with a mean fork length of 101 mm. The large variation in body size between years suggests annual variability in Seton and Anderson Lake rearing conditions for sockeye juveniles, although the mechanism involved is presently unknown. Section 4.2.5 evaluates density-dependent relationships between smolt abundance and body size.

Table 3. Mean forklengths of age-1 sockeye smolts captured in the Seton River, by study year [a].

	Night Sampling			Day Sampling			All Periods		
	Mean	**Std Dev**	**n**	**Mean**	**Std Dev**	**n**	**Mean**	**Std Dev**	**n**
2006	93	9	1239	-	-	-	93	9	1239
2007	98	7	1183	-	-	-	98	7	1183
2008	99	6	1049	102	6	394	100	6	1443
2009	109	6	1003	110	6	873	109	6	1876
2010	105	6	1246	106	6	464	105	6	1710
2011	94	7	1555	95	8	921	94	7	2476
2012	77	6	1499	78	6	1414	77	6	2913
2013	100	13	1042	99	12	560	100	13	1600
2014	101	9	1727	100	10	1004	101	10	2732

[a] *Daytime sampling was sporadic and opportunistic in 2006 and 2007*

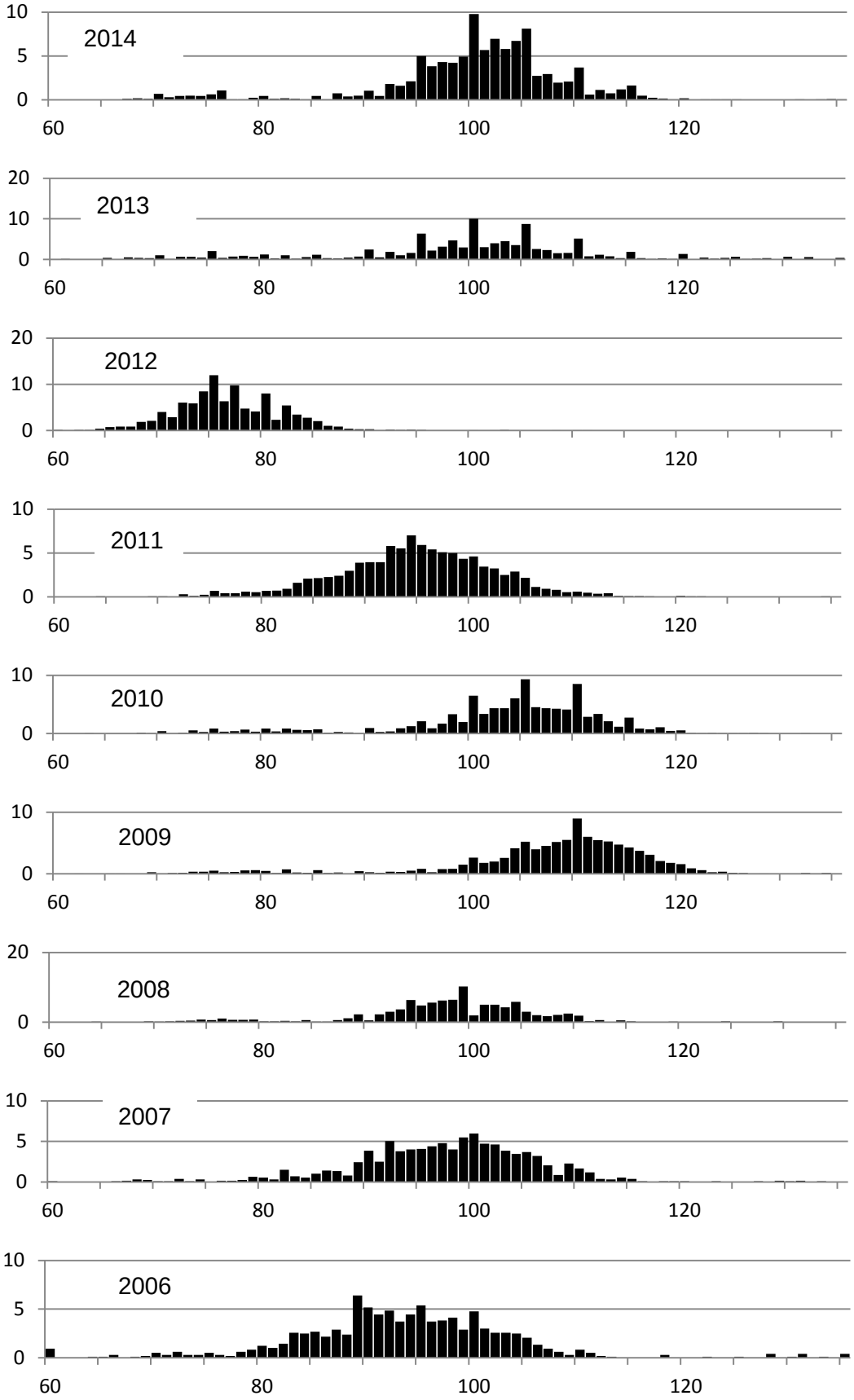

Figure 11. Smolt length frequency histograms for the 9 study years.

2.2.5 Smolt Abundance

Smolt abundance was determined by the Peterson mark-recapture method. The equation that calculates population size is:

$$N = MC/R$$

where N = population size
M = number smolts marked
C = number smolts captured in the sample
R = number of recaptures

Tables 4 and 5 show the mark recapture statistics for 2006 - 2014 during nighttime and daytime releases respectively. The dye experiments are run somewhat opportunistically depending on the availability of smolts from previous IPT catches. Experience has shown that dye-marked fish disperse out of the Seton River within several hours so each batch of dyed fish doesn't comingle with previous marked batches.

Table 4. Summary of nighttime mark-recapture experiment results (stratified by discharge) from the Seton River IPT, 2006 to 2014.

Study Year	Seton River Q ($m^3 \cdot s^{-1}$)	# of Trials	# of Marks Released	# of Marks Recaptured	% Recapture
2006	25 to 30	1	311	22	7.07
2007	25 to 30	1	416	26	6.25
	50+	3	1049	60	5.72
2008	25 to 30	3	1034	82	7.93
	31 to 35	1	660	38	5.76
2009	25 to 30	4	2310	212	9.18
2010	25 to 30	3	1012	105	10.38
2011	31 to 35	7	1517	90	5.93
2012	25 to 30	5	602	68	11.3
2013	25 to 30	2	248	18	7.26
2014	25 to 50	4	904	52	5.75
All years		34	10,063	773	7.68

Table 5 Summary of daytime mark-recapture experiment results from the Seton River IPT, 2006 to 2014.

Study Year	Seton River Q ($m^3 \cdot s^{-1}$)	# of Trials	# of Marks Released	# of Marks Recaptured	% Recapture Rate
2008	31 to 35	2	590	58	9.83
2009	25 to 30	2	1048	54	5.15
2010	25 to 30	1	386	25	6.48
	31 to 35	1	383	23	6.01
2011	31 to 35	5	748	62	8.29
2012	25 to 30	5	492	47	9.55
2013	25 to 30	1	119	6	5.04
2014	25 to 50	4	1236	38	3.07
All years		21	5002	313	6.25

In 2008 when an IPT was fished in the powercanal and mark-recapture experiments were conducted, 84% of the smolts were estimated to migrate via the powercanal when the power canal discharge was ca. 80 cms. This entrainment rate estimate has been utilized in all of the annual calculations of smolt abundance, including 2014.

There were 8 mark-recapture trials below the dam in 2014 (4 nighttime and 4 daytime) which yielded recapture rates of 5.75% during nighttime and 3.07 % during daytime. These values are somewhat lower than most of the previous trials likely reflecting relatively high flows in 2014 when trap efficiency was reduced. Additionally, there was an 8-d period after May 22 when the IPT was moved closer to shore in view of safety concerns associated with a higher flow (52 cms). A mark-recapture test on May 27 indicated lower recapture rates (2.3% day; 4.7% night) when compared with the 2014 average (3.07% day; 5.75% night). In view of the low number of migrating smolts at the tail end of the migration, no corrections were applied to account for this reduction in trap efficiency.

During previous years different approaches have been adopted to estimate smolt population size[3] and mortality rate. During 2014, the following procedure was applied for both daytime and nighttime calculations:

1) summarize the hourly trap catches by date in a date x time matrix,
2) scale the matrix by the inverse of recapture rate to obtain Seton smolt population estimates by day and by night,
3) expand the matrix to estimate the power canal population on an hourly basis by taking the Seton River smolt count multiplied by 0.84 (power canal diversion rate) and divided by 0.16 (proportion that passed through the Seton Dam),
4) sum the hourly values to obtain daily values,

[3] The different approaches have involved either the estimation of the hourly exposure of smolts under different operating conditions or mark-recapture experiments conducted above and below the dam.

5) estimate turbine mortality by multiplying the hourly powercanal population by 0.17 (assumed mortality rate utilized since 2006),
6) sum the hourly mortalities to obtain total mortality rate

Table 6 provides the annual time series of population estimates; the 2014 estimate was 2,336,600, the third highest number of smolts over the 9-year time series.

Table 6. Total population estimates for Seton-Anderson sockeye smolts.

Year	Seton River (Night)	Seton River (Day)	Power Canal (Day + Night)	Total Smolt Pop
2014	583,800	163,900	1,588,900	2,336,600
2013	188,000	10,700	253,000	452,000
2012	1,550,000	1,662,000	2,851,000	6,100,000
2011	3,074,000	102,700	1,656,100	4,800,000
2010	237,300	117,500	54,800	174,600
2009	166,500	99,700	46,100	312,300
2008	106,500	19,000	417,700	543,200
2007	889,900	220,000	1.070,000	2,200,000
2006	618,500	160,000	990,000	1,800,000

Seton sockeye smolt populations displayed a density-dependent effect of population size on smolt growth (Figure 12). Similar density dependence has been demonstrated for sockeye smolts in other sockeye lakes including Quesnel and Shuswap (DFO unpublished), Babine (Johnson 1958), Owikeno (Ruggles 1966) and various Alaskan lakes (Kyle et al. 1997).

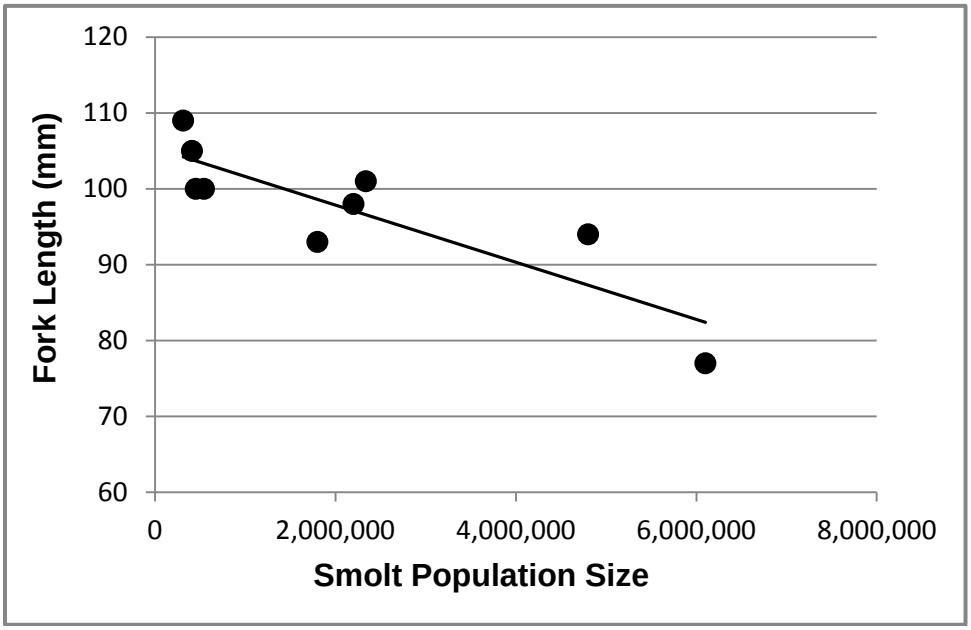

Figure 12. Smolt abundance vs. body size in the Seton River between 2006 - 2014.

2.2.6 Smolt Mortality

There was no need to estimate smolt mortality during 2014 as the Seton plant maintenance outage extended over the entire smolt migration period. Effectively there was no entrainment mortality. Table 7 provides the estimated mortality rate across years.

Table 7. Summary of estimated mortality rates for Seton-Anderson sockeye smolts, 2006 to 2014.

Study Year	Mortality Rate Estimate (%)
2014	0
2013	9.5
2012	8.0
2011	7.1
2010	4.0
2009	4.2
2008	13.5[1]
2007	-
2006	-

[1] Power canal sampling in 2008 precluded some plant shutdowns, contributing to a higher mortality estimate for that year.

3.0 Discussion and Recommendations

The Seton smolt monitoring program was implemented in 2014 for the 9th consecutive year. The primary purpose of the program is to monitor the effectiveness of smolt mortality mitigation via nightly plant shutdowns. The mortality target, as specified in the St'at'imc Hydro Agreement, is 5%. As shown in Table 6 this mortality rate has been exceeded in some years due to non-optimal nightly shutdown timing (i.e. 22:00 - 02:00) in relation to peak smolt migrations. During 2014, there was no entrainment mortality due to the maintenance shutdown that bracketed the smolt migration timing. It is recommended that future maintenance shutdowns be scheduled between April 20 - May 20 where practical as this timing would minimize turbine entrainment and would also protect daytime migrators when there are no shutdowns. Daytime migrations can be a significant component of seasonal migration in some years as occurred in 2012 when very high numbers of smolts migrated during daytime (Table 6).

During the smolt migration the Seton discharge was initially 38 cms and increased to 61 cms on May 22. In view of safety considerations the trap was adjusted for the higher flow by bringing it closer to shore where currents moderated. Under high flows it is recommended that a system be developed for hourly trap retrievals close to shore under reduced current velocities.

As in previous years, smolt emigration appeared to be triggered by increasing Seton River (and lake) temperatures in late April as the season progressed. Increasing photoperiod over this time period is another potential trigger for smolt emigration.

The smolt population size in 2014 was 2,336,600 which represents an intermediate level of abundance over the 9-year time series. The lowest population observed was 312,000 smolts in 2009 and the largest was 6,100,000 smolts in 2012. Smolts were average-sized in 2014 (mean fork length = 101 mm, standard deviation = 10). Taken together, these biological characteristics suggest that there will be a strong return of adult sockeye to the Seton system in 2016. This prediction doesn't distinguish between Gates Creek and Portage sockeye which have asynchronous cyclic dominance patterns. It is recommended that DNA sampling be undertaken on Seton River smolts in future to generate separate population estimates of these 2 distinct populations. Gates Creek sockeye comprise part of the Early Summer sockeye run to the Fraser, while Portage Creek sockeye are Late Run. It would be informative to enumerate the relative numbers of Gates and Portage smolts to determine whether there are downstream timing migration differences.

During 2014, daytime migrators comprised 13% of the total trap catches (Table 2). During the 2012 migration, the year when highest numbers of daytime migrators were observed, 48% of the trap catches occurred during daytime. In both years there was a seasonal time lag in outmigration behavior, with peak daytime migrations occurring about 1 week later than peak nighttime migrations (Figure 8). This pattern is also reflected in Figure 9.These observations suggest that the propensity of smolts to migrate during the daytime increases over the season due to physiological factors related to overall life cycle migration timing.

As in previous years, the greatest percentage (88%) of the 2014 nighttime migration occurred between the hours of 20:00 - 02:00. This pattern has been highly consistent between years (Figure 10) and verifies the effectiveness of the 20:00 - 02:00 plant closures.

The demonstration of density-dependent growth (Figure 12) for sockeye smolts in the Seton-Anderson system strongly suggests the operation of a within-lake growth and survival mechanism. The 2013 data point falls close to the trend line generated by the 9-year data set. In view of the prevailing fry migration pattern involving the rapid dispersal of Gates Creek fry into Seton Lake, this would be the likely habitat where mortality and growth mechanisms would likely operate. This question will be further addressed by BRGMON 6 during 2014. Marine survival of sockeye is related to smolt size; larger smolts survive better (Henderson and Cass 1991). During 2014, there was a medium-high density of average-sized smolts (mean fork length of 101 mm) while in other years e.g. 2012 there was a relatively high number of very small smolts (Figure 12). The marine survival consequences of the density-dependent growth patterns in freshwater could be an important component of sockeye production dynamics.

The objectives of the Computational Fluid Dynamics modeling study (Appendix 1) were to evaluate the hydraulics of the forebay and approach channel upstream of the SON facility during the period of operational shutdowns. The scope of the study included:

- Defining the flow scenarios during the nightly outages related to the smolt out-migration;
- Using computational fluid dynamics (CFD) models to characterize the velocity distribution in the SON forebays in the vicinity of the outlet structures; and,
- Identifying zones in the forebay that are of high risk for fish entrainment, and providing insight as to the effectiveness of nightly shutdowns at accommodating smolt outmigration

The following text has been abstracted from Appendix 1:

> *In evaluating the streamline diagrams presented in Appendix 1 (Figure 4) it is evident that in the high flow scenarios (Outage High Flow and Operational High Flow) the streamlines are parallel to one another, which indicates that walls do not have a substantial effect on the flow field in these high flow scenarios. During the low flow scenarios (Outage Low Flow and Operational Low Flow), where the total discharge through the facility is much lower, the streamlines become non-parallel as they exit the approach channel and enter the forebay in front of the dam. Under these scenarios the flow is more greatly impacted by the geometry of the forebay, and the flow may act in a direction that is not perpendicular to the dam face. It should be noted in the Idealised Outage scenario, which is a higher flow that these two lower flow scenarios, the streamlines still act in a manner similar to the two low flow scenarios. This is because, though the total non-power outlet discharge is greater than those of the low flow scenarios, the total discharge through the dam in this*

idealized scenario is much less than the two high flow scenarios where there is a substantial portion of the flow directed through the power canal.

In the Outage High Flow and Operational High Flow Scenarios where the power canal is active the flow accelerates as it enters the power canal due to a bottle-necking effect. This effect is localized and extends a few meters upstream of the dam face. When smolts encounter this zone, there would be a high probability of entrainment.

When the power canal is active, there is a strong flow field oriented near the right bank (looking downstream) that travels perpendicular to the dam face in the downstream direction. The magnitude of velocity in these conditions is highest (exceeding 1 m/s) within the approach channel, and exceeds 0.5 m/s at all distances upstream of the structure. Under these conditions there is a well established, slow moving, circulating eddy established, located near the left bank in front of the radial gate outlets. When the power canal is not active, the velocities in the forebay are greatly reduced. The direction of flow adjacent to the power canal outlets shifts by 90 degrees and is oriented parallel to the dam face, directing flow from the right to left bank, in the direction of the siphons. Under these scenarios, a low velocity zone is established at both the left and the right banks, however a strong circulation (or eddy) pattern is not established. In higher flow scenarios, when the power canal is not active, the peak velocity in the forebay is oriented towards the left bank, away from the power canal outlet. As out-migrating smolts will generally be attracted to higher velocities[4], this scenario is preferable for the night time outages. This will maximize the attraction of smolts to non-power outlets during the times of day that they are most active. In lower flow scenarios (where the power canal is not active) there may not be a substantial enough velocity gradient to guide fish towards these non-power outlets. Though the power house is not active in these scenarios, the power canal is not closed to fish access. In the absence of strong currents to guide fish towards the non-power outlets during the outage scenarios, smolts may still enter the power canal, and hold within the power canal until the outage timeframe has elapsed causing mortality.

The latter conclusion is an important one for BRGMON-13 to consider in future as the mitigation is predicated on the redirection of smolts away from the power canal and into bypass flow structures when shutdowns occur.

Preliminary evaluation of literature on sockeye smolt swimming behavior in relation to current flows is summarized in Appendix 1. Among other variables, the following parameters have been documented to influence salmon smolt swimming capacity in relation to entrainment:

- Swimming speeds
  - Burst
  - Critical
  - Sustained
- Orientation

[4] See Appendix 2

    - Lower critical swimming speed in darkness

- Physical characteristics affect fish swimming
    - Viscosity
    - Temperature

- Other factors
    - Temperature (15^{o}C is optimal for sockeye)
    - Size (manoeuvrability and speed)
    - Behavior
    - Physiological status (e.g. smolting)

- Salmon smolts approaching dams are generally surface oriented and follow flow

- Smolts typically become disoriented in dam forebays

To build on the monitoring approaches that have been adopted consistently since 2006, a program of acoustic tagging of sockeye smolts is recommended. This program would be undertaken on a trial basis in 2015 with a view towards documenting smolt vulnerability to entrainment under different operating conditions.

4.0 References

Groves, K.L., and P.S. Higgins. 1995. Seton Project: Overview study of downstream fish passage. BC Hydro Report No. H2768. WPR-259.

Henderson, M. A. and A. J. Cass.1991. Effect of smolt size on smolt-to-adult survival of Chilko Lake sockeye salmon (*Oncorhynchus nerka*). Can. J. Fish. Aquat. Sci. 48: 988-994.

Johnson, W.E. 1958. Density and distribution of young sockeye salmon *(Oncorhynchus nerka)* throughout a multibasin lake system. J. Fish. Res. Board Can. 15: 961-982.

Kyle, G.B., J.P. Koenings and J.A. Edmundson. 1997. An overview of Alaska lake-rearing salmon enhancement strategy: nutrient enrichment and juvenile stocking. Freshwaters of Alaska. Ecol. Studies 119: 205-227.

Levy, D.A. and C.C. Wood. 1992. Review of proposed mechanisms for sockeye salmon population cycles in the Fraser River. Bull. Math. Biol. 54: 241-261.

Levy, D.A., J. Sneep and S. Hall. 2008. Effectiveness of Seton Powerhouse shutdowns for reducing entrainment mortality of sockeye salmon smolts during 2008. Prepared for BC Hydro, Burnaby, BC.

Mundy, P.R. 1982. Computation of migratory timing statistics for adult Chinook salmon in the Yukon River, Alaska, and their relevance to fisheries management. N.Am.J.Fish.Mgmt. 4:359-370.

RL&L Environmental Services Ltd. 1999. Seton Dam fish diversion project, 1999 investigations and testing. Prepared for BC Hydro, Kamloops, BC.

Roos, J.F. 1991. Restoring Fraser River Salmon – a history of the International Pacific Salmon Fisheries Commission 1937-1985. Pacific Salmon Commission, Vancouver. 438p.

Ruggles, C.P. 1966. Juvenile sockeye studies in Owikeno Lake, British Columbia. Can. Fish Cult. 36: 3-22.

Sneep, J., S. Hall and LIllooet Tribal Council. 2012. Seton River sockeye smolt monitoring program: 2011 sampling results. Prep. for BC Hydro.

Appendix 1: Computational Fluid Dynamics Analysis
May 5, 2014

St'at'imc Eco-Resources
Box 2218
Lillooet, BC V0K 1V0

Attention: Bonnie Adolph, Project Coordinator

RE: Seton Dam Smolt Monitoring - Computational Fluid Dynamic Modeling

Dear Ms. Adolph,

It is my pleasure to provide you with the enclosed report on the computational fluid dynamics (CFD) study related to the Seton Dam Smolt Monitoring project.

St'at'imc Eco-Resources has retained the University of Alberta Department of Civil and Environmental Engineering (the Department) to complete a computational fluid dynamic (CFD) modeling study upstream of Seton dam (SON). This study investigates the hydraulics induced by the facility on the upstream forebay, approach channel and Seton Lake outlet. The current study specifically evaluates discharge scenarios that have been developed for the time frame in which there is a scheduled nightly outage to accommodate the out-migration of sockeye smolts. This occurs annually over a one-month period from April 20 – May 20.

This study was prepared exclusively for St'at'imc Eco-Resources. The quality of information, conclusions and estimates contained herein is consistent with the level of effort provided by the Department and are based on: i) information available at the time of preparation, ii) data supplied by outside sources, and iii) the assumptions, conditions and qualifications set forth in this report. This report is intended to be used St'at'imc Eco-Resources only. Any other use of, or reliance on, this report by any third party, without specific written authorization from the Department, is prohibited.

In reviewing these results, if there is anything that needs clarification, please let us know. You can reach me by email david.zhu@ualberta.ca or by telephone at 780-492-5813. Once again, thank you for the opportunity to be a part of this important project.

Yours truly,

David Z. Zhu, PhD, P.Eng.
University of Alberta – Department of Civil and Environmental Engineering

Enclosures

Seton Dam Smolt Monitoring - Computational Fluid Dynamic Modeling

Prepared for St'at'imc Eco-Resources

by

Mathew T. Langford, M.Eng., P.Eng.
Yu Qian, M.Sc.
David Z. Zhu, Ph.D., P.Eng.

University of Alberta
Department of Civil and Environmental Engineering
Edmonton, AB T6G 2W2

May 2014

1. Introduction

Background

The Seton Dam (SON) is a hydroelectric facility located on the Seton River operated by BC Hydro. The dam is located approximately 800 m downstream of the outlet of Seton Lake, west of the Town of Lillooet, BC. The dam is located just upstream of the confluence of the Seton River with the Fraser River. A site plan of the SON facility is included as Figure 1. The SON facility regulates outflow from Seton Lake, with the water surface elevation of the Lake remaining relatively constant over the course of the year. The Lake is regulated to geodetic elevations between 235.76 and 236.36 m. Under the approvals that are in place with the St'at'imc Nation, the reservoir may be drafted down to an elevation of 230.92 with notification in emergency scenarios (BC Hydro, 2011). For the purpose of the modelling exercise involved in this study, the reservoir level at SON was held consistent at 236.22 m, the average water surface elevation observed over the years 2004-2012.

The SON facility is composed of a 13.7 m tall concrete embankment that was constructed in 1956. The dam includes a number of outlets that transfer water to the Lower Seton River. The outlets of the SON facility include a fish water release gate, five siphons, a fish ladder, a radial gate and a power canal. The power canal conveys water approximately 3.7 km downstream to the SON generating station, just downstream of the confluence with the Fraser River. The discharge through the SON generating station travels solely through a single Francis-style turbine, with a generating capacity of 5- 48 MW. The CFD model that was developed for this study does not include the power canal downstream of the SON facility, nor the generating station.

The flow through the dam release and the power canal are combined, and assigned as the power canal inlet discharge for each model scenario. The maximum discharge capacity for each of the structures at the SON facility are as follows: fish water release gate at 14.1 m^3/s, five siphons at a combined 121.8 m^3/s, fish ladder at 1.3 m^3/s, radial gates at 247.7 m^3/s and power canal at 143.86 m^3/s (BC Hydro, 2011). In general the majority of discharge through the facility is through the power canal, with the radial gates being utilized infrequently. Also, generally siphon 1 (the south-most siphon) is used more frequently than the other four siphons. A minimum discharge of 5 m^3/s through outlets other than the power canal is required continually as an instream flow requirement for the Lower Seton River.

The Seton River system supports a diverse community of fish species including a number of anadromous salmonids. These fish species must be able to travel both downstream as well as upstream through the SON facility at different stages throughout their lifecycle. The SON facility has accommodated upstream fish passage with the inclusion of a fish ladder into the dam structure. Downstream fish passage is attained by passing fish to the Lower Seton River through non-power outlets, to minimize mortality through the generating station. The preliminary fish

entrainment risk assessment, which is a working document, has identified that the species of concern regarding fish entrainment including: Sockeye Salmon (*Oncorhynchus nerka*)(out-migrating smolts), Coho Salmon (*Oncorhynchus kisutch*)(out-migrating smolts), Chinook Salmon (*Oncorhynchus tshawytscha),* Pink Salmon (*Oncorhynchus gorbuscha),* Steelhead (*Oncorhynchus mykiss),* Rainbow Trout (*Oncorhynchus mykiss),* Gwenis and White Sturgeon (*Acipenser transmontanus)* (BC Hydro, In Draft). To accommodate the passage of out-migrating Sockeye salmon smolts, nightly powerhouse shutdowns during the period of April 20 - May 20 are used to limit the mortality, as smolts have been identified to most actively migrate during the night. The nightly shutdowns at the SON facility are scheduled to occur during the hours of 20:00 – 2:00 each evening during the outage period.

For the purpose of this report, the terminology “fish entrainment” will refer to any downstream passage of sockeye smolts into the facilities power canal. The normal lifecycles of anadromous fish upstream of dam must travel thorough the dam structure as smolt in order to migrate to the ocean. The method of passage through the dam structure (through a power or non-power intake) will affect the likelihood of mortality through the migratory obstacle. If fish are passed through and operational powerhouse, fish mortality can be caused by strong velocity shear, pressure gradient, turbulence, cavitation, direct impact of turbine blades, etc. (BC Hydro, 2006) and the impacts vary due to physical factors (turbine type and size, intake arrangement, discharge) and biological factors (fish size, swimming style, body orientation entering turbines, buoyancy) (Coutant and Whitney, 2000). High mortality rates can cause impacts to fish population conservation and recreational objectives. Previous work has been completed studying the use of physical, acoustic and lighting methods to repel fish from high risk zones (NPP, 2005). To ensure the efficiency of these operational devices, prediction of near intake velocity field upstream of the dam is necessary. Water velocity, temperature, depth, acceleration, etc. affects the habitat uses of fish species and their age classes. Hence, the upstream flow patterns at the facilities can provide valuable information on explaining fish movement.

CFD solvers have been used as a flow modeling tool for about a decade. Examples such as the CFD studies of the Wanapum dam (Meselhe and Odgaard, 1998), Dalles dam (Khan et al. 2004), Bonneville powerhouse (Rakowski et al., 2002), Howard Hanson dam (Wicklein et al., 2002), etc. are notable. In several occasions, CFD data was compared with physical model data and its reliability was ascertained (Meselhe and Odgaard, 1998). Previous studies including the collection of field data and CFD modeling have been completed at other BC Hydro site include Mica dam (Bhuyian and Zhu, 2007; Langford, et al. 2012(b)) Aberfeldie dam (Langford et al. 2012(a)), Hugh Keenleyside dam (Langford, et al. 2011), and the Seton, Carpenter and Downton Reservoirs (Langford et al. 2013). These studies integrated field observations with CFD modeling to predict and compare the hydraulics upstream of the facilities. The derived flow-field and habitat geometry was then used to identify the fish entrainment zone, and in estimating habitat displacement.

Objectives

The objectives of the current study are to evaluate the hydraulics of the forebay and approach channel upstream of the SON facility during the period of operational shutdowns. The information provided by this study, though not conclusive, does provide valuable information that St'at'imc Eco-Resources and BC Hydro can use to evaluate the effectiveness of the nightly outages on accommodating downstream sockeye smolt movement. The scope of this includes:

- Defining the flow scenarios during the nightly outages related to the smolt out-migration
- Using computational fluid dynamics (CFD) models to characterize the velocity distribution in the SON forebays in the vicinity of the outlet structures,
- Identifying zones in the forebay that are of high risk for fish entrainment, and providing insight as to the effectiveness of nightly shutdowns at accommodating out-migration.

2. Modeling Scenarios

Five operational scenarios were developed to be analyzed using the Seton forebay CFD model for the smolt monitoring program (see Table 1). These scenarios were developed based on the available historical data for the years 2006, 2007, 2008, 2012 and 2013. The data that was utilized is for the annual period of April 20 – May 20 inclusive, which are the scheduled dates for nightly shutdowns to mitigate smolt mortality through the generating station.

The "Outage" scenariors ("Outage High Flow" and "Outage Low Flow") were developed using the reported discharges for the hours 20:00 – 2:00 nightly. The "Operational" scenarios ("Operational High Flow" and "Operational Low Flow") were developed using the reported discharges for the hours 2:00-20:00 daily. In order to establish the high and low flows for each scenario the 90^{th} and 10^{th} percentile of the recorded discharges for each data set were used respectively.

As the discharge through other non-power outlets (Fish Water Release Gate, Radial Gate, Fish Ladder and Spawning Channel Siphons) do not fluctuate, the hourly data was interpolated from the daily data report by BC Hydro. The total discharge of the Non-power outlets is reported hourly by the downstream Water Survey of Canada Gauging Station (08ME003). The total discharge through the siphons is based on a mass balance, by subtracting the other non-power outlets from the total river discharge. In splitting the discharge between the siphons, BC Hydro's operational philosophy was followed, such that siphon 1 is opened first, followed by siphon 2. The maximum discharge of siphon 1 is 19.82 m^3/s, with the other four siphons being able to pass a maximum discharge of 25.48m^3/s.

It should be noted that though BC Hydro normally operates siphon 1 (and potential siphon 2 as well) during April and May, there are rare cases (2011 for example), where an alternate outlet has been used (siphon 3 in 2011). As there was not data available for 2011, this is not reflected in the scenarios that have been developed.

As normal operations over the years where records are available do not represent true outages (the timing generally does not strictly adhere to the scheduled 20:00 – 2:00 outages though outages do occur each evening), an idealized outage scenario was also included. The five scenarios that were evaluated in this study are outlines in Table 1 below. The discharge values indicated in this Table were included as mass flow rates for each of the respective outlet in the model setup.

Table 1 Seton Dam CFD Model Simulation Scenarios

Scenario	Power Canal (m^3/s)	FWRG (m^3/s)	Radial Gates (m^3/s)	Siphon 1 (m^3/s)	Siphon 2 (m^3/s)	Siphon 3 (m^3/s)	Siphon 4 (m^3/s)	Siphon 5 (m^3/s)	Fish Ladder (m^3/s)	Spawning Channel Siphons (m^3/s)
Outage High Flow	109.94	7.36	1.30	19.82	0.38	0.25	0.25	0.25	1.25	2.11
Outage Low Flow	0.00	3.71	0.00	14.90	0.00	0.00	0.00	0.00	1.18	2.11
Operational High Flow	112.92	7.36	1.30	19.82	0.38	0.27	0.27	0.27	1.25	2.11
Operational Low Flow	0.00	3.71	0.00	11.63	0.00	0.00	0.00	0.00	1.18	2.11
Idealised Outage (High Flow)	0.00	14.00	0.00	19.82	0.00	0.00	0.00	0.00	1.30	2.11

3. CFD Modeling

A CFD model has been developed for the Seton forebay, to assess the headpond hydraulics under varying operational conditions. The model that has been created for this study uses Ansys CFX version 14, a commercially available CFD solver (http://www.ansys.com/). This is a three-dimensional model which is able to assess the hydraulics across the entire headpond for the purpose of evaluating the potentially for smolt entrainment into the power canal at the SON facility.

Model Development

The CFD model that has been developed for SON extends from the dam face to 1 km upstream of the dock located at the Seton Lake outlet as shown on Figure 2. The models geometry (which also identifies the model domain) with bathymetry contours is presented in Figures 3. An unstructured tetrahedral mesh has been used in the numerical simulations. Local mesh refinements have been assigned near the outlets of each domain to refine the discretization and to resolve the small scale turbulent flows near the outlets with a high resolution. Coarser elements were

assigned for the rest of the domain. This resulted in 11.79 million nodes for the simulations of the SON forebay. The top wall of the model domain (water surface) was considered to have a free-slip boundary condition, which indicates that water flow is not influenced by the boundary, representing a free water surface. The other model boundaries are modeled as no slip walls, which indicate that water velocity is zero at each of these surfaces. A pressure regulated open boundary was modeled upstream. This boundary allows water inflow, and outflow from the model domain, much like an actual reservoir.

The model domain that was developed for the SON facility was based on the best available record information at the time of the study. This included the following information, provide by BC Hydro:

- Seton Lake bathymetry – pre flood contours
- Approach channel bed – 1955 contours
- Approach channel sides – 2010 lidar
- Approach channel, proximal to canal inlet – 1977 sounding data
- Radial gates, power canal inlet – BC hydro .dgn
- Siphons, fish water release gate, fish ladder – 1988 record drawings

It should be noted that the approach channel bed and Seton Lake bathymetry are based on relatively out-dated sources. As the approach channel is relatively shallow, the effects of the bed on the generated flow field are apparent. The uncertainty of the current bathymetry, and thus the model geometry in these locations should be taken into consideration when reviewing the results presented herein.

Governing Equations

The CFD solver solves the three dimensional Reynolds-Averaged Navier-Stokes equations, with the $k-\varepsilon$ turbulence model to assess the eddy viscosity. The governing equations are as follows (CFX, 2009),

$$\frac{\partial \rho}{\partial t}+\frac{\partial \rho u_j}{\partial x_j}=0$$

$$\frac{\partial \rho u_i}{\partial t}+\frac{\partial \rho u_j u_i}{\partial x_j}=-\frac{\partial p}{\partial x_i}+\frac{\partial}{\partial x_j}\left\{(\mu+\mu_t)\left(\frac{\partial u_i}{\partial x_j}+\frac{\partial u_j}{\partial x_i}\right)-\frac{2}{3}\rho k\delta_{ij}\right\}-(\rho-\rho_{ref})g_i$$

Equation 1

Where:

	ρ	is the density,
	k	is the turbulent kinetic energy,
	δ_{ij}	is the Kronecker delta,
	p	is the pressure,

μ is the molecular viscosity,

μ_t is the eddy viscosity, and

ρ_{ref} is the reference density.

To compute the eddy viscosity, the standard $k-\varepsilon$ turbulence model was used. The governing equations for the $k-\varepsilon$ turbulence model is,

$$\frac{\partial \rho k}{\partial t}+\frac{\partial \rho k u_j}{\partial x_j}=\frac{\partial}{\partial x_j}\left\{\left(\mu+\frac{\mu_t}{\sigma_k}\right)\frac{\partial k}{\partial x_j}\right\}+\mu_t\left(\frac{\partial u_i}{\partial x_j}+\frac{\partial u_j}{\partial x_i}\right)\frac{\partial u_i}{\partial x_j}-\rho\varepsilon$$

$$\frac{\partial \rho \varepsilon}{\partial t}+\frac{\partial \rho \varepsilon u_j}{\partial x_j}=\frac{\partial}{\partial x_j}\left\{\left(\mu+\frac{\mu_t}{\sigma_\varepsilon}\right)\frac{\partial \varepsilon}{\partial x_j}\right\}+C_1\frac{\varepsilon}{k}P_k-C_2\rho\frac{\varepsilon^2}{k}$$

$$\mu_t=\rho C_\mu\frac{k^2}{\varepsilon}$$

Equation 2

Standard values for the model constants were used, which are: C_1=1.44, $C_2=1.92$, $\sigma_k=1.0$, $\sigma_\varepsilon=1.3$, and $C_\mu=0.09$. At the no-slip wall, the CFX solver uses a no-flux boundary condition for the kinetic energy equation. For the dissipation (ε) equation, the following equation is used,

$$\varepsilon=\frac{\rho u^* C_\mu^{3/4}k^{3/2}}{\mu\kappa\tilde{y}^*}$$

Equation 3

Where: κ is the von-Karman constant,

$\tilde{y}^*$ is $\rho u^*\Delta y/\mu$ or 11.06, whichever is larger,

Where: Δy is the distance of the first grid point from the wall, and

u^* is computed by,

$$u^*=C_\mu^{1/4}k^{1/2}$$

Equation 4

4. Results and Discussions

The purpose of the CFD modeling exercise is to visualize the flow field induced upstream of the SON facility during both daytime (powerhouse operational) and nighttime outage (powerhouse not operational) conditions during the smolt out-

migration period. In order to visualize the flow field generated by the dam, a number of techniques were used including streamlines, vector plots and contours of velocity.

Streamlines provide an excellent visual depiction of the flow field in faster moving open channels. These plots can be used to identify the manner of which a particle will travel through a given flow domain (i.e. can be used to visualize the flow field in a Lagrangian framework). Streamlines were generated for SON under each of the dams operating scenarios showing flow paths through the approach channel and forebay. Figure 4 depicts the streamlines of the flow field approaching SON under each of the operational scenarios. The streamlines shown here are in three-dimensional space and track the location of 50 different discrete particles trajectories through the forebay. Though in some scenarios it appears that streamlines cross one another, there is no actual intersection in three-dimensions.

In evaluating the streamlines presented in Figure 4 it is evident that in the high flow scenarios (Outage High Flow and Operational High Flow) the streamlines are parallel to one another, which indicates that walls do not have a substantial effect on the flow field in these high flow scenarios. During the low flow scenarios (Outage Low Flow and Operational Low Flow), where the total discharge through the facility is much lower, the streamlines become non-parallel as they exit the approach channel and enter the forebay in front of the dam. Under these scenarios the flow is more greatly impacted by the geometry of the forebay, and the flow may act in a direction that is not perpendicular to the dam face. It should be noted in the Idealised Outage scenario, which is a higher flow that these two lower flow scenarios, the streamlines still act in a manner similar to the two low flow scenarios. This is because, though the total non-power outlet discharge is greater than those of the low flow scenarios, the total discharge through the dam in this idealized scenario is much less than the two high flow scenarios where there is a substantial portion of the flow directed through the power canal.

Vector plots depicting the velocity and direction of flow were generated for each of the operation scenarios. It should be noted that the vectors in these plots have been normalized and the length of the vector does not reflect the magnitude of the velocity at each point. Vector plots of the simulated hydraulics upstream of SON under each of the operational scenarios are included as Figure 5. These vector plots represent the velocity at a geodetic elevation of 235.00 m. Plan contours of velocity at the intakes elevation as well as profile contours for the SON canal intake and siphon 1 were generated as part of the current study. The purpose of depicting the velocity vectors and contours for the forebay in these areas is to provide insight to the actual velocity experienced by fish in these zones of the forebay. This also provides a visualization of the flow field in an Eulerian framework. It should be noted that all the velocity contours presented in this study depict the velocity magnitude, not the individual directional components of velocity. Plan contours of velocity magnitude at a geodetic elevation of 235.00 m are includes as Figure 6. Profile contours of the middle of the power canal (extending perpendicular from the dam face upstream) as

well as siphon 1 (extending perpendicular from the dam face upstream) are included as Figures 7 and 8 respectively.

The vector plot presented as Figure 5 provide information on the direction of flow in each of the operational scenario as well as the presence of slow moving recirculation zones. In the high flow scenarios (Outage High Flow and Operational High Flow), where there is a substantial amount of water traveling through the power canal outlet, higher velocity flows, oriented in a direction perpendicular to the power canal outlets are recognized against the right bank (facing downstream). A well developed, slow moving recirculation zone, or eddy, is established on the left bank in front of the dam's radial gates in these scenarios. This low velocity zone is present in the lower discharge scenarios (Outage Low Flow, Operational Low Flow and Idealised Low Flow), however the circulation eddy is less prominent. In these scenarios a low velocity eddy is also formed against the right bank which is similar in size. Flow adjacent to the power canal in these scenarios is parallel to the dam face proceeding in a direction from the right to the left bank, toward siphon 1.

The plan velocity contours included in Figure 6 of this report outline the change in velocity magnitude throughout the forebay area. The approach channel both widens and deepens as it enters the forebay of the dam (within 150 m of the dam face). In the high flow scenarios, the velocities are much high than the three lower flow scenarios. It is noted that in these scenarios, where the power canal is active, a high velocity zone oriented against the right bank, approaching the power canal exists. In these higher flow scenarios the velocity in the approach channel exceeds 1 m/s, and in the forebay, velocities exceeding 0.5 m/s exist at all distances upstream. Smolts that are located in these zones during higher flows (during the day, or during the outage timeframe if the 20:00 – 2:00 schedule is not maintained) are at risk of being entrained into the flow, or directed towards the power canal. In the low flow scenarios and the Idealised High Flow scenario, where the power canal is not active, the peak velocities are located towards the left side of the forebay instead of the right side. Though the velocity magnitudes are much lower than the power canal active (high flow) scenarios, substantial velocities may exist depending on the discharge through the fish water release gate. In the idealised High Flow scenario, velocities in the range of 0.2 m/s exist at all distances upstream of the intakes. Reducing flow through the power canal is effective at establishing higher velocities against the left (as opposed to right) bank which should attract fish towards non-power outlets and reduce mortality.

In evaluating the profile contours for the power canal (Figure 7) and the operational siphon (siphon 1, Figure 8), it is apparent that there is not significant variation in velocity at different depths. Generally the fishes orientation within the water column will affect the pressure forces experienced by the fish (due to hydrostatic pressure), however generally will not have a substantial impact on the velocities felt by the fish. As the power canal span the entire depth of the forebay there is little to no variation in velocity with depth in all scenarios. In the Outage High Flow and Operational High Flow Scenarios where the power canal is active the flow accelerates as it enters the

power canal due to a bottle-necking effect. This effect is localized and only extends a few metres upstream of the dam face. Upstream of this, velocity is uniform with depth. There is a localized zone (within approximately 5 m) of the siphons where there is some variation in velocity with depth as the siphons require the water to re-direct from a parallel to upward direction in this zone. Upstream of this the velocities are generally uniform with depth.

In order to evaluate how the velocity field develops as it approached the dam, cross-sectional velocity profile plots at various distances upstream of the dam face were included as well. This allows assessment of how the flow field changes as it opens from the downstream end of the approach channel into the forebay area in front of the SON structure. Figure 9 depicts the simulated cross-sectional velocity profiles for sections located 5 m, 25 m, 50 m, 100 m and 150 m upstream of the power canal for each of the modeled scenarios.

Looking at the velocity cross-sections of the forebay and approach channel at various distances upstream of the dam allows the ability to visualize how the flow field develops as it approaches the dam. Figure 9 shows the impact of operational scenario on this flow field development. It can be noted that the highest velocities will be experienced by surface oriented fish in each of the scenarios. The drag induced by the bed will provide lower velocities adjacent to the bed. As noted previous this zone is quite small, and generally the velocities are close to uniform with depth. At some locations in the forebay, surface oriented fish may be exposed to higher velocities than those oriented deeper in the water column. The highest velocities within the model domain are consistently noted within the approach channel, where the channel is narrower and shallower. When the power canal is active, the peak velocity at each cross section is generally oriented towards the right side of the forebay. This is shifted to the left side of the forebay when the power canal is not active. This is most noticeable in the Idealized Outage (High Flow) scenario. The increased total discharge in this scenario (compared to the Outage Low Flow and Operational Low Flow scenarios) facilitates the formation of a higher velocity zone on the left portion of the forebay. The high velocity should increase the attraction of fish to the non-power outlets in these scenarios. As noted previously, in the two high flow scenarios, maximum velocities exceeding 1 m/s existing in the approach channel and velocities exceeding 0.5 m/s exist at all cross-sections. In the low flow scenarios velocities exceeding 0.1 m/s only exist in the approach channel. The velocities at all sections within the forebay are less than 0.1 m/s. In the Idealised Outage scenario, velocities exceeding 0.2 m/s exist at all sections, with peak velocities of over 0.3 m/s simulated in the approach channel.

5. Conclusions

A computational fluid dynamics (CFD) modeling study was completed to evaluate the forebay hydraulics upstream of the Seton dam (SON) facility during the annual nightly outages to accommodate sockeye salmon smolt out-migration. The purpose

of the nightly outages, which are scheduled to occur between the hours of 20:00 and 2:00 for the month of April 20 to May 20, is to reduce smolt mortality during this key timeframe in their lifecycle.

In using CFD to simulate the flow field under varying operational conditions that occur over the course of these flow modifications, some analysis as to the effectiveness of outages at accommodating fish passage can be ascertained. A total of five operational scenarios were simulated using a numerical model to gain an understanding as to the effects of flow modification on the upstream hydraulics at SON.

When the power canal is active, there is a strong flow field oriented near the right bank (looking downstream) that travels perpendicular to the dam face in the downstream direction. The magnitude of velocity in these conditions is highest (exceeding 1 m/s) within the approach channel, and exceeds 0.5 m/s at all distances upstream of the structure. Under these conditions there is a well establish, slow moving, circulating eddy establish, located near the left bank in front of the radial gate outlets. When the power canal is not active, the velocities in the forebay are greatly reduced. The direction of flow adjacent to the power canal outlets shifts by 90 degrees and is oriented parallel to the dam face, directing flow from the right to left bank, in the direction of the siphons. Under these scenarios, a low velocity zone is established at both the left and the right banks, however a strong circulation (or eddy) pattern is not established. In higher flow scenarios, when the power canal is not active, the peak velocity in the forebay is oriented towards the left bank, away from the power canal outlet. As out-migrating smolts will generally be attracted to higher velocities, this scenarios is preferable for the night time outages. This will maximize the attraction of smolts to non-power outlets during the times of day that they are most active. In lower flow scenarios (where the power canal is not active) there may not be a substantial enough velocity gradient to guide fish towards these non-power outlets. Though the power house is not active in these scenarios, the power canal is not closed to fish access. In the absence of strong currents to guide fish towards the non-power outlets during the outage scenarios, smolts may still enter the power canal, and hold within the power canal until the outage timeframe has elapsed causing mortality. The velocity gradient threshold that effect smolt attraction is not evaluated in this study and should be assessed by a qualified fisheries biologist. Though some preliminary discussions as to impacts of varying flow field on smolt behaviour have been presented, these conclusions should be evaluated by a qualified fisheries biologist if they are to be used for decision making.

The modeling that is presented in this study has been completed using a CFD model that performs independent of mesh size (the mesh has been refined such that mesh size has no impact on the results of the simulations). The model has not been validated with field or laboratory measurements. If a field measurement program is eventually included as part of the smolt monitoring or fish entrainment strategies at Seton dam it is recommended that a comparison between the field measurements and the CFD model be completed to evaluate the effectiveness of the model. If

updated information regarding the bathymetry of the approach channel and forebay becomes available, it is recommended that the model domain be revised and the simulations revisited, especially if there is substantial variation from the historical data.

References

BC Hydro (In Draft), *Seton Lake Reservoir – Bridge River System Fish Entrainment Risk Screening,* BC Hydro.

BC Hydro (2006), *Fish Entrainment Risk Screening and Evaluation Methodology,* BC Hydro, Report No. E478.

BC Hydro (2011), *Bridge River Power Development Water Use Plan March 17, 2011* Revised for Acceptance for the Comptroller of Water Rights.

Bhuiyan, F., Zhu, D.Z., (2009), Computational Fluid Dynamics Modeling of Flow Pattern Induced by Hydropower Intakes in Revelstoke and Mica Dams – Prepared for BC Hydro.

CFX (2009), *ANSYS CFX Solver Theory Guide*, Release 12.0, ANSYS Inc., PA 15317.

Coutant, C.C., Whitney, R.R. (2000), *Fish Behaviour in Relation to Passage through Hydropower Turbines: A Review,* Transactions of the American Fisheries Society, 129:2, 351-380

EPRI (1992), *Fish Entrainment and Turbine Mortality Review and Guidelines.* Stone & Webster Environmental Service, Boston, Massachusetts.

Khan, L.A., Wicklein, E.A., Rashid, M., Ebner, L.L., and Richards, N.A., (2004),"Computational fluid dynamics modeling of turbine intake hydraulics at a hydropower plant", Journal of Hydraulic Research, 42(1), 61-69.

Langford, M.T., Baki, A.B.M.., Zhu. D.Z. (2013) *Bridge-Seton Fish Entrainment Strategy – Computational Fluid Dynamics Modeling of Seton Carpenter and Downton Reservoirs.*

Langford, M.T., Islam, M. R., Morrison, K., Zhu. D.Z. (2012(a)) *Aberfeldie Dam Fish Entrainment Hydraulics: Computational Fluid Dynamic Modeling and Field Study – Interim Report.*

Langford, M.T., Robertson, C.B., Islam, M.R., Zhu. D.Z. (2011) *Hugh Keenleyside Dam Fish Entrainment Hydraulics: Computational Fluid Dynamic Modeling and Field Study – Interim Report.*

Langford, M.T., Robertson, C.B., Zhu. D.Z. (2012(b)) *Mica Dam Fish Entrainment Hydraulics: Computational Fluid Dynamic Modeling and Field Study – Interim Report.*

Meselhe, E.A., and Odgaard, A.J.,(1998), "3D numerical flow model for fish diversion studies at Wanapum dam", Journal of Hydraulic Engineering, 124 (12), 1203-1214.

NPP (2005), Fish Entrainment and Mortality Study, Vol 1, Niagra Power Project, New York Power Authority.

Rakowski, C.L., Richmond, M.C., Serkowski, J.A., Ebner, L. (2002), *Three dimensional simulation of forebay and turbine intakes flows for the Bonneville project*, Proceedings of HydroVision 2002, Oregon.

RL&L (2000), Resident Fish Entrainment Information Review, RL&L Information Services Ltd.

Wicklein, E.A., Khan, L.A., Rashid, M., Deering, M.K., and Nece, R.E., (2002), *A three dimensional computational fluid dynamics model of the forebay of Howard Hanson dam*, Washington, Proceedings of Hydro Vision 2002, Portland, Oregon.

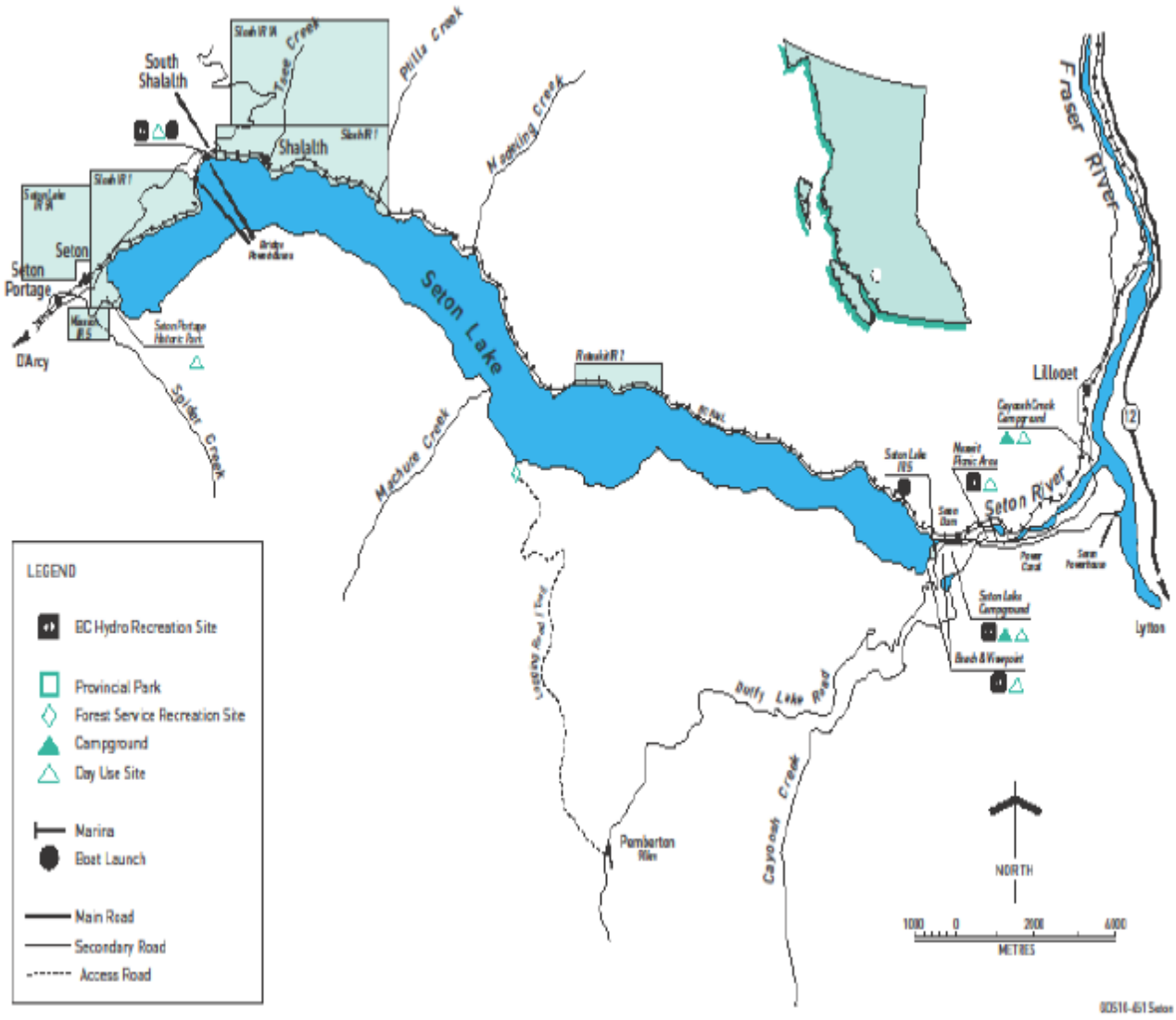

Figure 1 Seton Site Plan.

Figure 2 Seton Model Domain.

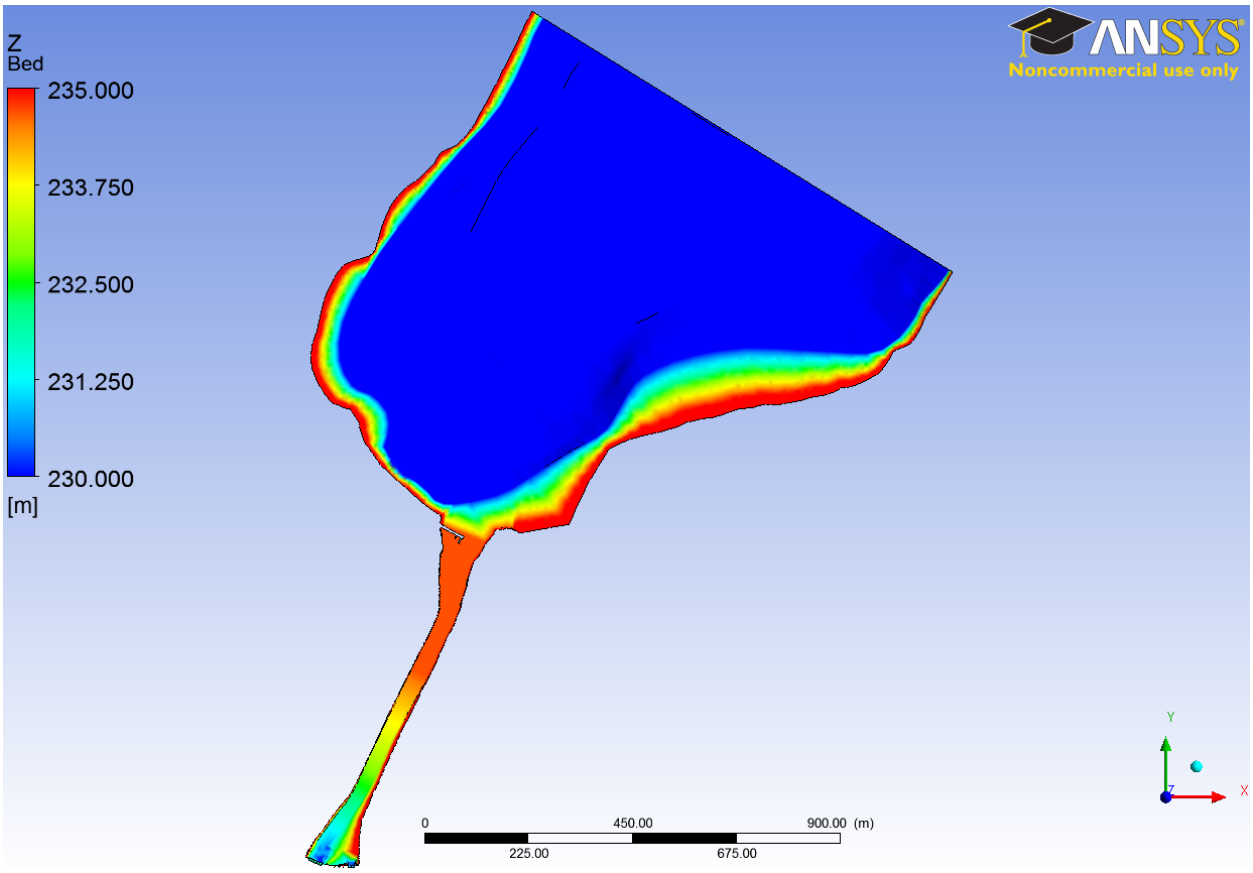

Figure 3 Seton CFD Model Geometry – Bathymetry Contours.

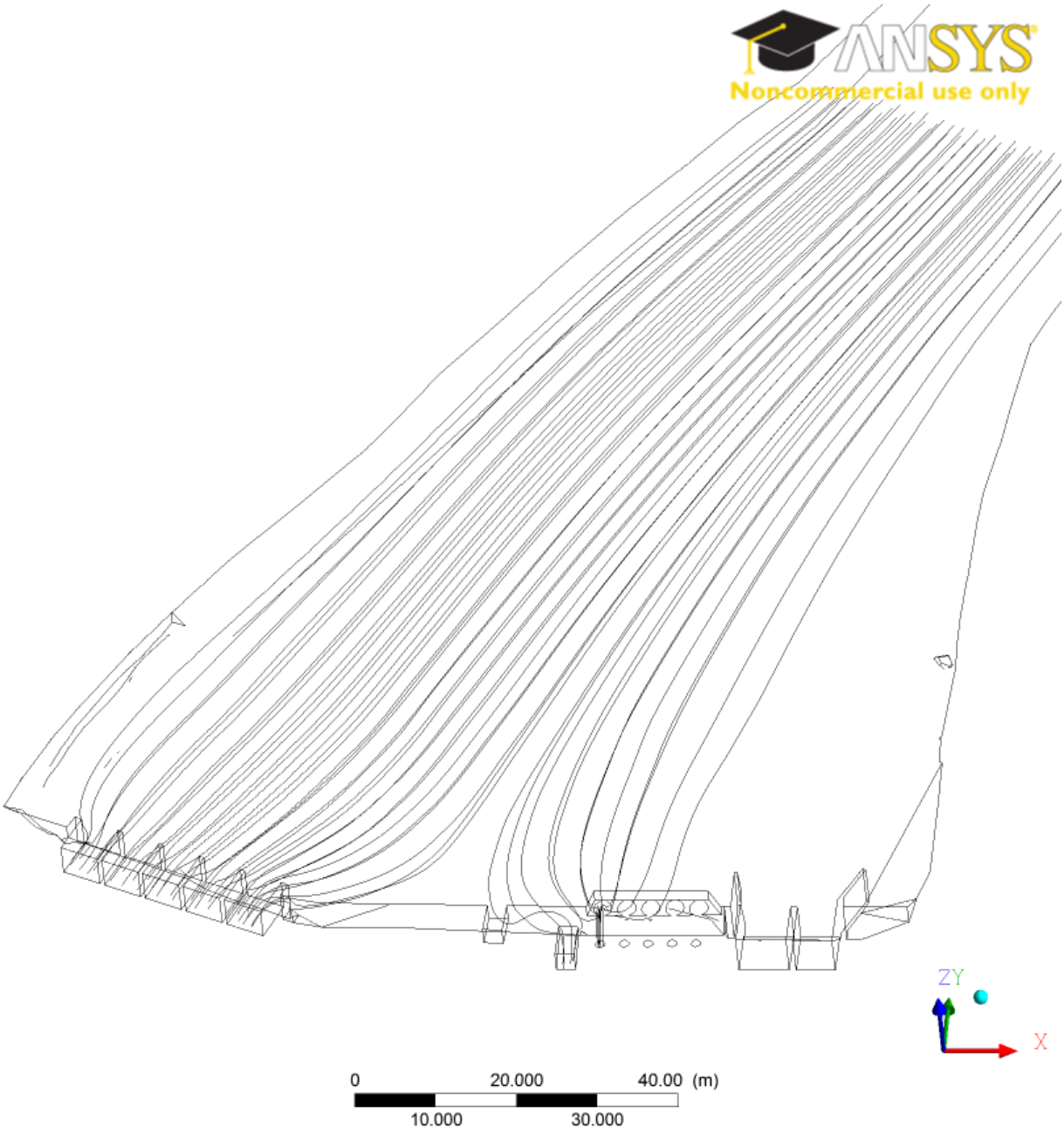

(a)

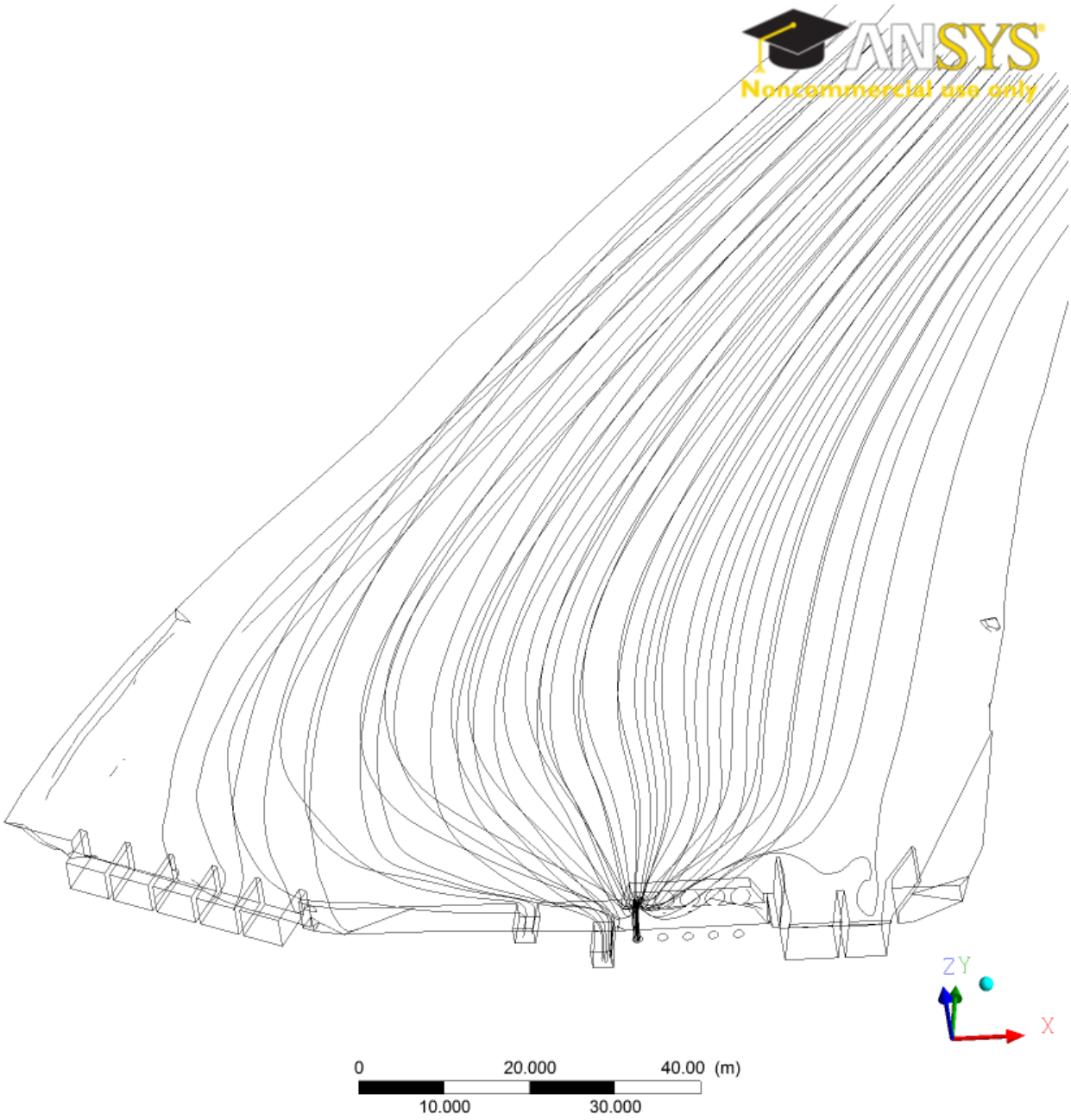

(b)

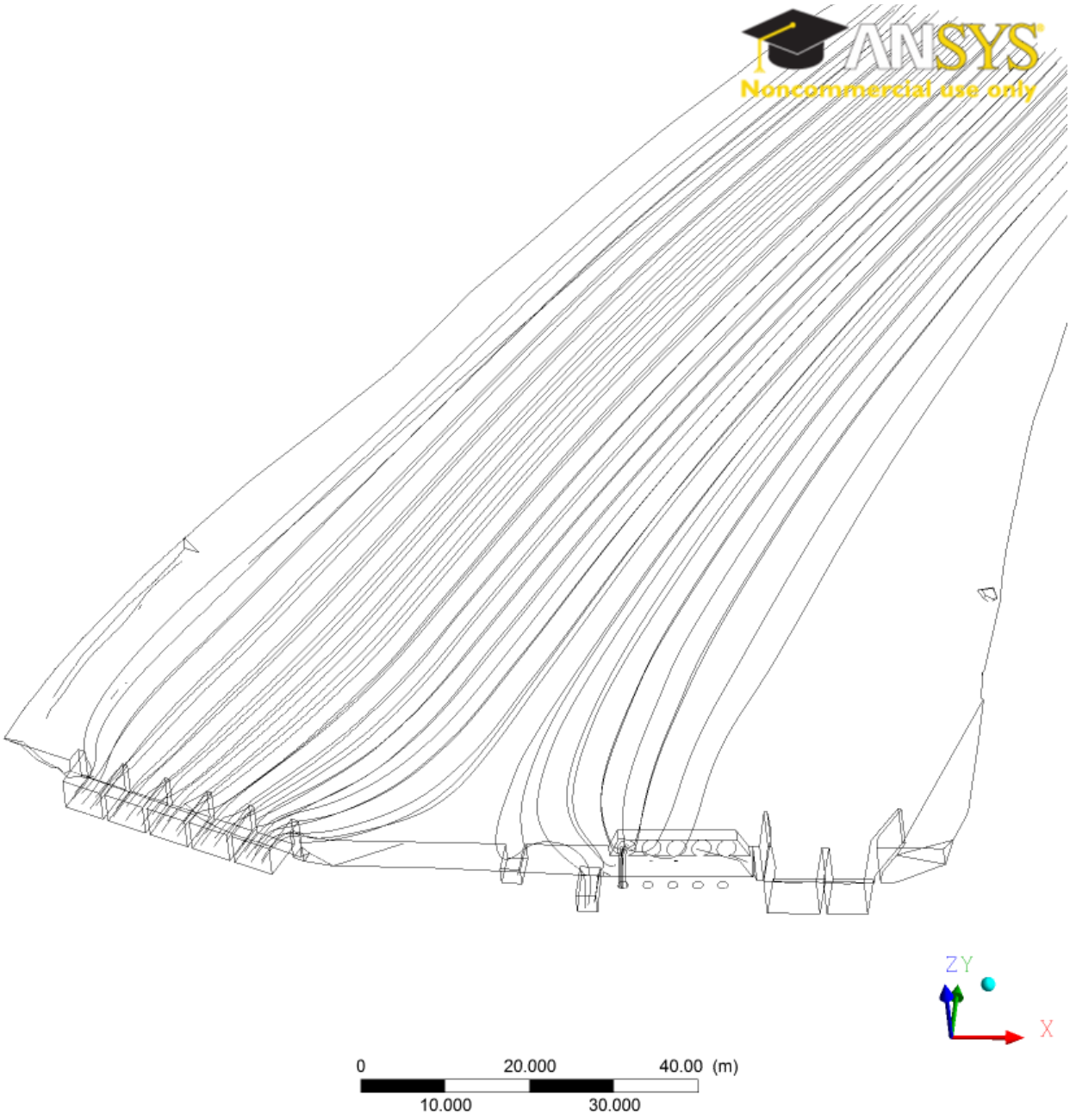

(c)

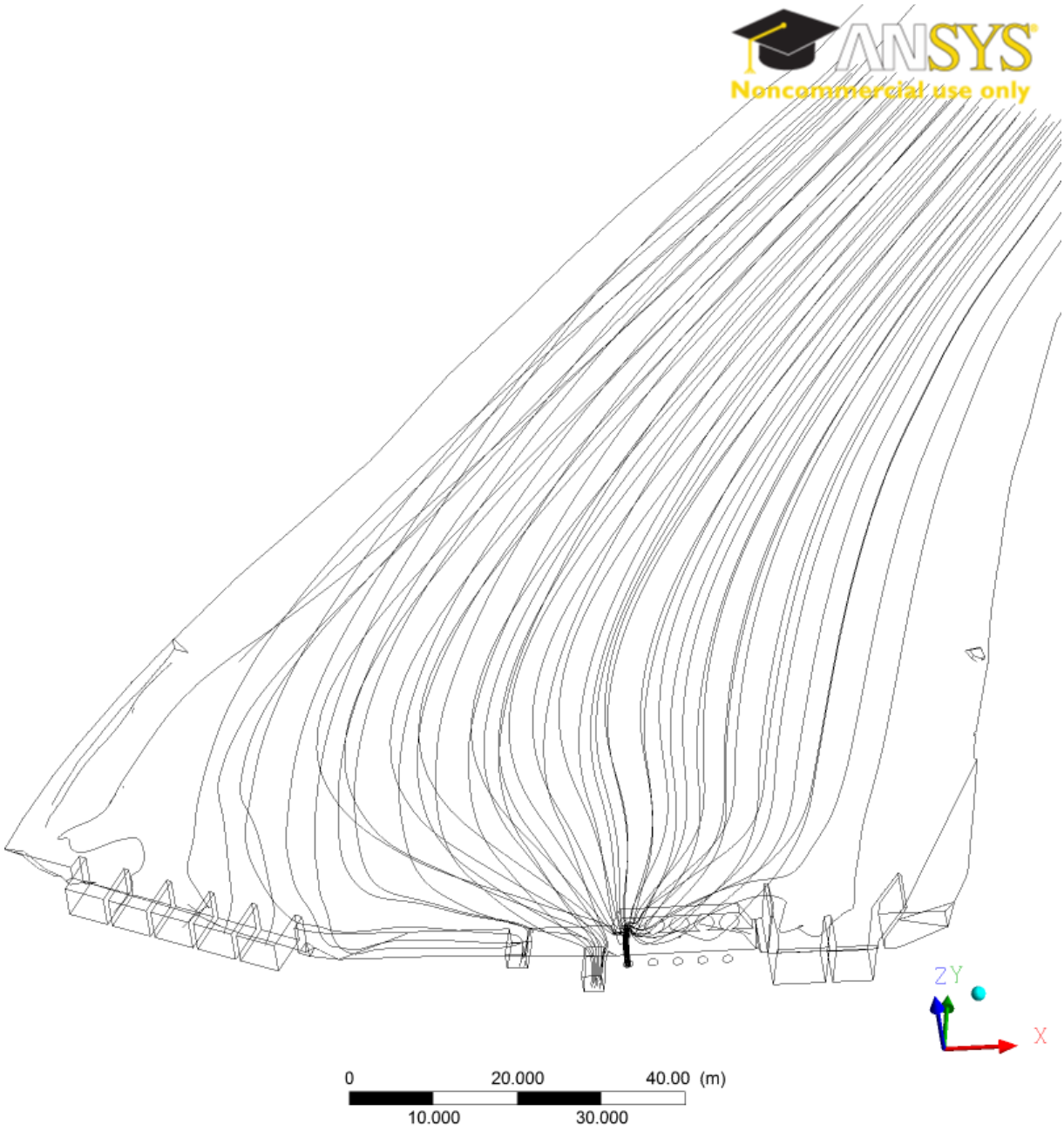

(d)

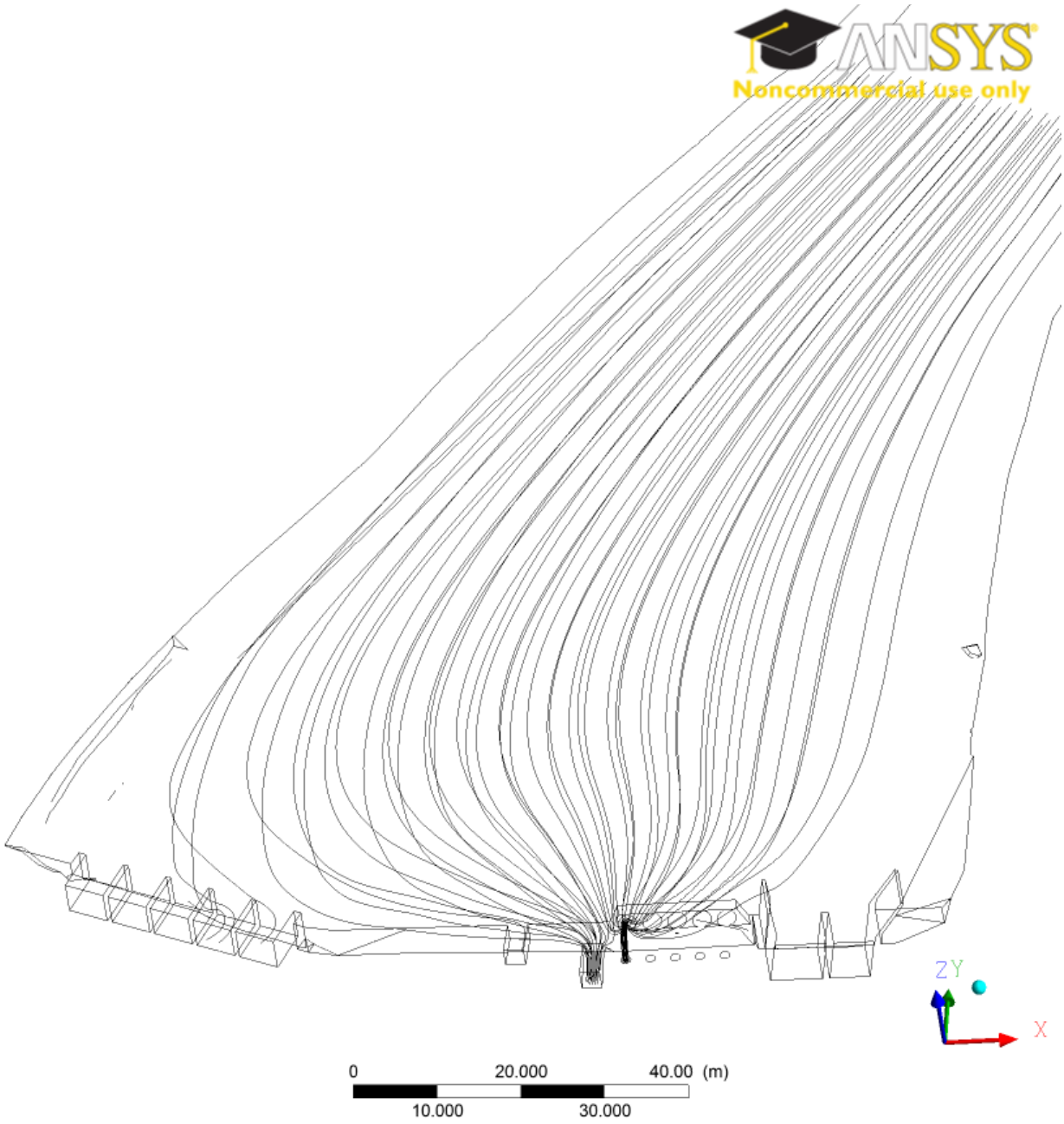

(e)

Figure 4 Seton Streamlines (a) Outage High Flow; (b) Outage Low Flow; (c) Operational High Flow; (d) Operational Low Flow; (e) Idealised Outage (High Flow).

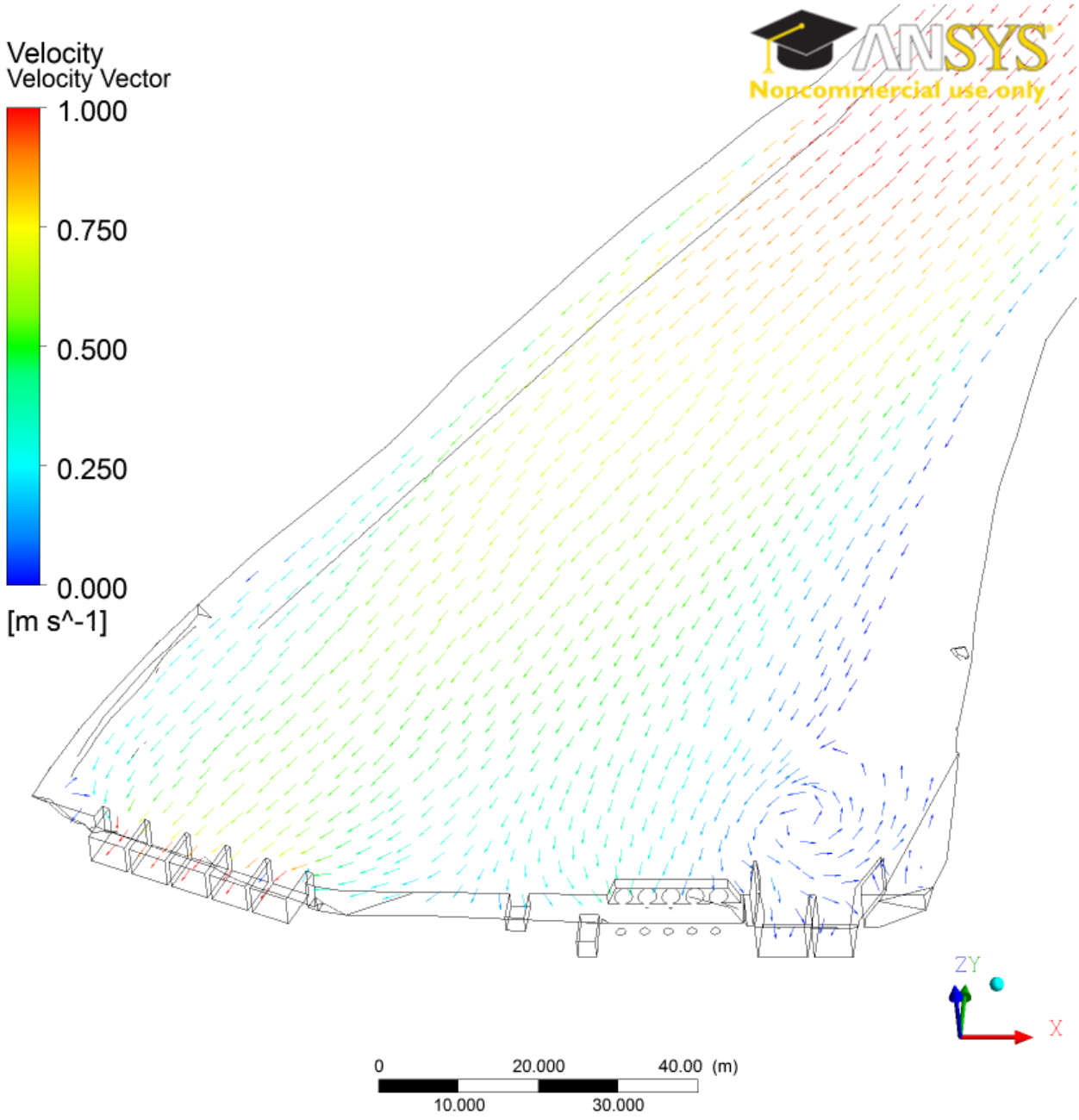
Velocity
Velocity Vector
1.000
0.750
0.500
0.250
0.000
[m s^-1]
ANSYS
Noncommercial use only
ZY
X
0
20.000
40.00 (m)
10.000
30.000

(a)

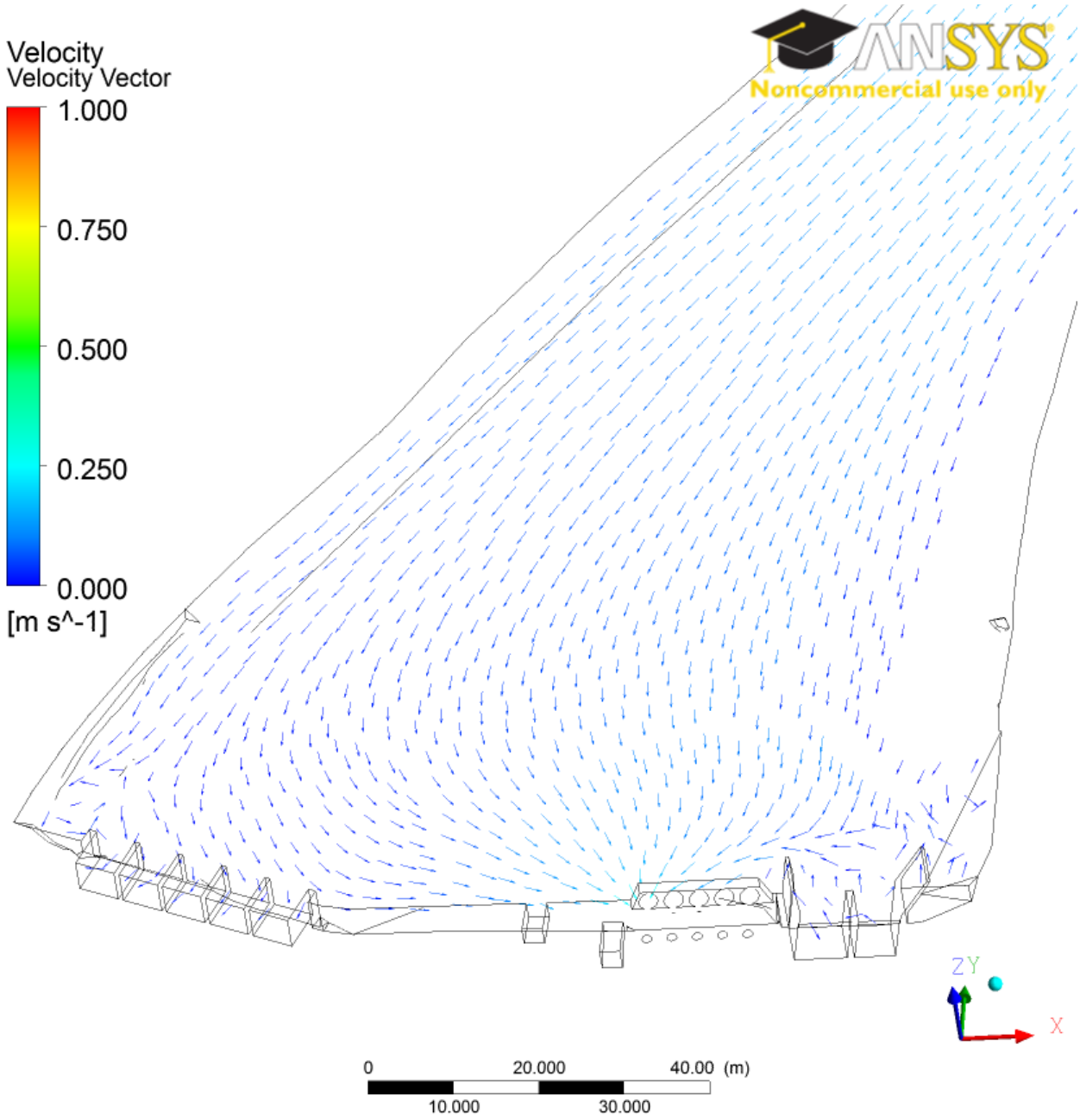
Velocity
Velocity Vector
1.000
0.750
0.500
0.250
0.000
[m s^-1]
ANSYS
Noncommercial use only
Z Y
X
0
20.000
40.00 (m)
10.000
30.000

(b)

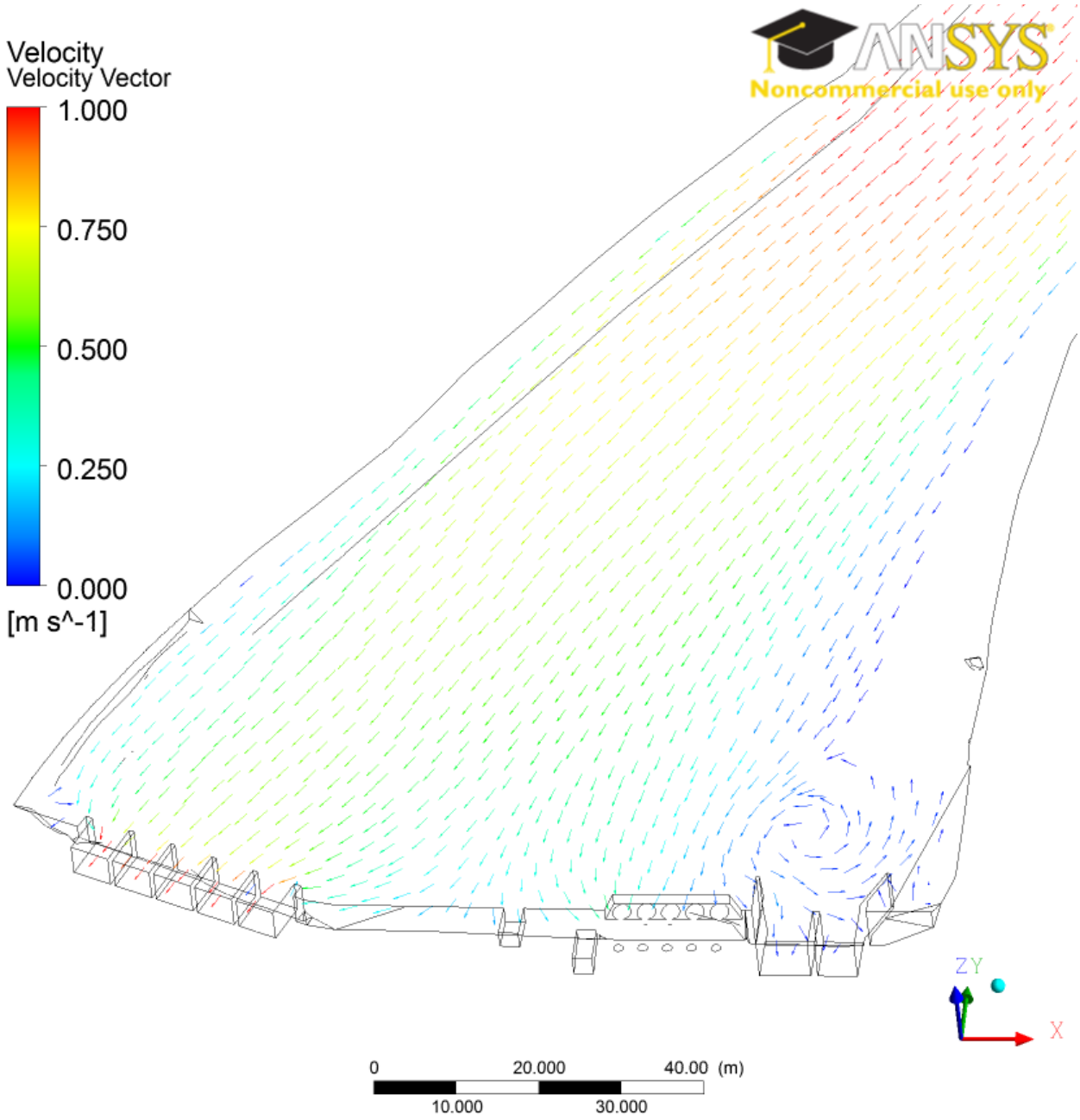
Velocity
Velocity Vector
1.000
0.750
0.500
0.250
0.000
[m s^-1]
ANSYS
Noncommercial use only
ZY
X
0
20.000
40.00 (m)
10.000
30.000

(c)

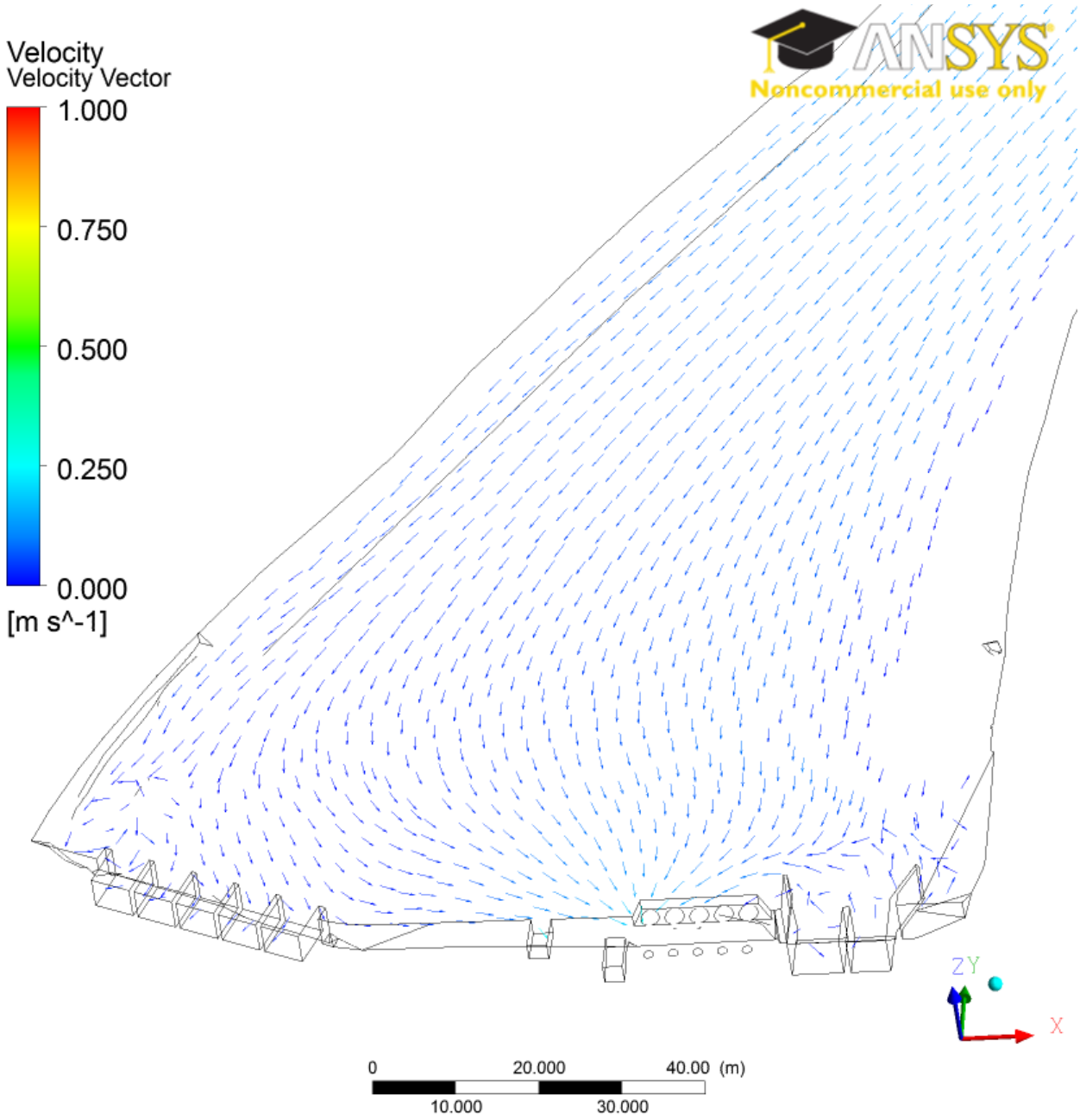
Velocity
Velocity Vector
1.000
0.750
0.500
0.250
0.000
[m s^-1]
ANSYS
Noncommercial use only
Z Y
X
0
20.000
40.00 (m)
10.000
30.000

(d)

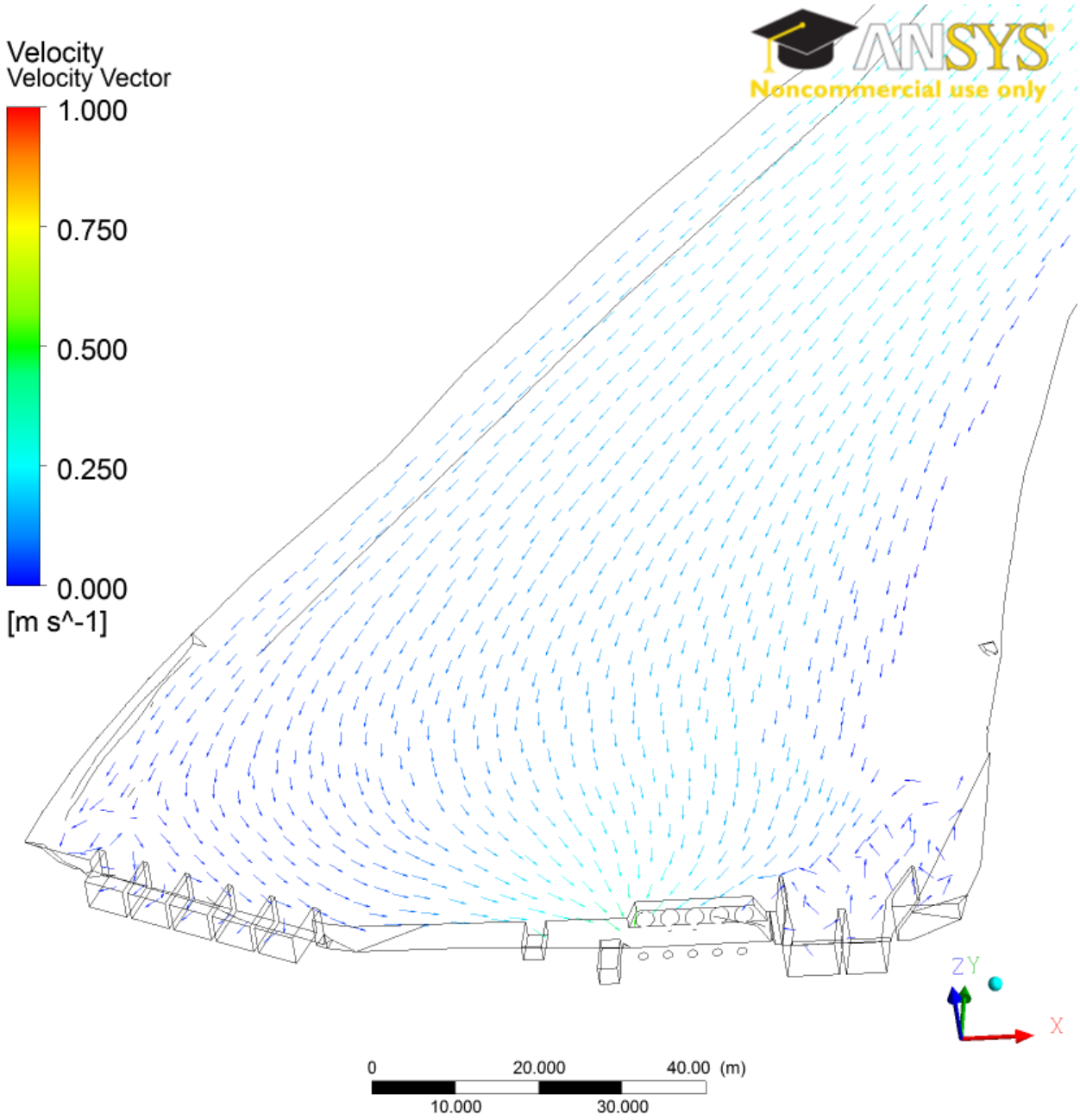

(e)

Figure 5 Seton Vector Plot at Elevation 235.00m (a) Outage High Flow; (b) Outage Low Flow; (c) Operational High Flow; (d) Operational Low Flow; (e) Idealised Outage (High Flow).

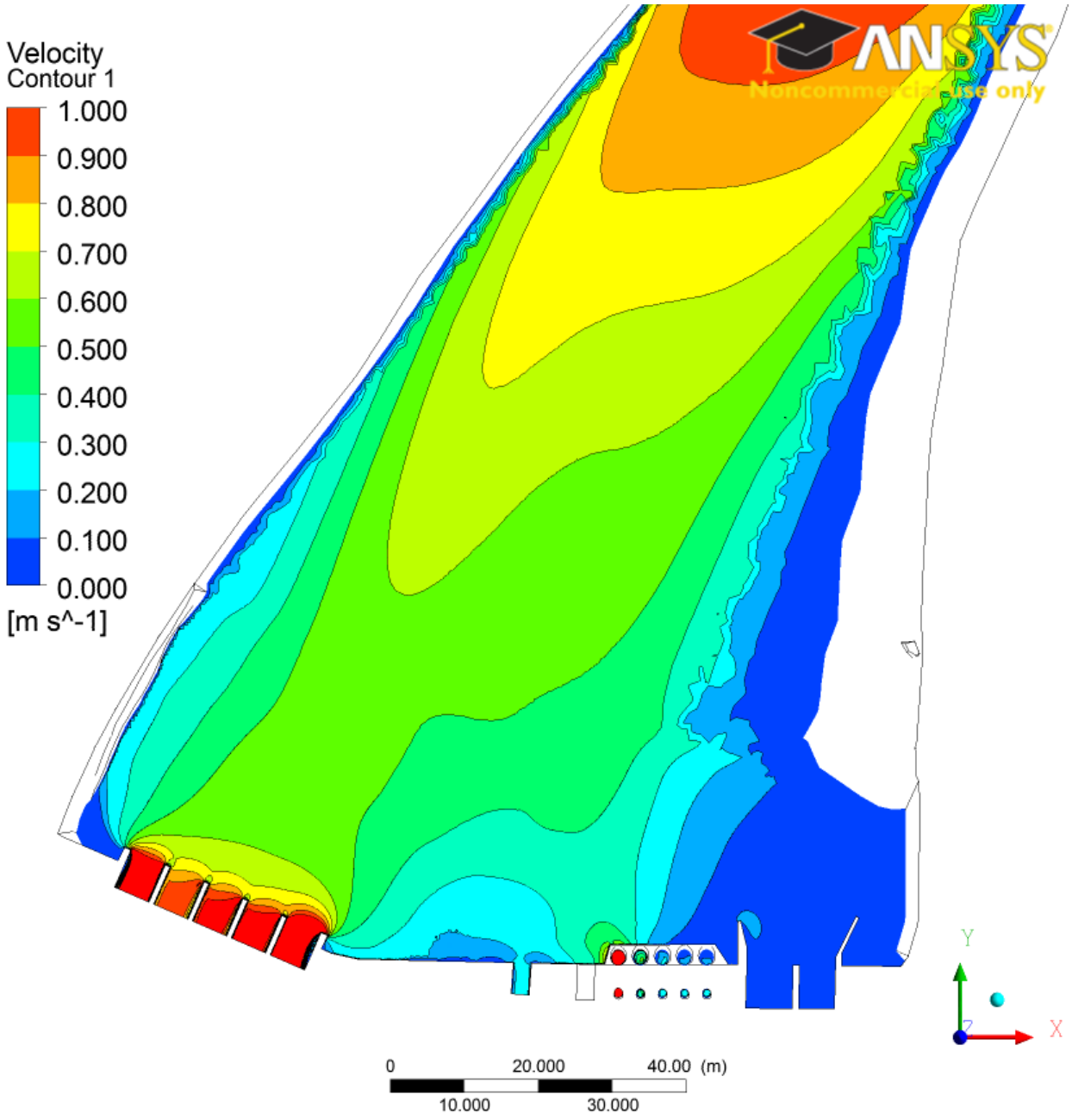
Velocity
Contour 1
1.000
0.900
0.800
0.700
0.600
0.500
0.400
0.300
0.200
0.100
0.000
[m s^-1]
ANSYS
Noncommercial use only
Y
X
Z
0
20.000
40.00 (m)
10.000
30.000

(a)

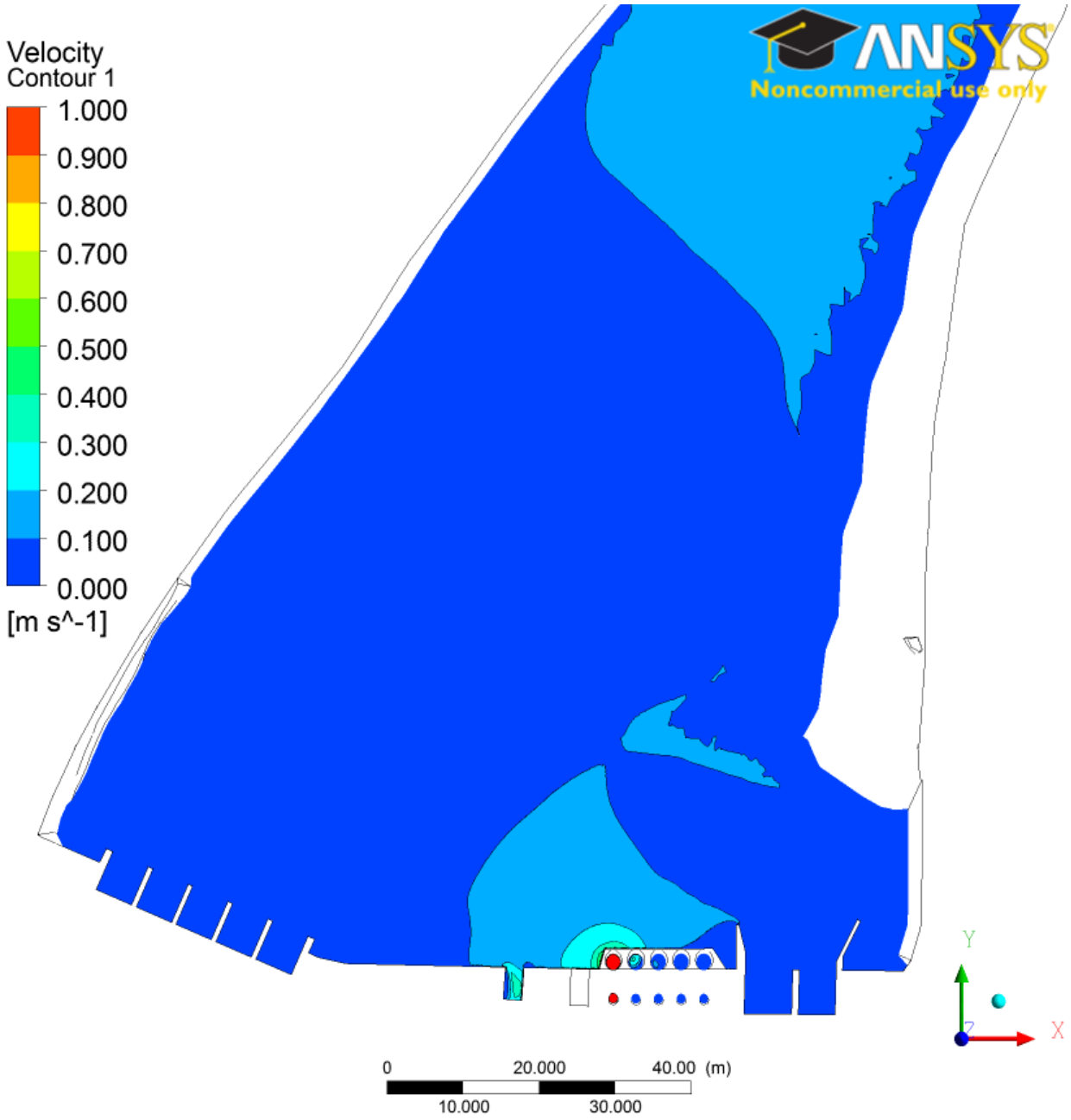
Velocity
Contour 1
1.000
0.900
0.800
0.700
0.600
0.500
0.400
0.300
0.200
0.100
0.000
[m s^-1]
ANSYS
Noncommercial use only
Y
Z
X
0
20.000
40.00 (m)
10.000
30.000

(b)

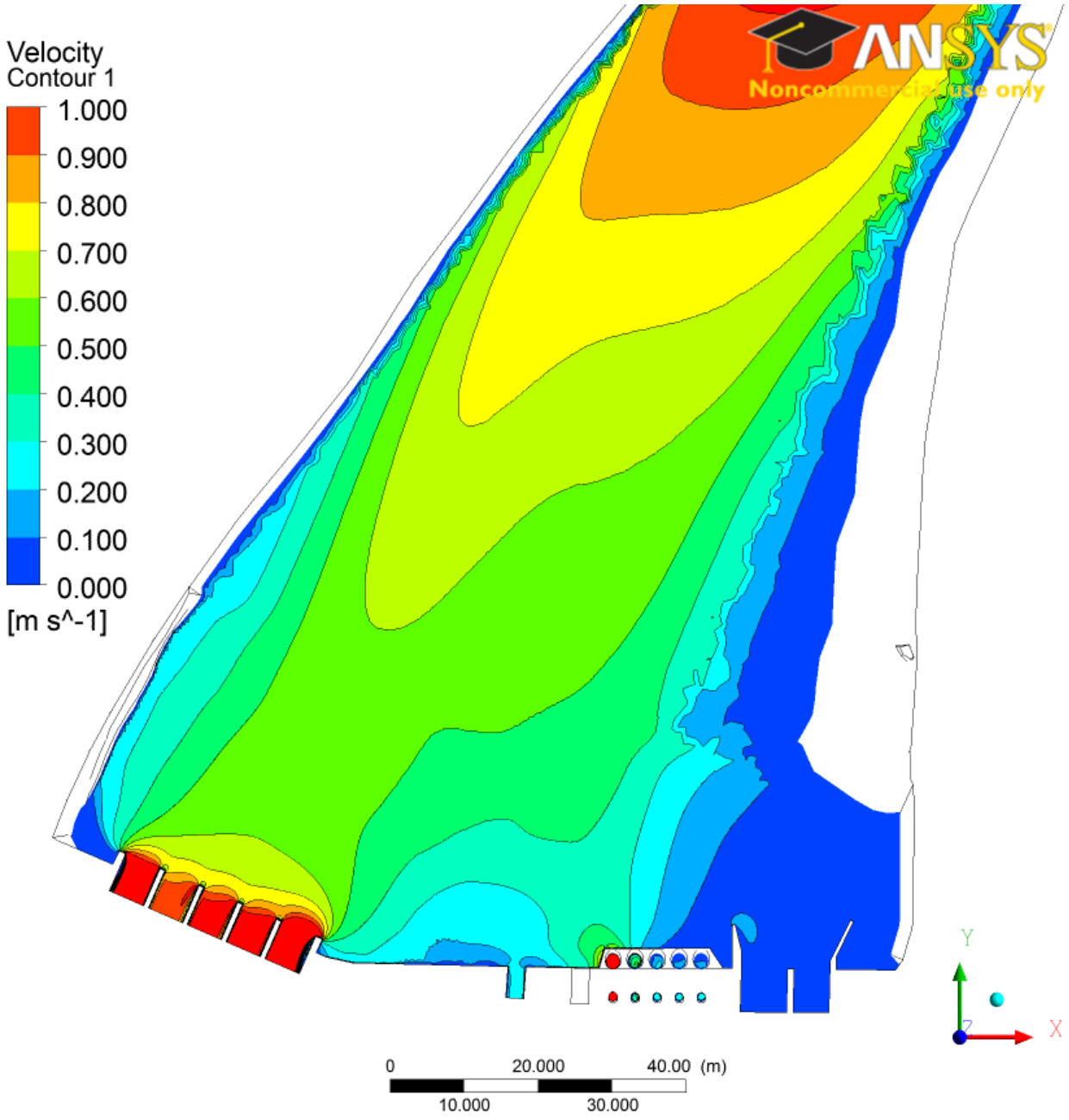
Velocity
Contour 1
1.000
0.900
0.800
0.700
0.600
0.500
0.400
0.300
0.200
0.100
0.000
[m s^-1]
ANSYS
Noncommercial use only
Y
Z
X
0
20.000
40.00 (m)
10.000
30.000

(c)

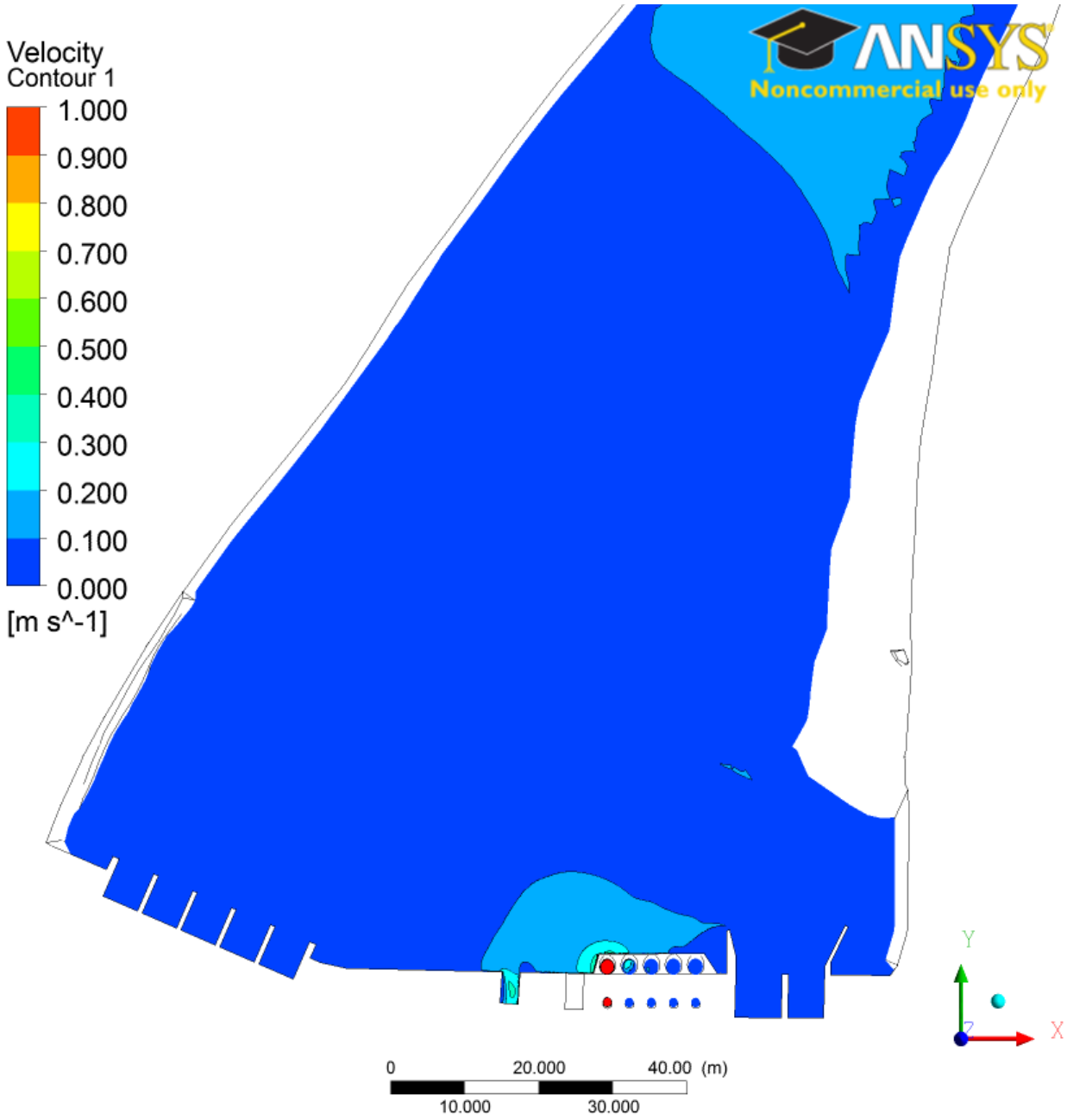
Velocity
Contour 1
1.000
0.900
0.800
0.700
0.600
0.500
0.400
0.300
0.200
0.100
0.000
[m s^-1]
ANSYS
Noncommercial use only
Y
Z
X
0
20.000
40.00 (m)
10.000
30.000

(d)

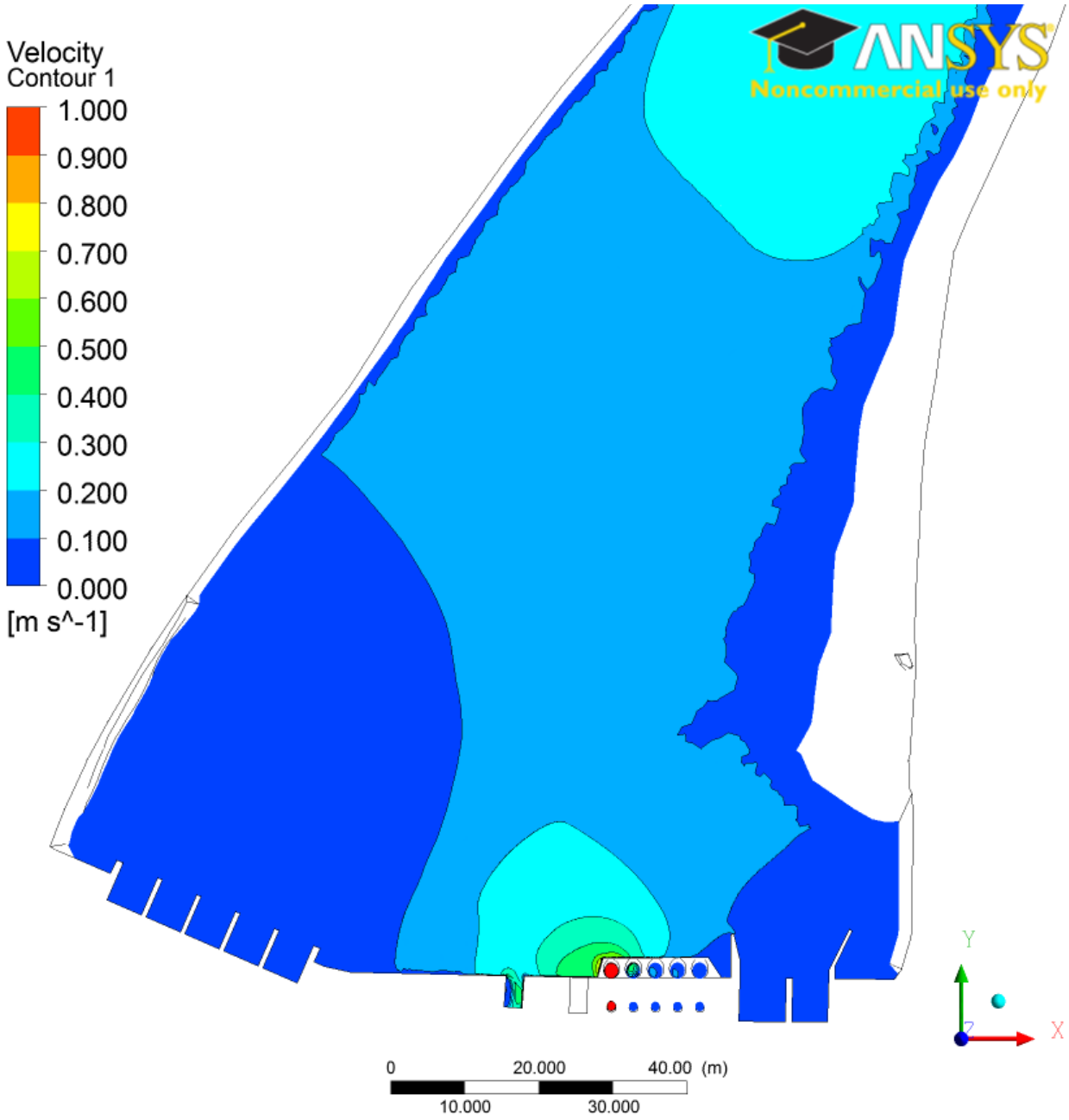

(e)

Figure 6 Seton Velocity Plan Contours at Elevation 235.00m (a) Outage High Flow; (b) Outage Low Flow; (c) Operational High Flow; (d) Operational Low Flow; (e) Idealised Outage (High Flow).

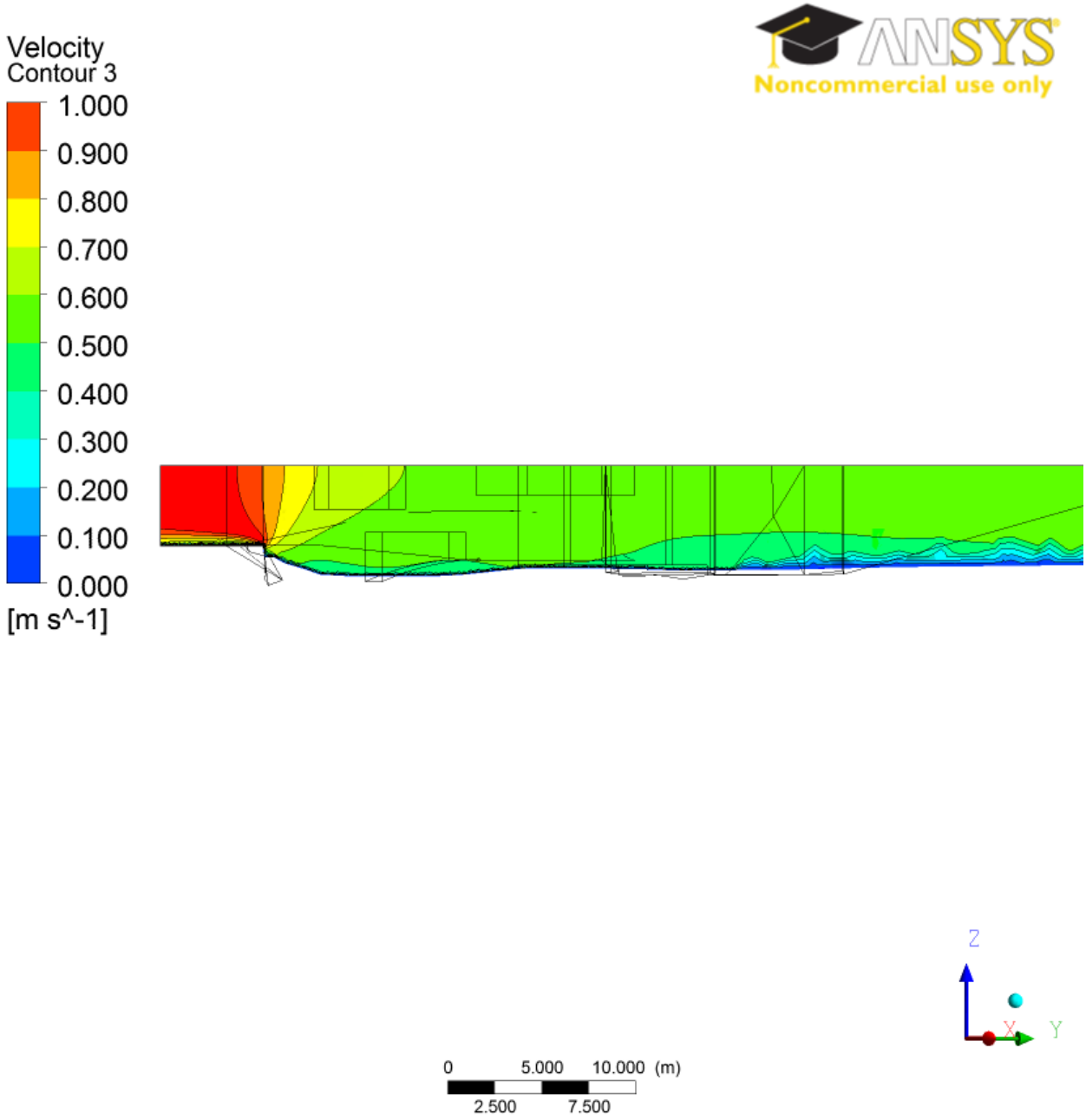
Velocity
Contour 3
1.000
0.900
0.800
0.700
0.600
0.500
0.400
0.300
0.200
0.100
0.000
[m s^-1]
ANSYS
Noncommercial use only
Z
Y
X
0
5.000
10.000 (m)
2.500
7.500

(a)

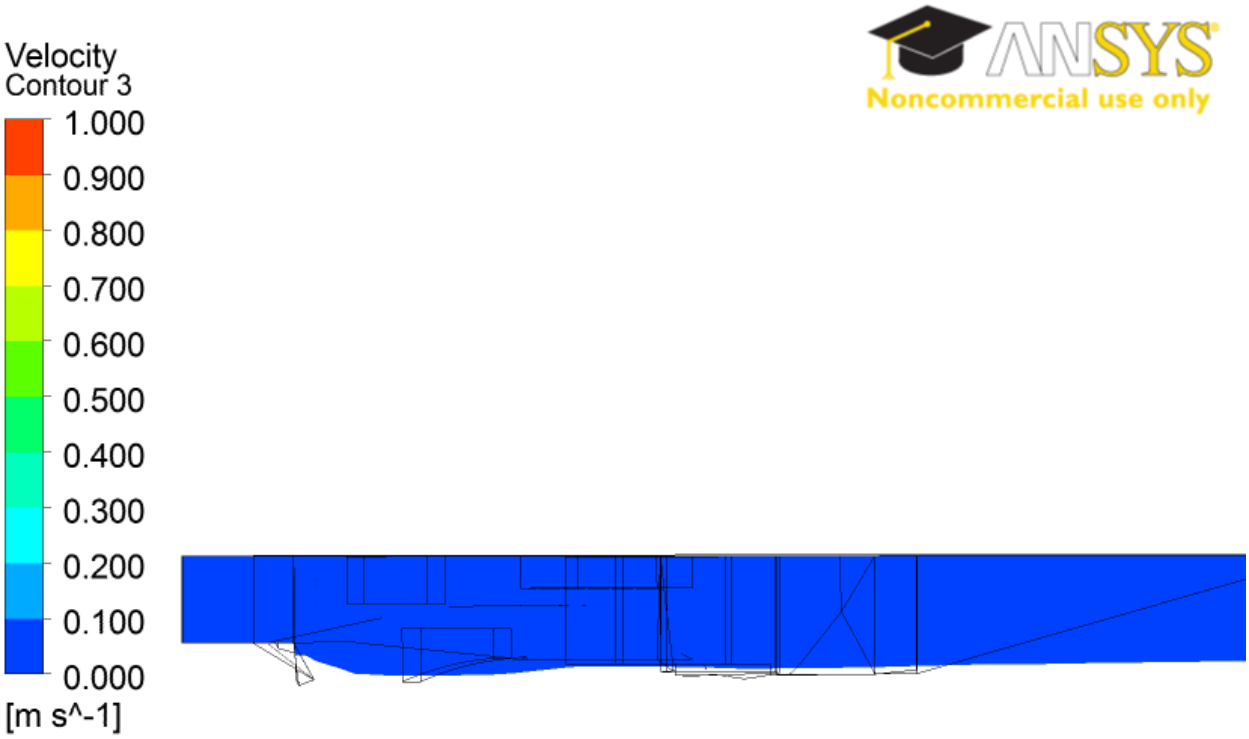
Velocity
Contour 3
1.000
0.900
0.800
0.700
0.600
0.500
0.400
0.300
0.200
0.100
0.000
[m s^-1]
ANSYS
Noncommercial use only

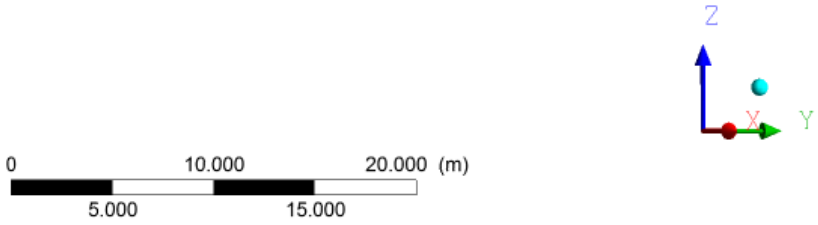
Z
Y
X
0
10.000
20.000 (m)
5.000
15.000

(b)

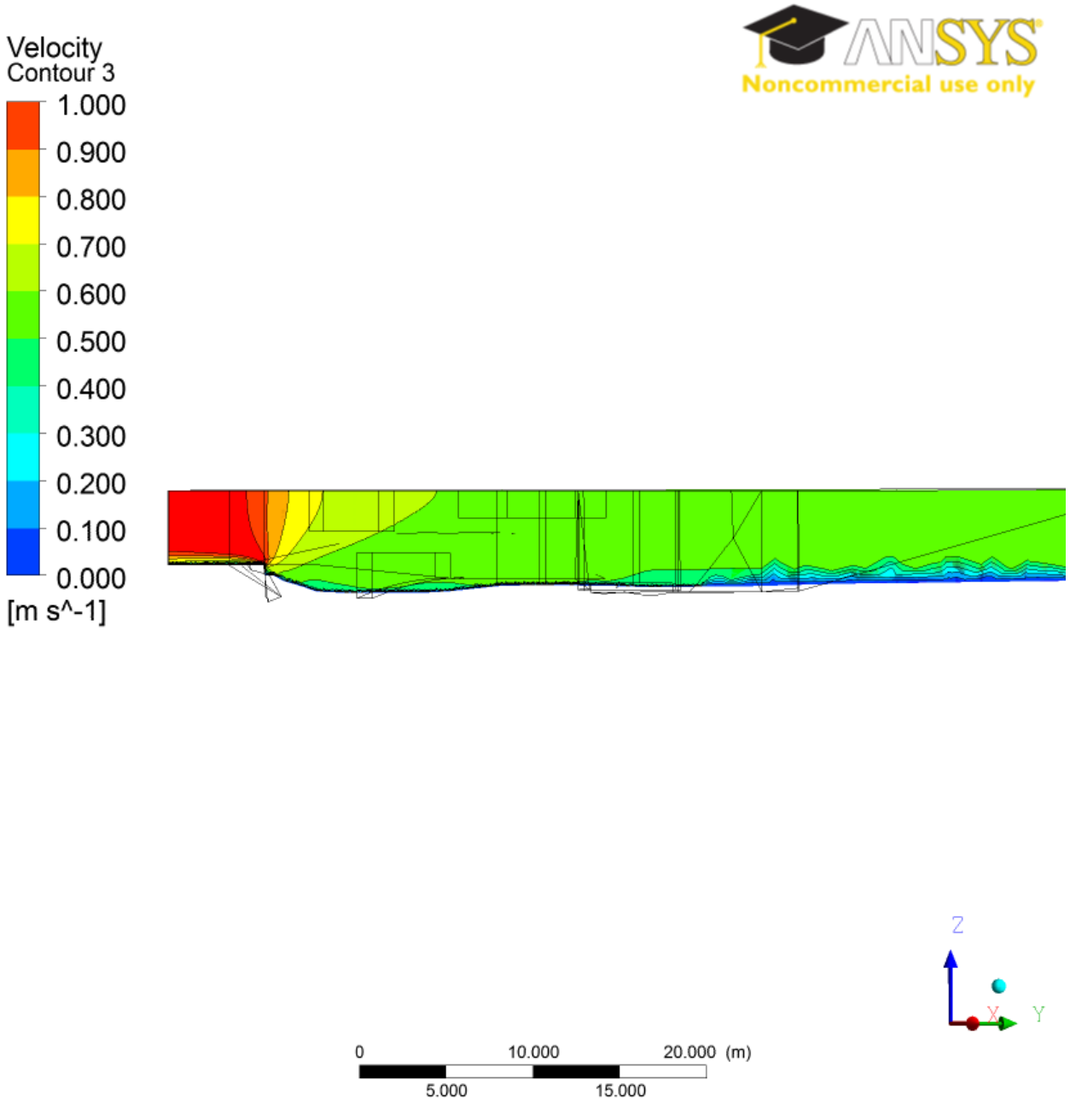
Velocity
Contour 3
1.000
0.900
0.800
0.700
0.600
0.500
0.400
0.300
0.200
0.100
0.000
[m s^-1]
ANSYS
Noncommercial use only
Z
X
Y
0
10.000
20.000 (m)
5.000
15.000

(c)

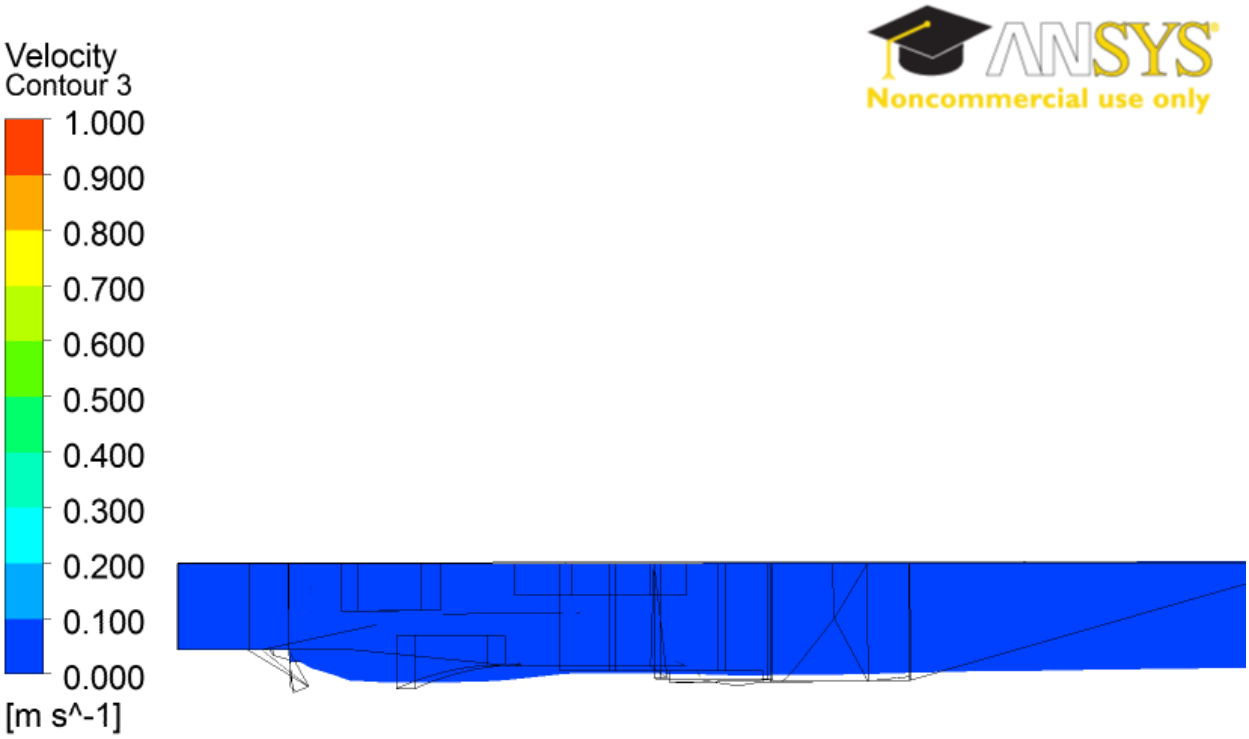
Velocity
Contour 3
1.000
0.900
0.800
0.700
0.600
0.500
0.400
0.300
0.200
0.100
0.000
[m s^-1]
ANSYS
Noncommercial use only

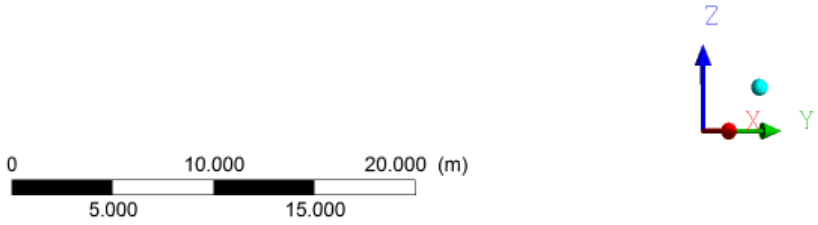
Z
X
Y
0
10.000
20.000 (m)
5.000
15.000

(d)

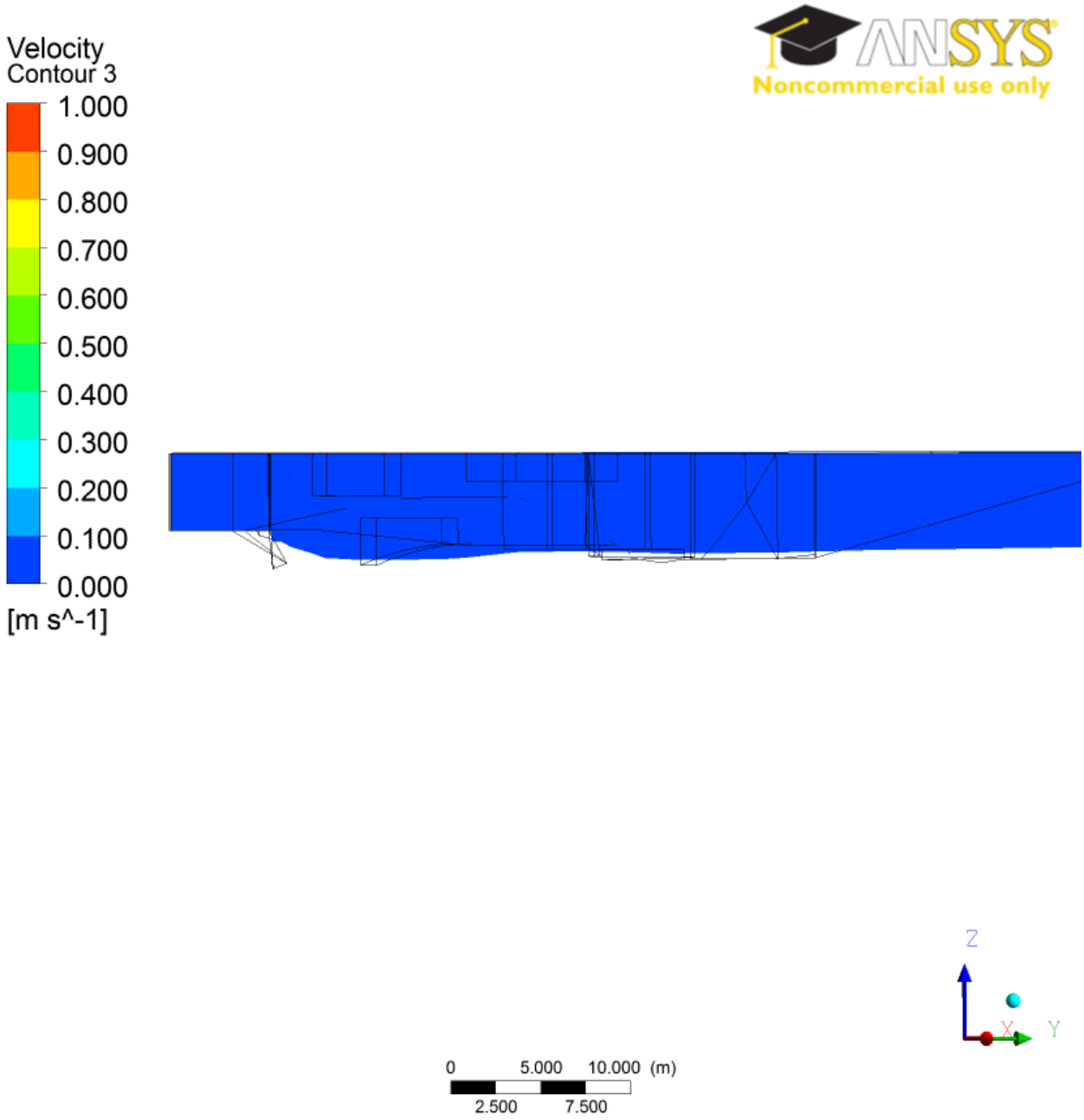

(e)

Figure 7 Seton Canal Inlet Velocity Profile Contours (a): Outage High Flow; (b): Outage Low Flow; (c): Operational High Flow; (d): Operational Low Flow; (e): Idealised Outage (High Flow).

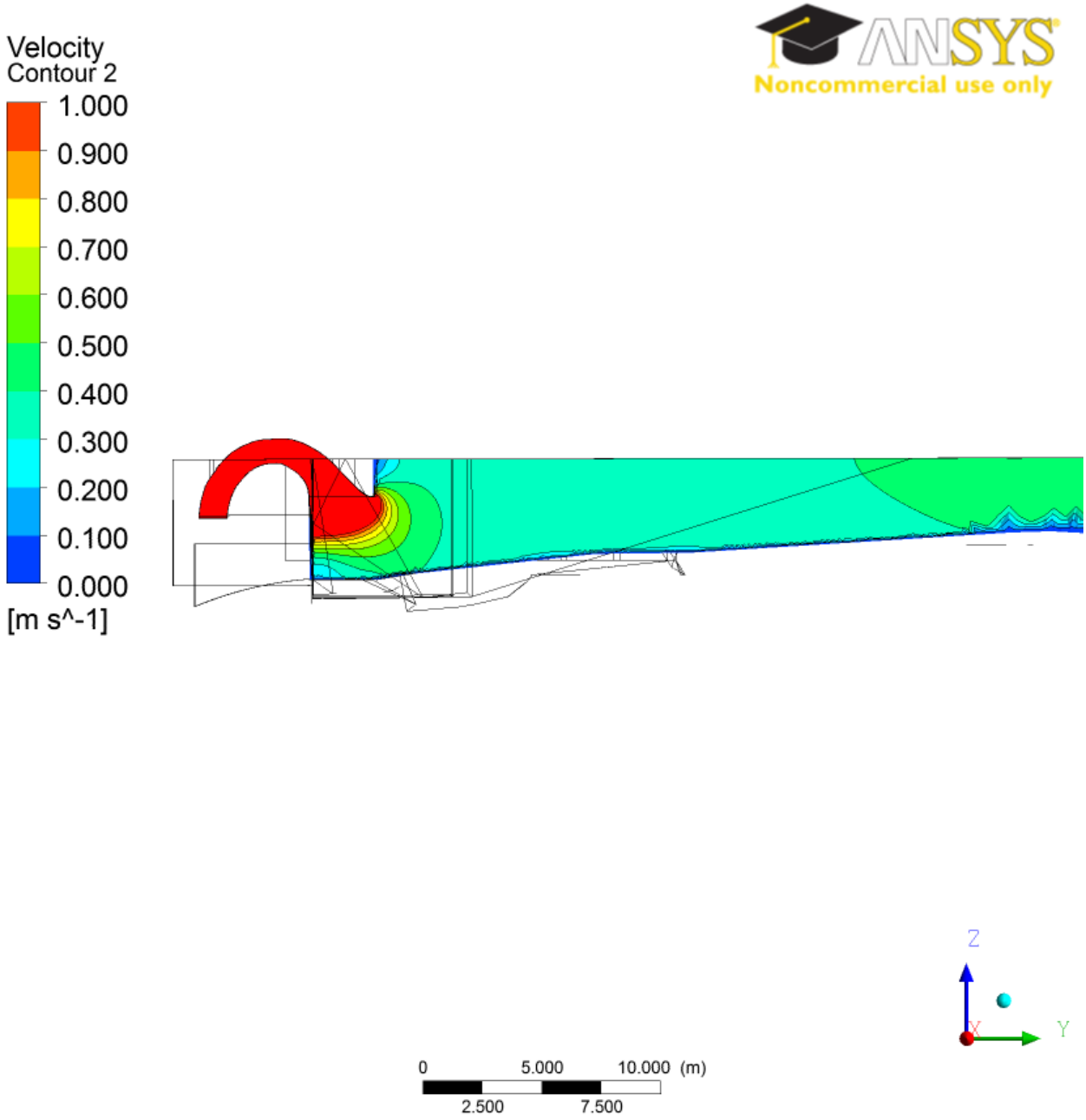
Velocity
Contour 2
1.000
0.900
0.800
0.700
0.600
0.500
0.400
0.300
0.200
0.100
0.000
[m s^-1]
ANSYS
Noncommercial use only
Z
Y
X
0
5.000
10.000 (m)
2.500
7.500

(a)

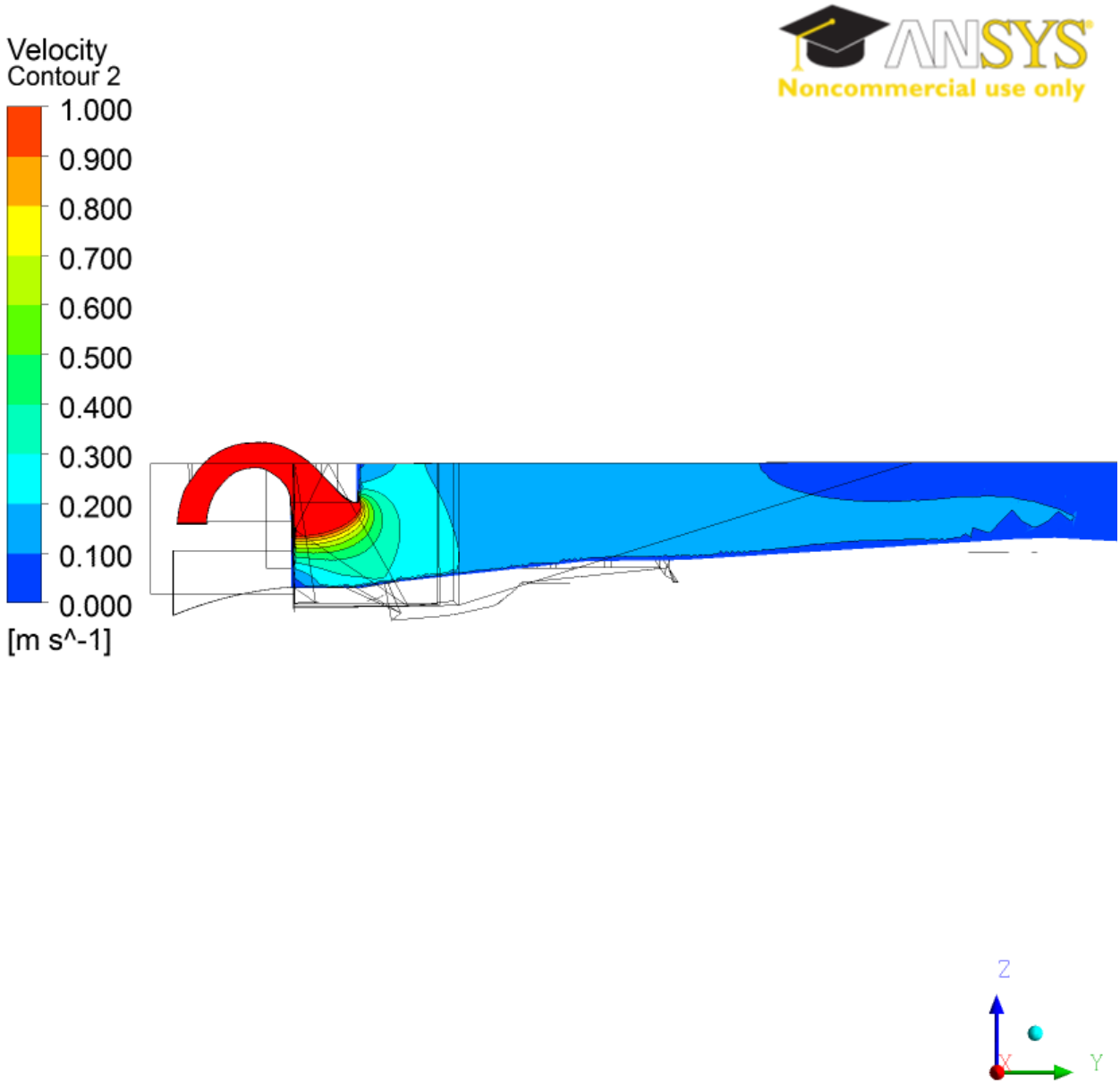
Velocity
Contour 2
1.000
0.900
0.800
0.700
0.600
0.500
0.400
0.300
0.200
0.100
0.000
[m s^-1]
ANSYS
Noncommercial use only
Z
Y
X
0
5.000
10.000 (m)
2.500
7.500

(b)

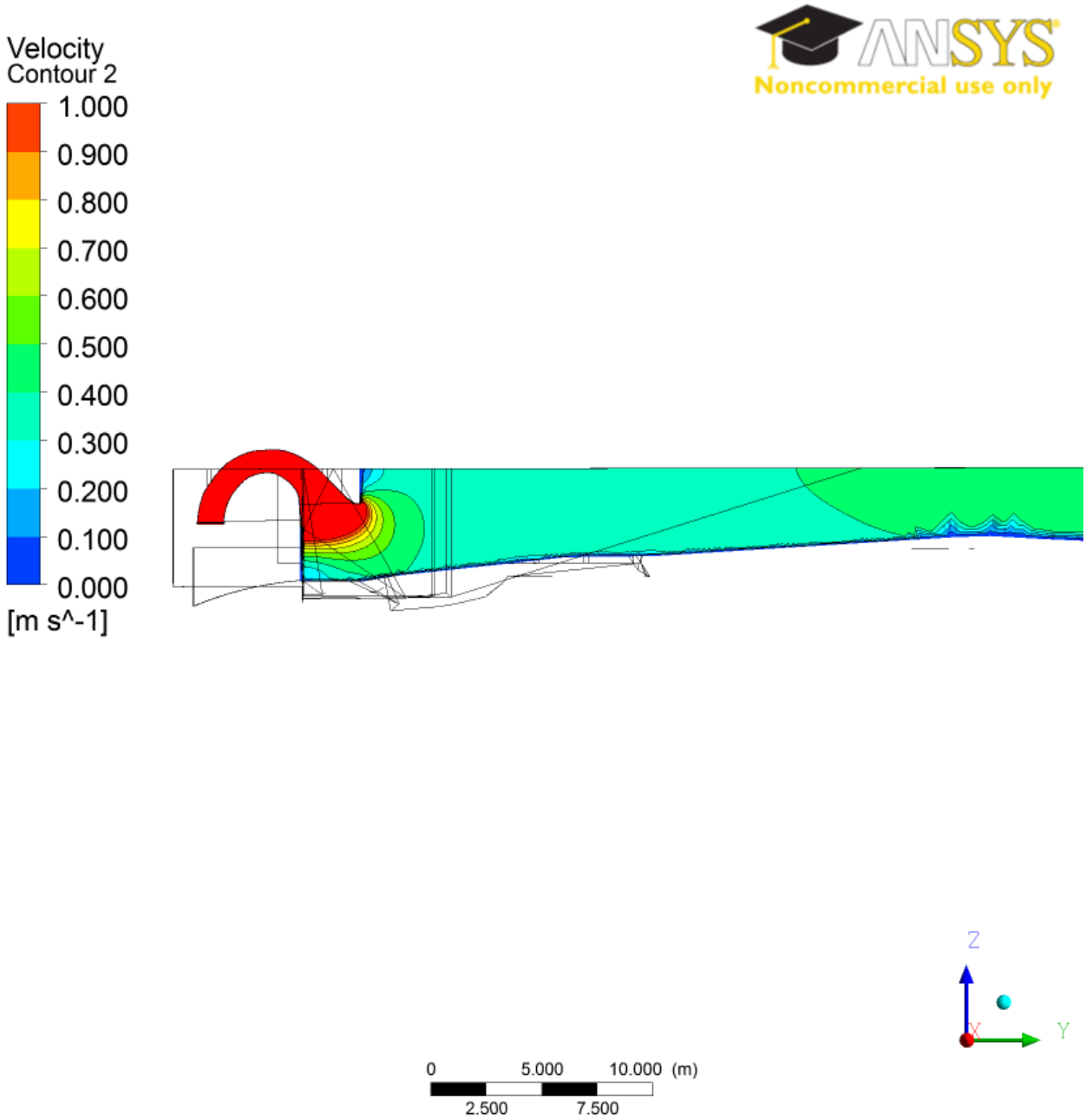
Velocity
Contour 2
1.000
0.900
0.800
0.700
0.600
0.500
0.400
0.300
0.200
0.100
0.000
[m s^-1]
Noncommercial use only
Z
Y
X
0
5.000
10.000 (m)
2.500
7.500

(c)

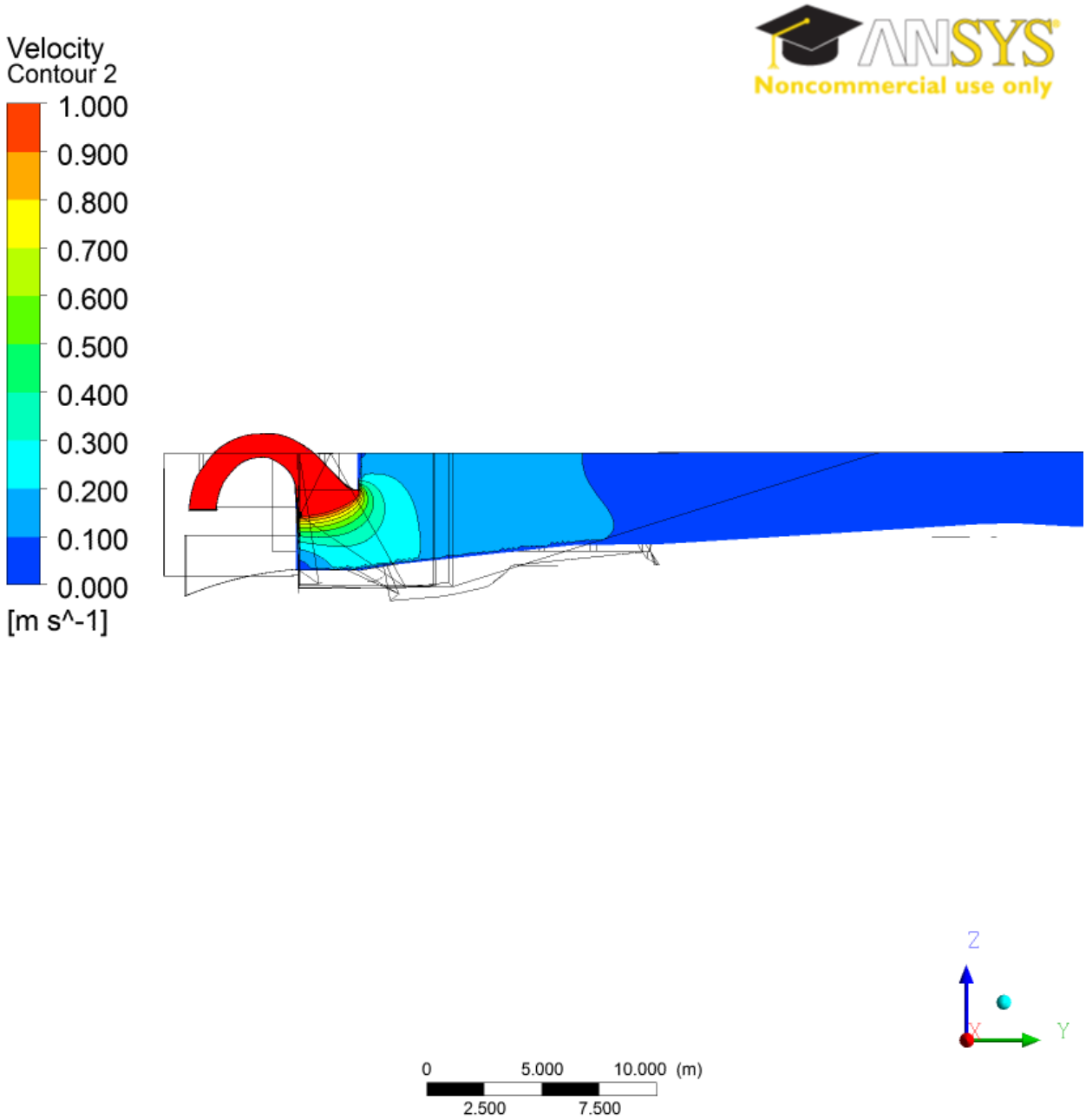
Velocity
Contour 2
1.000
0.900
0.800
0.700
0.600
0.500
0.400
0.300
0.200
0.100
0.000
[m s^-1]
Noncommercial use only
Z
Y
X
0
5.000
10.000 (m)
2.500
7.500

(d)

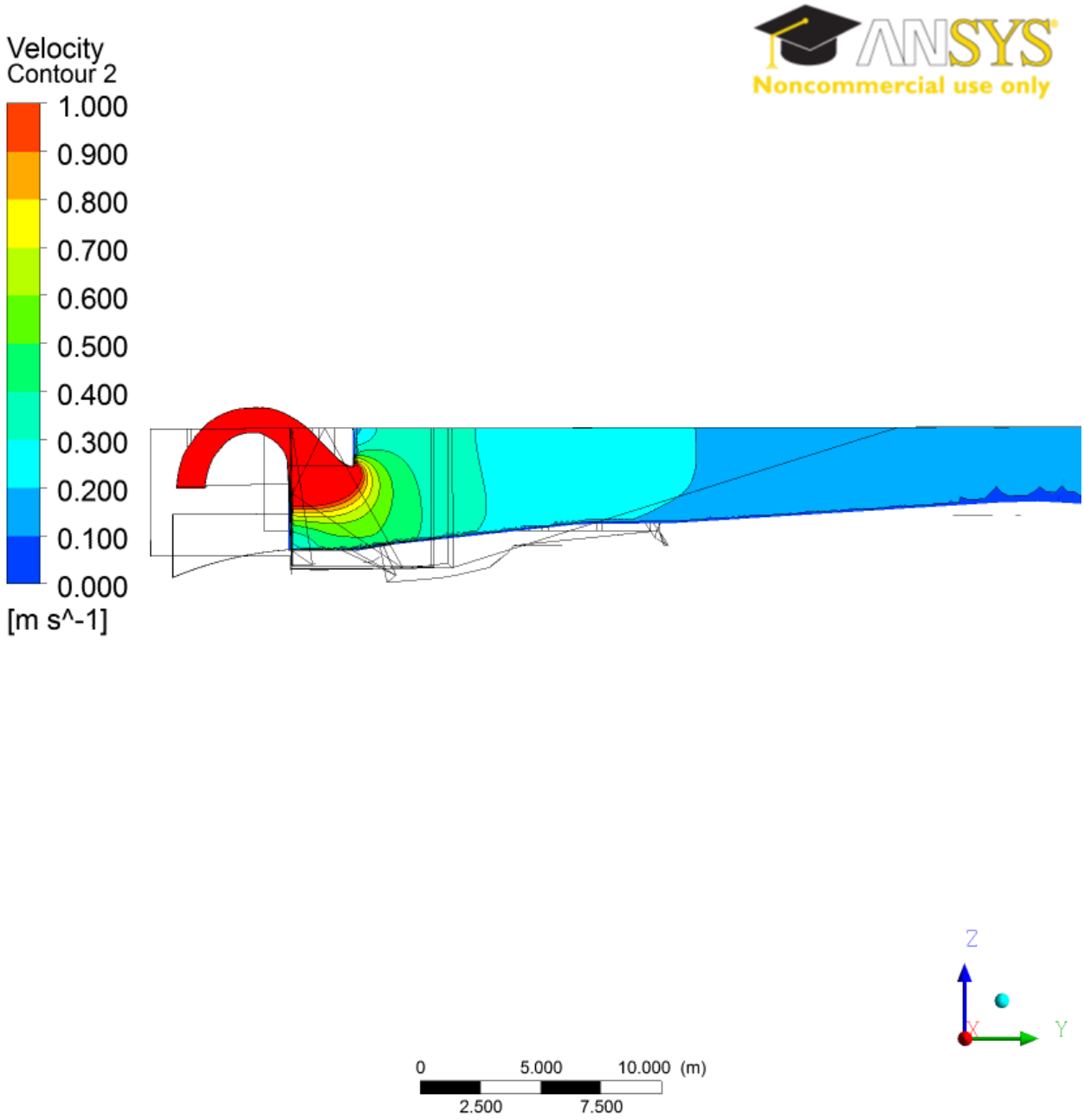

(e)

Figure 8 Seton Siphon 1 Velocity Profile Contours (a) Outage High Flow; (b) Outage Low Flow; (c) Operational High Flow; (d) Operational Low Flow; (e) Idealised Outage (High Flow).

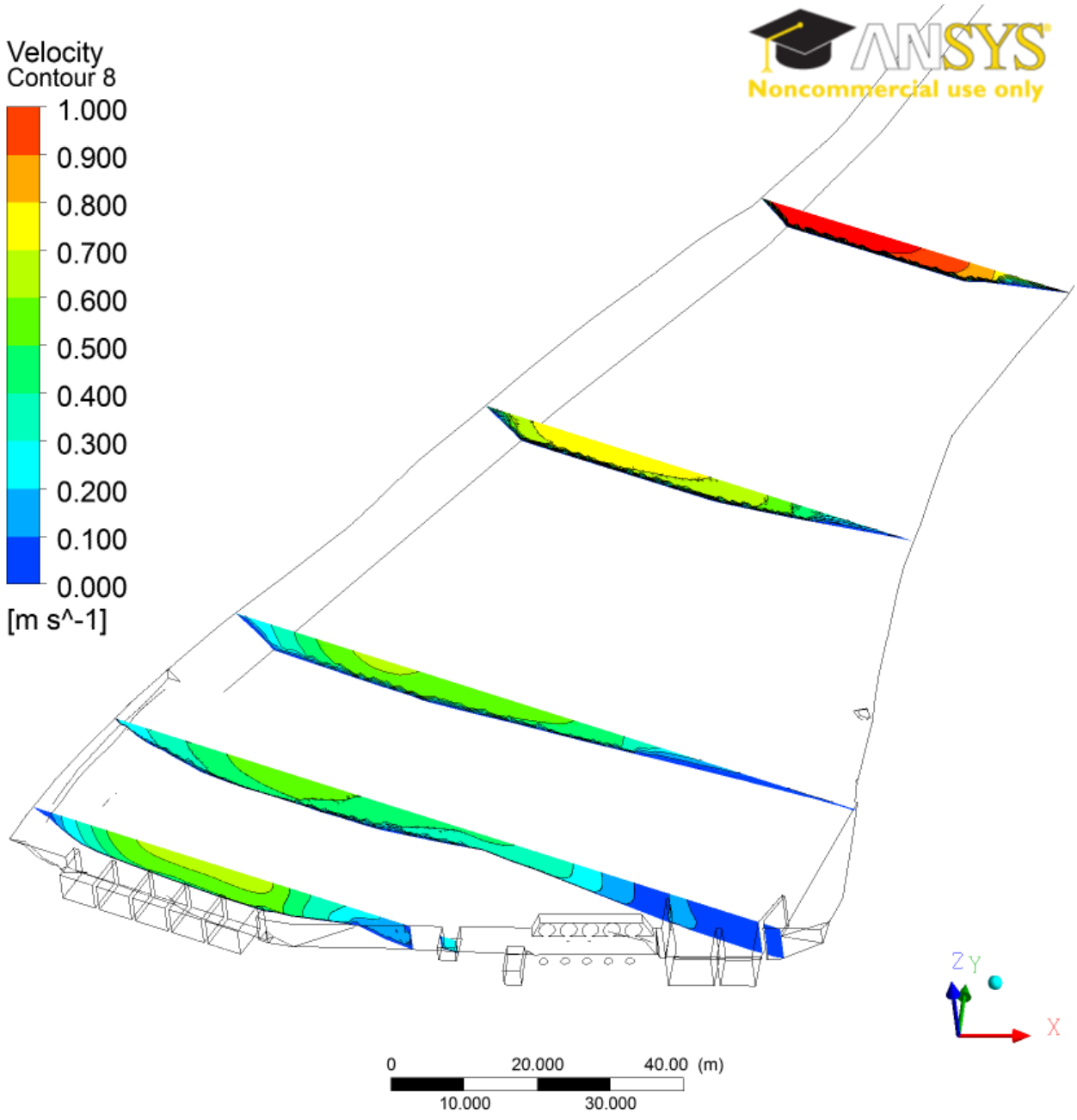
Velocity
Contour 8
1.000
0.900
0.800
0.700
0.600
0.500
0.400
0.300
0.200
0.100
0.000
[m s^-1]
ANSYS
Noncommercial use only
Z
Y
X
0
20.000
40.00 (m)
10.000
30.000

(a)

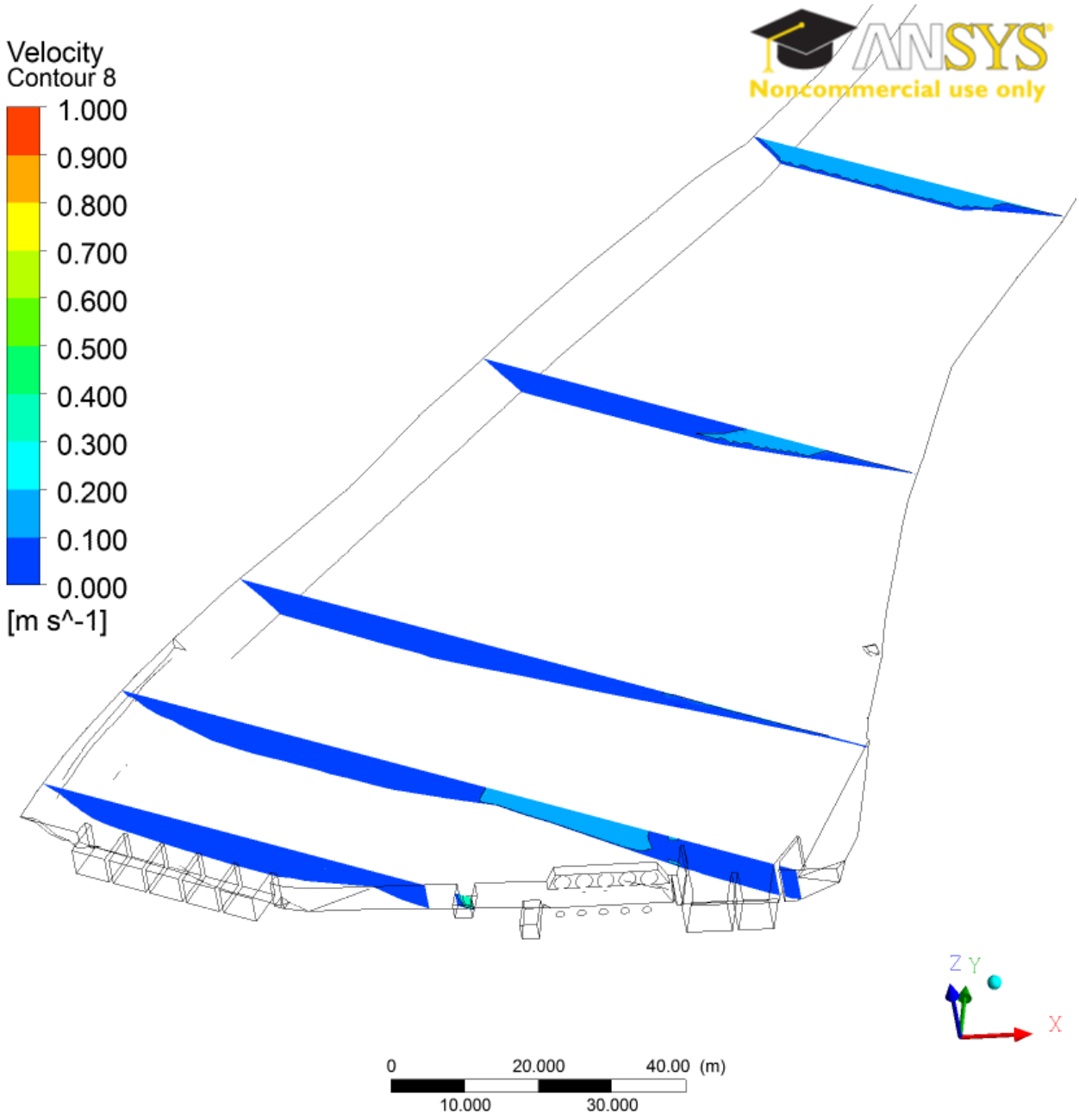
Velocity
Contour 8
1.000
0.900
0.800
0.700
0.600
0.500
0.400
0.300
0.200
0.100
0.000
[m s^-1]
ANSYS
Noncommercial use only
Z Y
X
0
20.000
40.00 (m)
10.000
30.000

(b)

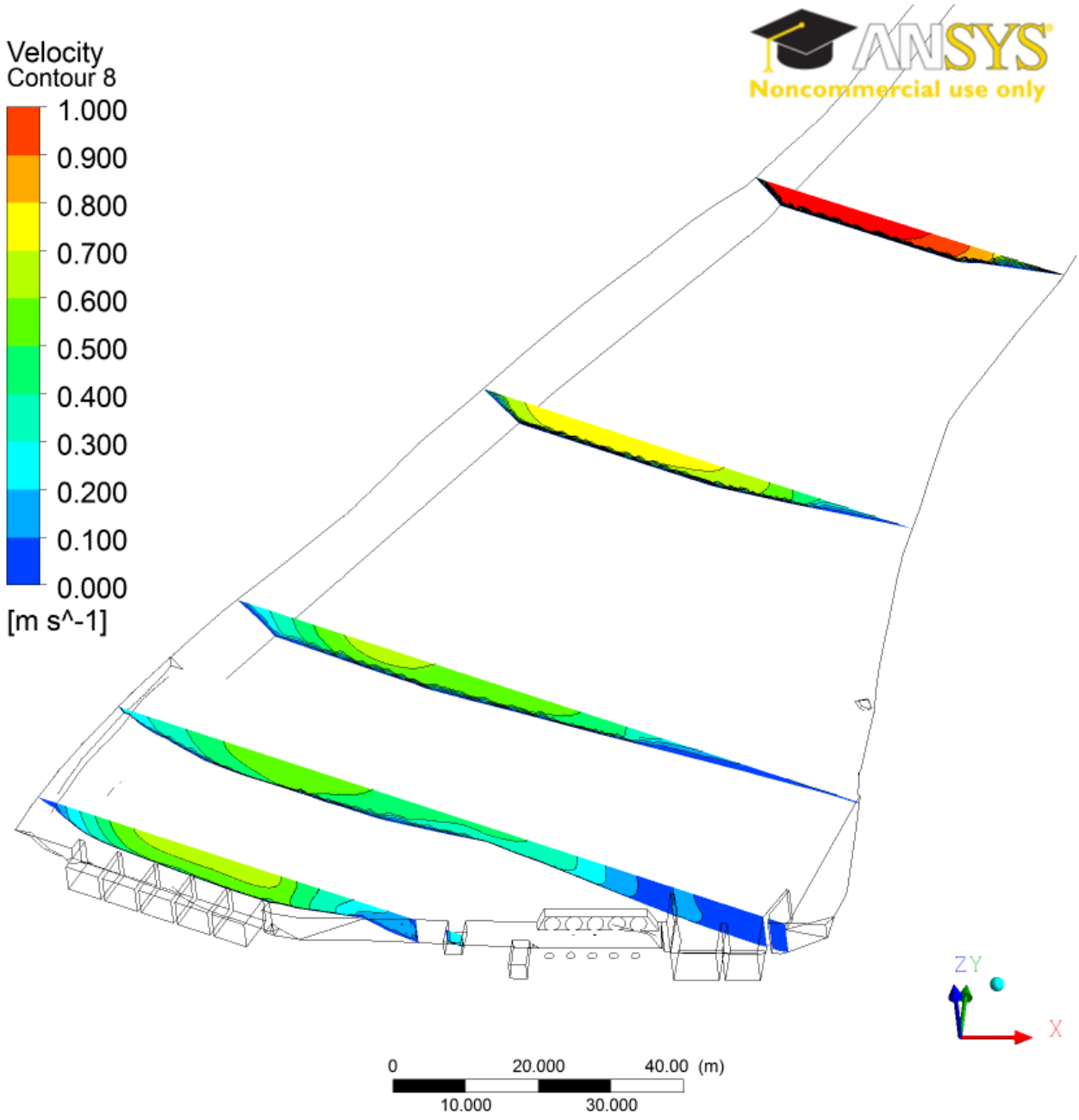
Velocity
Contour 8
1.000
0.900
0.800
0.700
0.600
0.500
0.400
0.300
0.200
0.100
0.000
[m s^-1]
ANSYS
Noncommercial use only
Z Y
X
0
20.000
40.00 (m)
10.000
30.000

(c)

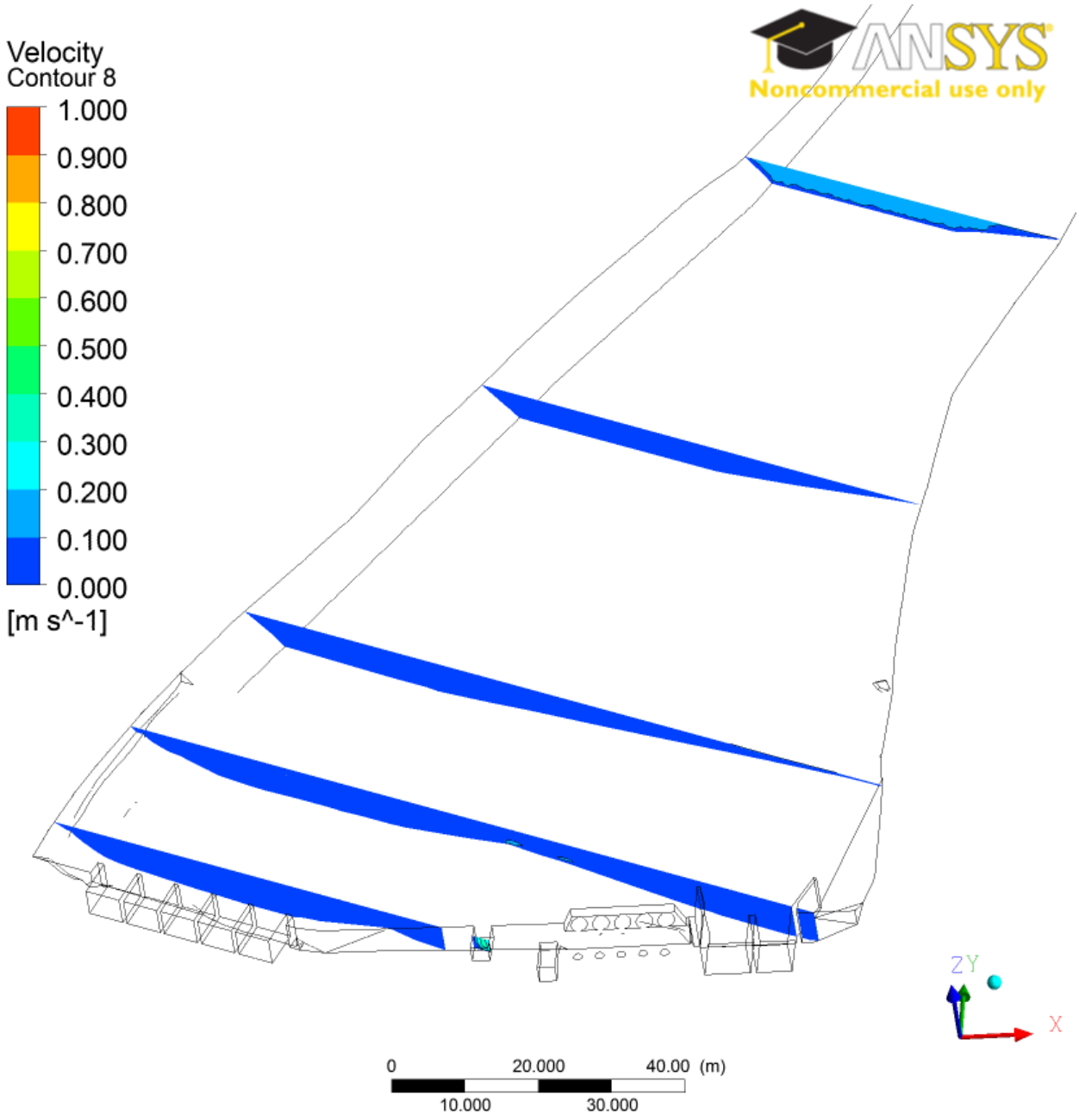
Velocity
Contour 8
1.000
0.900
0.800
0.700
0.600
0.500
0.400
0.300
0.200
0.100
0.000
[m s^-1]
ANSYS
Noncommercial use only
Z Y
X
0
20.000
40.00 (m)
10.000
30.000

(d)

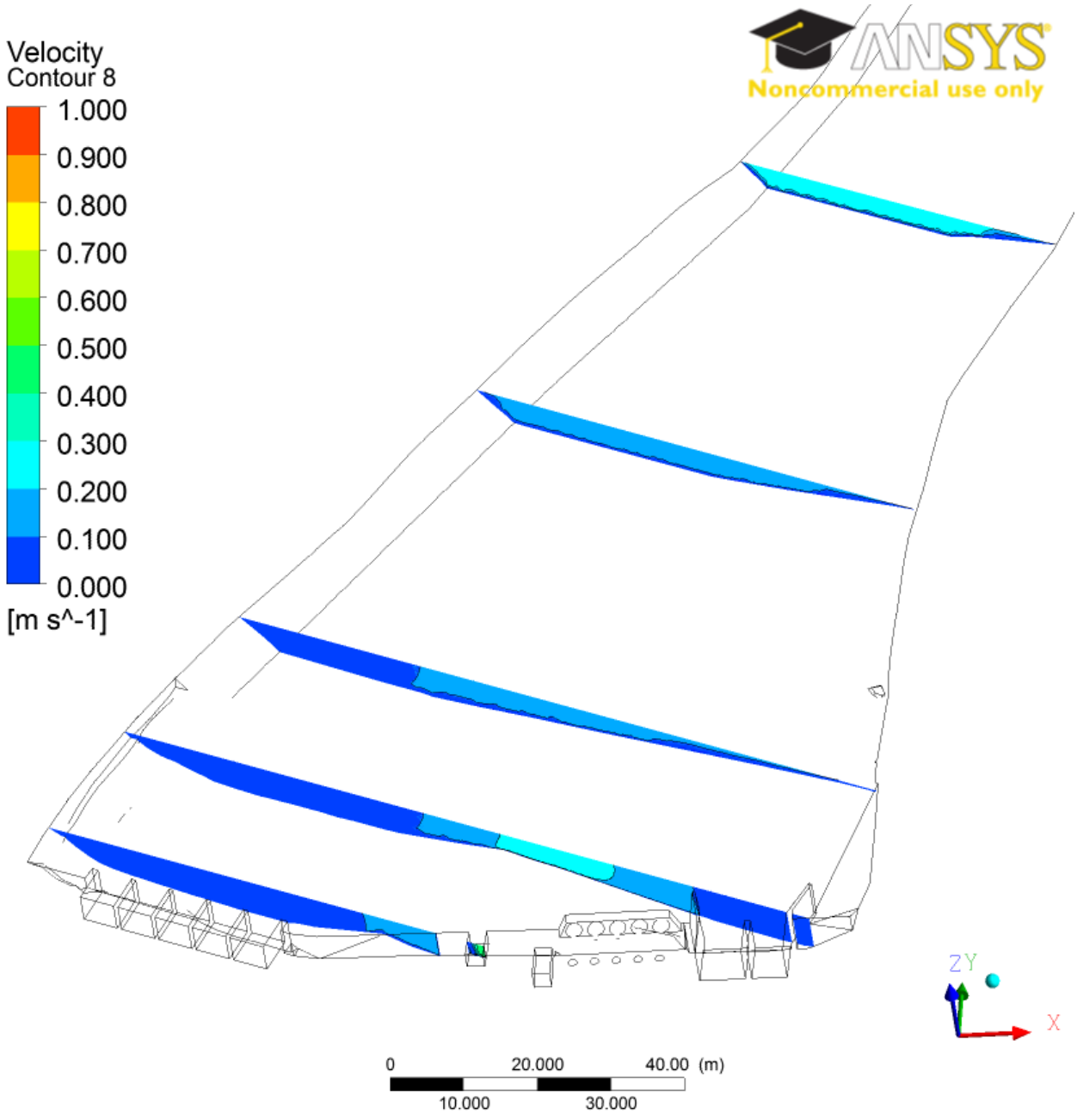

(e)

Figure 9 Seton Cross-Section Velocity Profile Count at Transects 5m, 25m, 50m, 100m and 150m, (a) Outage High Flow (b) Outage Low Flow; (c) Operational High Flow; (d) Operational Low Flow; (e) Idealised Outage (High Flow).

Appendix 2: Sockeye Smolt Swimming Behavior

MEMO

To:	Bonnie Adolph Jessie Hopkins
c.c.	David Zhu Mat Langford
From:	Dave Levy
Date:	March 11, 2014
Re:	Sockeye smolt swimming behavior

This memo reports the results of a cursory review of the scientific literature on salmon smolt swimming behavior. The intent was to survey papers that are relevant for the BRGMON-13 project including the Computational Fluid Dynamics modeling to be undertaken by the University of Alberta. Papers were obtained via Google Scholar. There is a large literature in this area, a reflection of the importance of fish entrainment in hydro and cooling water intakes.

Three key papers contained the most relevant information for our purposes:

Brett, J.R. and N.R. Glass. 1973. Metabolic rates and critical swimming speeds of sockeye salmon (*Oncorhynchus nerka*) in relation to size and temperature. J.Fish. Res. Board Can. 30: 379-382.

Feist, B.E. and J.J. Anderson. 1991. Review of fish behavior relevant to fish guidance systems. Univ. of Washington, Fisheries Research Inst. 92p.

Coutant, C.C. and R. Witney. 1999. Fish behavior in relation to passage through hydropower turbines: a review. Trans. Am. Fish. Soc. 129: 351-380.

On the pages that follow, information that is relevant for sockeye smolt entrainment at the Seton Dam has been extracted from these 3 sources.

Conclusions from this analysis include:

1. Regression relationships are available for sockeye that relate critical swimming speeds (=maximum 60-min sustained swimming speed) to fish length (total length, cm[5]). This is important to apply at Seton since we have observed significant between-year differences in smolt size. By implication entrainment may vary as a function of smolt size.

[5] Tip of head to tip of tail

2. Isopleths are available for critical swimming speeds in relation to fish size and temperature. If we know fish size and water temperature, we can extrapolate critical swimming speed.

3. Different types of swimming behavior are burst, critical and sustained. Burst swimming speed is the maximum velocity a fish can swim for 15 sec or less, analogous to sprinting in humans. Burst swimming velocities consume tremendous amounts of energy - metabolic rate required for burst swimming is 40 times higher than that required for sustained swimming. Critical swimming velocity is determined by increasing water velocity in experimental flumes by a constant interval every 15 min and noting the velocity at which the subject becomes exhausted. Lastly, sustained swimming is the velocity a fish can maintain for an hour or more without variation in performance, analogous to walking in humans.

4. Orientation in moving water (rheotropism) is accomplished mainly with visual and tactile sensation along with the lateral line system. Because of this, most fish (especially juveniles) invariably have a lower critical velocity in darkness than in light. This implies that entrainment risk at Seton may be lower during daytime rather than nighttime periods.

5. Physical characteristics of water have an effect on fish swimming. Water viscosity is the dominant factor in larval fish locomotion with associated low Reynolds numbers. Water viscosity is 30% greater at 10°C than at 20°C. For large fish, inertial forces of the water are the dominant factor; thus it is more difficult to accelerate and easier to glide. With larval fish, acceleration is less difficult, but gliding is more difficult. For example, smaller fish (10 cm) in total length can attain burst speeds of 25 body lengths per second (at 14°C), whereas larger fish (about 100 cm TL) can reach 6 bls. The power needed for propulsion equals the drag that the fish has to overcome, and fish morphology and locomotion are the main factors affecting drag.

6. A number of other factors contribute significantly to fish's ability to swim: temperature, size or age, species, stock, ecology/behavior and physiological status (such as smolting). Vision and the lateral line system are the key sensory inputs for a fish's response to currents.

7. Maximum burst speeds are on the order of 10 bls. Sustained swimming speeds for for sockeye and coho salmon were 3.0 and 3.4 bls

8. Temperature has a large impact on fish's swimming ability. In general 15°C is considered the optimal temperature for most species of Pacific salmon (Figures 1 and 2).

9. The length of a fish governs the ability to manoeuvre but also its burst, sustained and critical swimming speed and time to exhaustion.

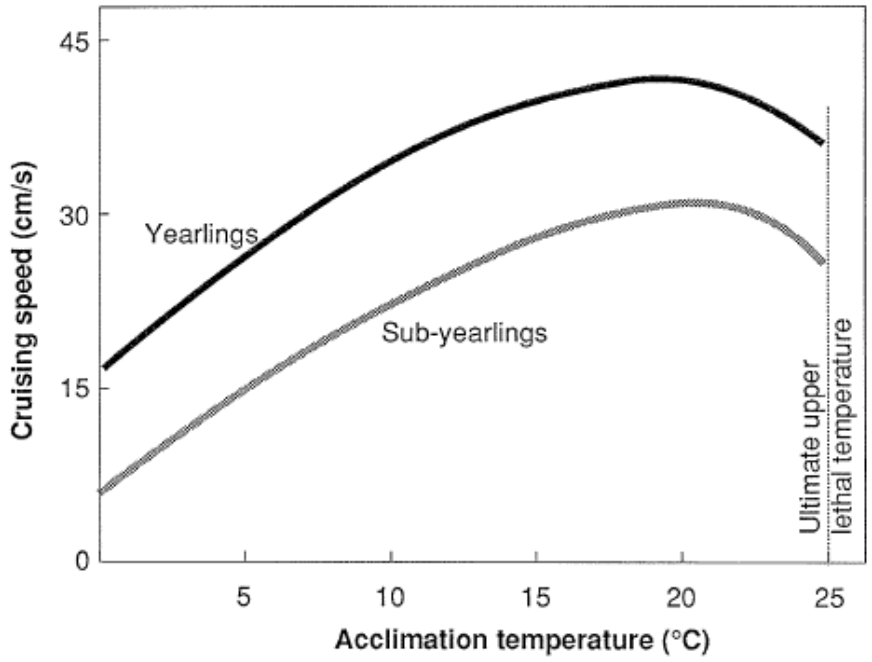

Figure 1 Effect of temperature on cruising speed of yearling and subyearling coho salmon, adjusted to common mean lengths of 3.5 and 2.1 in (8.9 and 5.4 cm), respectively (Brett et al. 1958).

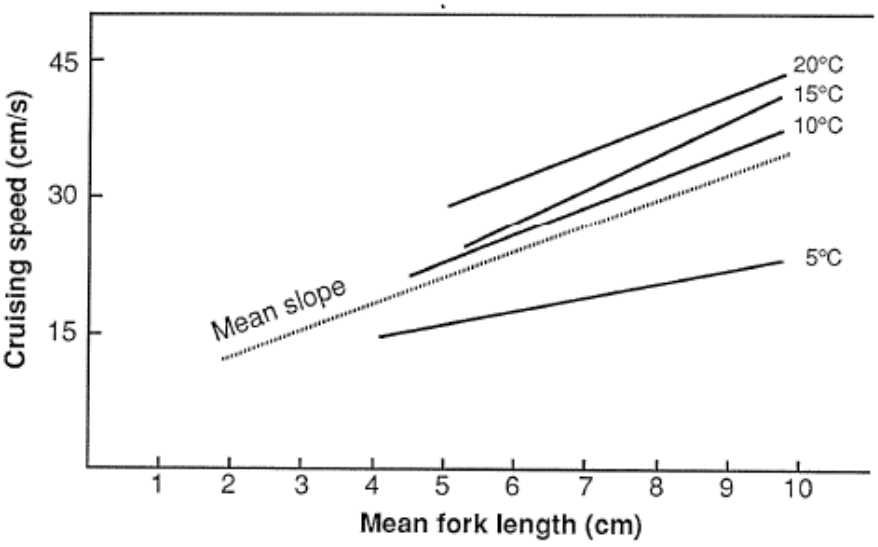

Figure 2 elationship between yearling and subyearling coho salmon cruising speeds as a function of TL at various temperatures. On the basis of the mean slope, cruising speed increasing about 0.1 fps (3 cm/s) for each 0.4 in (1 cm) increase in TL (Brett et al. 1958).

10. A behavior of juvenile salmonids that complicated behavioral studies is the tendency for the fish to seek zones of lower water velocity in both experimental and *in situ* situations. Thus one cannot assume that outmigrating fish will necessarily seek high current velocities.

11. Young salmon migrants can discriminate water velocities much lower than those which must be maintained in order to not delay them at dams.

12. Coutant and Whitney (2009) focused on aspects of fish behavior that could be used for computational fluid dynamics (CFD) modeling of fish trajectories through turbine systems. Salmon smolts approaching dams are generally surface oriented and follow flow. They can be diverted from turbines by spills or bypasses, with varying degrees of effectiveness. Smolts typically become disoriented in dam forebays.